Optimal Scheduling of a Natural Gas Processing Facility with Real-time Price Demand Response

Mohammed Abahussain

A dissertation

submitted in partial fulfillment of the

requirements for the degree of

Doctor of Philosophy

University of Washington

2015

Reading Committee:

Richard D. Christie, Chair

Daniel Kirschen

Miguel A. Ortega Vazquez

Program Authorized to Offer Degree:

Electrical Engineering

University of Washington

Abstract

Optimal Scheduling of a Natural Gas Processing Facility with Real-time Price Demand Response

Mohammed M Abahussain

Chair of the Supervisory Committee:
Professor Richard D. Christie
Electrical Engineering

Demand Response (DR) has been a hot topic since the introduction of the smart grid concept. The USA, Canada, and some European countries are researching the benefits of DR programs and their integration methodology into the electricity market. In the Gulf Region, smart grid received more attention, especially in the area of DR after the implementation of the Gulf Grid Interconnection and the ongoing deregulation effort of the electricity sector in Saudi Arabia.

Real-Time Price (RTP) DR (RTPDR) is a type of consumer-based DR (CBDR) that responds to a change in the RTP of electricity. RTPDR can reduce the volatility of energy prices, consumption of fuel and the range of loading. It can also defer capital investment in generation and transmission, improve social welfare, and enable stochastic energy resources that are carbon-free, once it is implemented. RTPDR has not been widely implemented because of the

sociological barriers that inhibit its implementation which are not as strong in industrial processes compared to inconvenience. The benefits of RTPDR are the motivation to overcome these barriers as industrial participation is a function of the benefit of RTPDR to the facility's owner.

Current literature discusses the implementation of utility-based DR, which involves involuntary control by the utility, in the industrial sector. The literature also discusses the implementation of CBDR, which involves voluntary control by the consumer, in the residential sector.

The contribution of this work is a methodology to quantify the benefits of RTPDR that will influence decisions about implementing RTPDR at a large industrial facility. RTPDR benefits are analyzed by presenting an optimal scheduling algorithm for the industrial facility, which owns a co-generation system. RTPDR is implemented at the facility by adjusting its production level and the co-generation system output to respond to the RTP of electricity by reducing the consumption of utility power and even supply power to the utility. A design study of the parameters that affect the implementation of RTPDR at the process facility is introduced. Then, a study of the integration of a considerable penetration level of RTPDR load into the Saudi Grid is proposed.

TABLE OF CONTENTS

List of Figures v

List of Tables viii

Glossary ii

Chapter 1. Introduction 1

1.1 Literature Review 3

1.2 Summary and Research Direction 10

Chapter 2. Optimal Instantaneous Scheduling of a Natural Gas Processing Facility with RTPDR 13

2.1 Introduction 13

2.2 Choosing a Plant 13

2.3 System Description 14

2.4 Plant Economics 15

2.5 Profit Maximization Problem Formulation for a Gas Processing Facility 17

2.5.1 System Constraints 18

2.5.2 Thermal Generation Constraints: 19

2.5.3 Power and Steam Demand Constraints 20

2.5.4 Co-generation System Power & Steam Relationship 21

2.6 Simulation Results and Discussion 21

2.7 Proposed Sensitivity Analysis to the Natural Gas Price 27

2.8 Conclusion 27

Chapter 3. Time-horizon scheduling of a Natural Gas Processing Facility with RTPDR 29

3.1 Saudi Grid Load & Price Profile 30

3.2 Profit Maximization for a Gas Processing Facility over a Time-Horizon 33

3.2.1 System and Thermal Generation Constraints 36

3.2.2 Cogeneration System Dynamic Constraints 37

3.2.3 Boiler Constraints 42
3.2.4 Power and Steam Demand Constraints 43
3.2.5 Transmission System Constraints 45
3.2.6 Process System Dynamic Constraints 45
3.3 Rolling Time-horizon Scheduling 54
3.3.1 Co-generation System 56
3.3.2 Boiler System 58
3.3.3 Process System 58
3.3.4 Storage System 59
3.4 Discussion and Analysis 59
3.4.1 Subsidized Fuel Price Case 59
3.4.2 Unsubsidized Fuel Price Case 63
3.5 Effects of Real Time Price Volatility and Price Forecast Accuracy 67
3.5.1 Effects of RTP Volatility 68
3.5.2 Effects of Price Forecast Accuracy 80
3.6 Conclusion 87

Chapter 4. Optimal Design Study of a Natural Gas Processing Facility for RTPDR Implementation 90

4.1 Introduction 90
4.2 Parameters that Affect Process Facility's RTPDR Profit 91
4.3 Co-generation Design Study and Sizing 92
4.4 Production Capacity Economic Evaluation and Sizing 96
4.5 Storage Tank Economic Evaluation and Sizing 98
4.6 Optimization over Process Facility's Parameters 100
4.6.1 Objective Function 100
4.6.2 Discussion 101
4.7 Conclusion 102

Chapter 5. Real-time Price Demand Response Effects on the Electricity Market and Power System 105

5.1 Introduction 105
5.2 Discussion 108
5.3 The Single-bus Test System 109
5.3.1 Introduction to Social Welfare 110
5.3.2 Modelling the Saudi Grid 116
5.3.3 The Saudi Grid single-bus Analysis 126
5.3.4 Fuel Price Sensitivity Analysis 128
5.3.5 Effects of Higher Penetration Levels of RTPDR Injections on Economic Incentives and the Electricity Market 131
5.4 The Three-bus Test Case 134
5.4.1 Scenario-I 136
5.4.2 Scenario-II 141
5.4.3 Scenario-III 148
5.5 The Saudi Electricity Market 151
5.5.1 Objective 151
5.5.2 Overview of the Saudi Electricity Market 151
5.5.3 Development of the Saudi Grid Test System 154
5.5.4 Testing the Saudi Grid System 160
5.6 Conclusion 162

Chapter 6. Contributions of the Research Work and Future Research Directions 164

6.1 Identification of Suitable RTPDR Facilities 164
6.2 Quantification of RTPDR Benefits for an Industrial Facility 165
6.3 A Method for Design Study to Modify an Industrial Facility to Improve its RTPDR Capability 165
6.4 A Method for Quantification of RTPDR Benefits for the Electricity Market and Society 166
6.5 Future Work 167
6.5.1 Identification of Characteristics of Suitable RTPDR Facilities 167
6.5.2 Expand DR Participation to Other Components of the Load 168
6.5.3 Expansion of the Detailed Model of the Industrial Facility's Process System 168

6.5.4 Expanding the Analysis for the Saudi Grid Test System 169
6.5.5 A Multi-objective Design Study for the Gas Processing Facility Using the Saudi Grid RTP Data 169
6.6 Conclusion 170
Bibliography 171

LIST OF FIGURES

Figure 1.1. Single-line diagram of GCC interconnection project [1]. 2
Figure 2.1. Block diagram of the process facility 15
Figure 2.2. Production level of the process facility at different RTP. 22
Figure 2.3. Steam production of the process facility at different RTP. 23
Figure 2.4. Demand curve for the process facility at different RTP 25
Figure 2.5. Co-generation unit-1 power output at different RTP 26
Figure 2.6. Co-generation unit-2 power output at different RTP 26
Figure 2.7. The gas facility's profit at different RTP 27
Figure 3.1. Weather profile for Houston, TX (left) and Dammam, Saudi Arabia (right) [42, 43] 31
Figure 3.2. Load profile of the Saudi Grid 33
Figure 3.3. Comparison of the price profile between the fixed price, subsidized fuel, and unsubsidized fuel cases 33
Figure 3.4. Block diagram of the process flow 46
Figure 3.5. Comparison between the fixed and adaptive contractual constraints 48
Figure 3.6. Forecast accuracy as a function of horizon length; [50] re-produced from [51] 55
Figure 3.7. Rolling time-horizon scheduling showing initial conditions carry-over 55
Figure 3.8. RTP profile for event-1 74
Figure 3.9. Production level during event-1 75
Figure 3.10. Cogen-1 power output during event-1 75
Figure 3.11. Cogen-2 power output during event-1 75
Figure 3.12. Purchased power from the utility during event-1 76
Figure 3.13. Boiler system steam output during event-1 76
Figure 3.14. Instantaneous profit of the process facility during event-1 76
Figure 3.15. RTP profile for event-2 77
Figure 3.16. Production level for event-2 78

Figure 3.17. Cogen-1 power output for event-2 78
Figure 3.18. Cogen-2 power output for event-2 78
Figure 3.19. Purchased power from the utility for event-2 79
Figure 3.20. Boiler system steam output for the RTPDR scenario in event-2 79
Figure 3.21. Instantaneous profit of the process facility for event-2 79
Figure 3.22. ANN structure for the price forecasting algorithm 82
Figure 4.1. Profit of the process facility at different generation system capacities 95
Figure 4.2. Curve fitting for the quadratic coefficient of generator's cost curve 96
Figure 4.3. Profit of the process facility at different production capacities 98
Figure 5.1. The single-bus test system 110
Figure 5.2. The worth of an elastic load (left); the worth of an inelastic load (right) 110
Figure 5.3. The cost of serving an elastic load (left); the cost of serving an inelastic load (right) 111
Figure 5.4. Social welfare of an elastic load (left); Social welfare of an inelastic load (right) 111
Figure 5.5. Effects of treating a partially-elastic load as an inelastic load (case-1) 114
Figure 5.6. Social welfare change from treating an elastic load as an inelastic load (case-1) 114
Figure 5.7. Effects of treating a partially-elastic load as an inelastic load (case-2) 115
Figure 5.8. Social welfare change from treating an elastic load as an inelastic load (case-2) 115
Figure 5.9. The equivalent power injection of a RTPDR facility 117
Figure 5.10. The equivalent social welfare contribution of a RTPDR facility 117
Figure 5.11. Bid Curve for the negative RTPDR injection 121
Figure 5.12. Cost function for the negative RTPDR injection 122
Figure 5.13. Bid Curve for the positive RTPDR injection 122
Figure 5.14. Cost function for the positive RTPDR injection 122
Figure 5.15. RTPDR surplus of a negative injection (example-1) 123
Figure 5.16. RTPDR surplus of a negative injection (example-2) 124
Figure 5.17. RTPDR surplus of a negative injection (example-3) 124

Figure 5.18. RTPDR surplus of a negative injection (example-4) 125
Figure 5.19. RTPDR profit of a positive injection (example-1) 125
Figure 5.20. RTPDR profit of a positive injection (example-2) 126
Figure 5.21. Demand curve for the lumped RTPDR injection in the Saudi Grid single-bus model using the subsidized and unsubsidized fuel prices 130
Figure 5.22. Social welfare effects for different penetration levels of RTPDR injections (load-reduction case) 132
Figure 5.23. Social welfare effects for different penetration levels of RTPDR injections (load-increase case) 133
Figure 5.24. The single-line diagram of the 3-bus test system for scenario-I [69] 136
Figure 5.25. The single-line diagram of the 3-bus test system for scenario-II 141
Figure 5.26. The electricity market structure in Saudi Arabia prior to deregulation [38] 152
Figure 5.27. The Electricity market structure in Saudi Arabia after phase-I completion [38] 153
Figure 5.28. The Electricity market structure in Saudi Arabia after complete deregulation [38] 153
Figure 5.29. Generation and transmission systems for the Central and Eastern regions [84] 155
Figure 5.30. System topology of the Saudi Grid 157
Figure 5.31. Feasibility region for the transmission line violation constraint [79] 159

LIST OF TABLES

Table 1.1. Overview of Installed Capacity in Saudi Arabia in 2007 [2] 2
Table 1.2. Overview of DR Classification in the Literature 7
Table 2.1. Frac Spreads for a Typical NGL Process Facility 16
Table 2.2. Expected Effect of Frac Spread on RTPDR 17
Table 2.3. Generation Cost Curve Breakpoints 20
Table 2.4. Equipment Status at Critical Production Levels (1: ON, 0: OFF) 23
Table 3.1. Comparison between the Fixed Price, Subsidized Fuel, and Unsubsidized Fuel Cases 32
Table 3.2. A Generator Startup Cost Constraint Example 39
Table 3.3. A Minimum Uptime Constraint Example ($MUT = 5$) 41
Table 3.4. A Minimum Downtime Constraint Example ($MDT = 4$) 42
Table 3.5. Enforcement of the Minimum Uptime ($t = 6, MUT = 5, su_{g,2} = 1$) 42
Table 3.6. A Contractual Constraint Example 49
Table 3.7. An Example of the Startup Constraint for the Process Facility 54
Table 3.8. Computational Time as a Function of the Horizon Length 56
Table 3.9. An Example of the MUT Initial Condition Calculation 57
Table 3.10. An Example of the MDT Initial Condition Calculation 58
Table 3.11. Profit Comparison for Different Scenarios (subsidized fuel case) 60
Table 3.12. Cost and Revenue Allocation for Different Scenarios (subsidized fuel case) 60
Table 3.13. Total Generated Power for Different Scenarios (subsidized fuel case) 60
Table 3.14. Total Production for Different Scenarios (subsidized fuel case) 60
Table 3.15. Total Power Export to the Grid for Different Scenarios (subsidized fuel case) 62
Table 3.16. Steam Production for Different Scenarios (subsidized fuel case) 62
Table 3.17. Comparison between Fuel Prices in the Subsidized and Unsubsidized Fuel Cases 63

Table 3.18. Profit Comparison for Different Scenarios (unsubsidized fuel case)..... 64
Table 3.19. Cost and Revenue Allocation for Different Scenarios (unsubsidized fuel case) 65
Table 3.20. Total Generated Power for Different Scenarios (unsubsidized fuel case) 65
Table 3.21. Total Production for Different Scenarios (unsubsidized fuel case) 65
Table 3.22. Total Power Export to the Grid for Different Scenarios (unsubsidized fuel case)..... 65
Table 3.23. Steam Production for Different Scenarios (unsubsidized fuel case)..... 65
Table 3.24. Steam Production for Different Boilers during a High RTP Event (day-150) 67
Table 3.25. Comparison between the Subsidized Fuel, Unsubsidized Fuel, and ERCOT Cases..... 68
Table 3.26. Profit Comparison for Different Scenarios (ERCOT System) 70
Table 3.27. Cost and Revenue Allocation for Different Scenarios (ERCOT system)..... 70
Table 3.28. Total Generated Power for Different Scenarios (ERCOT system)..... 70
Table 3.29. Total Production for Different Scenarios (ERCOT system)..... 70
Table 3.30. Total Power Export to the Grid for Different Scenarios (ERCOT system) 70
Table 3.31. Steam Production for Different Scenarios (ERCOT system) 71
Table 3.34. Effects of High RTP Volatility on the Process Facility's Profit..... 87
Table 4.1. Expansion Cost of the Process Facility's Co-generation System [64]..... 92
Table 4.2. A Cost-benefit Analysis of the Co-Generation System Expansion 93
Table 4.3. Marginal Costs of 245 MW And 250 MW Generation Units..... 95
Table 4.4. Cost Curve Parameters for Different Generators..... 96
Table 4.5. Capital Cost of Two NGL Plants in Saudi Arabia [65, 66] 97
Table 4.6. Cost of Increasing the Production Capacity of the Process Facility..... 97
Table 4.7. A Cost-benefit Analysis of the Production Capacity Expansion..... 97
Table 4.8. Cost of Incoming Product Storage System at the Process Facility..... 99
Table 4.9. Cost-benefit Analysis of the Storage System Expansion..... 99
Table 4.10. The Process Facility's Profit at Different Generation and Storage System sizes (K$)..... 102

Table 5.1. Social Welfare Change from Treating an Elastic Load as an Inelastic Load (case-1) 113
Table 5.2. Cost for Different Types of Fuel at the Subsidized Fuel Price [55] 116
Table 5.3. RTPDR Effects on the Single-bus Model Using the Subsidized Fuel Price...127
Table 5.4. Fuel Cost at the Subsidized and Unsubsidized Fuel Price [53, 54, 55] 130
Table 5.5. RTPDR Effects on the Single-bus Model Using the Unsubsidized Fuel Price 131
Table 5.6. Effects of Higher Penetration Level of RTPDR Injections on RTP Volatility 133
Table 5.7. Comparison of RTPDR Effects between a Single and Multiple RTPDR Injections 133
Table 5.8. Effects of Multiple RTPDR Injections on the Process Facility's Profit 134
Table 5.9. Transmission System Data (scenario-I) [69] 137
Table 5.10. Generation Cost Data for Scenario-I [69] 137
Table 5.11. Market Effects of the RTPDR injection (scenario-I) 138
Table 5.12. Generation Dispatch (scenario-I) 138
Table 5.13. LMP Data (scenario-I); the RTPDR Injection Located at Bus-3 138
Table 5.14. Load Payment for the Three-Bus Test Case (scenario-I) 139
Table 5.15. Generation Revenue for the Three-Bus Test Case (scenario-I) 139
Table 5.16. Social Welfare for the Three-bus Test Case (scenario-I) 140
Table 5.17. The RTPDR Injection Market Benefit for the Three-bus Test Case (scenario-I) 140
Table 5.18. Transmission System Data (scenario-II) 141
Table 5.19. Generation Cost Data (scenario-II) [63] 142
Table 5.20. Market Effects of the RTPDR Injection (scenario-II) 143
Table 5.21. Generation Dispatch (scenario-II) 143
Table 5.22. LMP Data for the Three-bus Test Case (scenario-II) 143
Table 5.23. Generation Cost Data (modified scenario-II) [63] 144
Table 5.24. Market Effects of the RTPDR Injection (modified scenario-II) 145
Table 5.25. Generation Dispatch (modified scenario-II) 145

Table 5.26. LMP Data for the Three-bus Test Case (modified scenario-II)..... 145
Table 5.27. Load payment for the Three-bus Test Case (modified scenario-II)..... 146
Table 5.28. Generation Revenue for the Three-bus Test Case (modified scenario-II)... 147
Table 5.29. Social Welfare for the Three-bus Test Case (modified scenario-II)..... 147
Table 5.30. Market Benefit of the RTPDR Injection for the Three-bus Test Case (modified scenario-II)..... 148
Table 5.31. Generation Cost Data (scenario-III) [63]..... 149
Table 5.32. Load Data at Bus-3 (scenario-III)..... 149
Table 5.33. Generation Dispatch for Different Cases (scenario-III) 150
Table 5.34. LMP Data for Different Cases (scenario-III)..... 150
Table 5.35. Generation Capacity by Region [55, 38, 2, 72, 84, 35, 77, 70, 71] 155
Table 5.36. Generation Mix of the Central and Eastern Systems [70] 156
Table 5.37. Major Transmission Lines between the Eastern and Central Regions 158

GLOSSARY

A/P	Capital recovery, $\frac{i(1+i)^N}{(1+i)^N-1}$.
AE(i)	Annualized cost of co-generation system expansion based on interest rate of *i*, in $/year.
A_s	Slope of the fitted line, which corresponds to the incremental process steam, in Mlb/MB.
$A_{s,b}$	Marginal cost of boiler *b*, in $/Mlb.
$A_{s,g}$	Linear coefficient of steam output of co-generation unit *g*, in Mlb/MW.
a	Fixed coefficient of power demand, in MW.
B	Total number of boilers at the natural gas facility.
$B_{s,b}$	Intercept which corresponds to no-load cost of boiler *b*, in $/hr.
$B_{s,g}$	Fixed coefficient of steam output of co-generation unit *g*, in Mlb.
$BP_{M_{\dot{v}}}$	Break point $M_{\dot{v}}$.
b	Linear coefficient of power demand, in MW/MB.
$C(P_u)$	Cost of purchasing power from or selling power to the utility, in $/hr.
$C(P_{u,t})$	Cost of purchasing power from or selling power to the utility at time step *t*, in $/hr.
C_b	Cost function for boiler *b*.
C_g	Cost function for generator *g*.
$C_b\,(S_b)$	Cost function of boiler *b* that produces S_b, in $/hr.
$C_b\,(S_{b,t})$	Cost function of boiler *b* that produces $S_{b,t}$ at time step *t*, in $/hr.
$C_g\,(P_g)$	Cost function of generator *g* that produces P_g, in $/hr.
$C_g\,(P_{g,t})$	Cost function of generator *g* that produces $P_{g,t}$ at time step *t*, in $/hr.
C_{raw}	Raw material cost in $/MB.
CSU_b	Startup cost of boiler *b*, in $.
$CSU_{b,t}$	Startup cost of boiler *b* at time step *t*, in $.

CSU_g	Startup cost of generator g, in \$.
$CSU_{g,t}$	Startup cost of generator g at time step t, in \$.
$CSU_{\dot{v},t}$	Startup cost of the process system at time step t, in \$.
CS	Consumer surplus, in \$.
c	Quadratic coefficient of power demand, in MW/MB^2.
$c_{v,l}$	Linear cost coefficient, in \$/MW.
$cost_a$	New equipment cost.
$cost_b$	Reference equipment cost.
D	Demand
$DT_{aux_{\dot{v},t}}$	Dummy variable used for the calculation of the initial down-time status of the process system.
$DT_{aux_{g,t}}$	Dummy variable used for the calculation of the initial down-time status of generator g.
$DT_{g,ini}$	Number of periods that generator g has been de-committed up to period $t-1$, in hrs.
$DT_{\dot{v},ini}$	Number of periods that the process system has been de-committed up to period $t-1$, in hrs.
day	Number of days in the study period.
$f_p(P_l)$	Penalty cost as a function of the real power flow at branch l, in \$.
Fs	Frac Spread obtained from selling one MB of NGL products, in \$.
F_t	Cash flow at time t, in \$.
FV_l	Transmission constraint violation for branch l, in MW.
G	Total number of co-generation units at the natural gas facility.
i	Interest rate used for economic analysis; internal process facility requirement is 7.5%.
IC	Incremental cost.
IS_g	Initial status of generation unit g.
k	Shrinkage factor of the process system.

$K_{b,t}$	Cost of bringing online boiler *b* at time step *t*, in $.
$K_{g,t}$	Cost of bringing online generator *g* at time step *t*, in $.
L	Number of transmission lines in the electricity grid.
$L_{Bus_i}^{residential}$	Residential load at Bus_i, in MW.
L_g^{up}	Number of hours that generator *g* has to be committed to meet the minimum up-time constraint, in hrs.
L_g^{down}	Number of hours that generator *g* has to be de-committed to meet the minimum down-time constraint, in hrs.
$L_{total}^{residential}$	Total residential load of the province, in MW.
$L_{\dot{v}}^{up}$	Number of hours that the process system has to be committed to meet the minimum up-time constraint, in hrs.
$L_{\dot{v}}^{down}$	Number of hours that the process system has to be de-committed to meet the minimum down-time constraint, in hrs.
$limit_l$	Transmission line limit for branch *l*.
LMP_j	Locational marginal price at bus *j*.
M_g	Number of segments of the piece-wise cost function of generator *g*.
$M_{\dot{v}}$	Number of segments of the piece-wise power demand function of the process system.
M	Maintenance cost, in $/year.
MB	Thousand barrels.
MC_{g,M_g}	Marginal cost of segment M_g of generator *g*, in $/MWh.
MDT_g	Minimum down-time constraint for generator *g*, in hrs.
$MDT_{\dot{v}}$	Minimum down-time constraint for the process system, in hrs.
$MMSCF$	Million standard cubic feet.
$MP_{M_{\dot{v}}}$	Marginal power of segment $M_{\dot{v}}$, in MW/MB.
MUT_g	Minimum up-time constraint for generator *g*, in hrs.
$MUT_{\dot{v}}$	Minimum up-time constraint for the process system, in hrs.
MW	Million watts.

N	Number of years.
N_d	Remaining number of days for the weekly contractual constraint, in days.
NLC_{g}	No-load cost of generator *g*, in $/hr.
NLP	No-load power of the process facility, in MW.
n	Exponential factor of the economy of scale, 0.7 for a petro-chemical process.
$P(BP_{M_{\dot{v}}})$	Power demand at break point $M_{\dot{v}}$, in MW.
P_D	Power demand of the process facility, in MW.
$P_D(V)$	power demand as a function of volume, in MW.
$P_{D,t}$	Power demand of the process facility at time step *t*, in MW.
$P_{D,t}\,(\dot{v}_t)$	Power demand as a function of processed material flow rate at time *t*, in MW.
P_g	Output power of generator *g*.
$P_{g,ini}$	Initial power output of generator *g*.
$P_{g,\,M_g}$	Amount of power in segment *m* for generator *g*, in MW.
$P_{g,\,M_g,t}$	Amount of power in segment *m* for generator *g* at time step *t*, in MW.
$P_{g,max}$	Maximum real power output constraint of generator *g*, in MW.
$P_{g,min}$	Minimum real power output constraint of generator *g*, in MW.
$P_{g,t}$	Output power of generator *g* at time step *t*, in MW.
P_l	Real power flow at branch *l*.
P_u	Amount of power purchased from or sold to the utility, in MW.
$P_{u,t}$	Purchased power from or sold to the utility at time step *t*, in MW.
PU_t	Power import from the utility at time step *t*, in MW.
$PW(i)$	Capital cost of co-generation system expansion, in $.
p_u	Price of purchasing power from the utility, in $/MW.
$p_{u,t}$	Predicted real-time price of energy at time step *t*, in $/MWh.
R_{TH}	Ratio of the study period length to a daily period length (1.5).
RD_b	Steam decrease ramp rate constraint of boiler *b*, in Mlb/hr.

RD_g	Power decrease ramp rate constraint of generator *g*, in MW/hr.
$RD_{\dot{v}}$	Production level decrease ramp rate constraint, in MB/hr.
RU_b	Steam increase ramp rate constraint of boiler *b*, in Mlb/hr.
RU_g	Power increase ramp rate constraint of generator *g*, in MW/hr.
$RU_{\dot{v}}$	Production level increase ramp rate constraint, in MB/hr.
S	Size of equipment.
S_b	Output steam of boiler *b*, in Mlb.
$S_{b,ini}$	Initial steam output of boiler *b*, in Mlb.
$S_{b,min}$	Minimum steam output constraint of boiler *b*, in Mlb.
$S_{b,max}$	Maximum steam output constraint of boiler *b*, in Mlb.
$S_{b,t}$	Output steam of boiler *b* at time step *t*, in Mlb/hr.
S_D	Total steam demand of the process facility, in Mlb.
$S_D(V)$	Steam demand as a function of volume, in Mlb.
$S_{D,t}$	Total steam demand of the process facility at time step *t*, in Mlb/hr.
S_g	Output steam of co-generation unit *g*, in Mlb.
$S_{g,t}$	Output steam of co-generation unit *g* at time step *t*, in Mlb/hr.
$sd_{\dot{v},t}$	Shutdown status of the process system at time step *t* (1: OFF, 0: ON).
$sd_{g,t}$	Shutdown status of generator *g* at time step *t* (1: OFF, 0: ON).
$su_{\dot{v},t}$	Startup status of the process system at time step *t* (1: ON, 0: OFF).
$su_{b,t}$	Startup status of boiler *b* at time step *t* (1: ON, 0: OFF).
$su_{g,t}$	Startup status of generator *g* at time step *t* (1: ON, 0: OFF).
SP	Supplier's profit, in $.
SW	Social welfare, in $.
T	Time-horizon of the gas facility's optimal scheduling, in hrs.
TAC	Total annualized cost, in $/yr.
TL_{max}	Maximum transfer capacity between the gas facility and the utility, in MW.

t_g^{off}	Number of hours that generator g has been de-committed up to period $t-1$, in hrs.
$u_{\dot{v},t}$	Status (flow, no flow) of the incoming raw material flow rate.
u_b	Status (on, off) of boiler b.
$u_{b,t}$	Status (on, off) of boiler b at time step t.
u_g	Status (on, off) of generator g.
$u_{g,ini}$	Initial status (on, off) of generator g.
$u_{\dot{v},ini}$	Initial status (on, off) of the process system.
$u_{g,t}$	Status (on, off) of generator g at time step t.
$UT_{aux_{\dot{v},t}}$	Dummy variable used for the calculation of the initial up-time status of the process system.
$UT_{aux_{g,t}}$	Dummy variable used for the calculation of the initial up-time status of generator g.
$UT_{g,ini}$	Number of periods that generator g has been committed up to period $t-1$, in hrs.
$UT_{\dot{v},ini}$	Number of periods that the process system has been committed up to period $t-1$, in hrs.
V	Production volume, in MB.
$V_{c,target}$	Target contractual constraint for each study period, in MB.
V_{max}	Maximum production level of the gas processing facility, in MB.
V_{min}	Minimum production level of the gas processing facility, in MB.
$V_{tot,d}$	Total volume of end products at the end of day d, in MB.
$V_{tot,ini}$	Initial volume of end products at the beginning of the study period, in MB.
$V_{T,min}$	Minimum Volume of processed materials at the end of the time-horizon T, in MB.
V_T	Volume of processed raw material at the end of the study time horizon T, in MB.
V_{ini}	Processed volume at the beginning of the study period, in MB.

V_i	Production volume of segment *i*, in MB.
V_t	Volume of the processed raw material at time step *t*, in MB.
$V_{s,T}$	Volume of raw material in the storage tank at the end of the study horizon *T*, in MB.
$V_{s,ini}$	Initial volume of raw material in the storage tank, in MB.
$V_{s,t}$	Volume of raw material in the storage tank at time step *t*, in MB.
$V_{s,max}$	Maximum storage capacity of the gas processing facility in MB.
$V_{w,t}$	Target volume for week *w*, in MB.
$W(P_d)$	Worth function of load P_d, in $/hr.
$Week$	Number of weeks in the study period.
X_a	New equipment size.
X_b	Reference equipment size.
$Y_{M_{\dot{v}},t}$	Set of binary variables that indicate the active segment of the production flow rate.
$Z_{M_{\dot{v}},t}$	Set of continuous variables in the interval [0, 1].
δ	Duration of one time step, in hrs.
ζ_b	Thermal time constant of boiler *b*, in hrs.
ζ_g	Thermal time constant of generator *g*, in hrs.
$\kappa_{\dot{v}}$	Fixed startup cost of the process system, in $.
κ_b	Fixed cost of bringing online boiler *b*, in $.
κ_g	Fixed cost of starting-up generator *g*, in $.
$\dot{v}_{M_{\dot{v}},t}$	Processed raw material flow rate in segment $M_{\dot{v}}$ at time *t*, in MB/hr.
$\dot{v}_{in,t}$	Flow rate of raw material entering the gas processing facility at time step *t*, in MB/hr.
$\dot{v}_{ini}$	Initial flow rate of raw material at the beginning of the study period, in MB/hr.
$\dot{v}_{max}$	Maximum flow rate of raw material at the gas processing facility, in MB/hr.

$\dot{v}_{min}$	Minimum flow rate of raw material at the gas processing facility, in MB/hr.
$\dot{v}_{o,t}$	End product flow rate at time step *t*, in MB/hr.
$\dot{v}_{s,t}$	Flow rate of raw material entering the storage tank at time step *t*, in MB/hr.
$\dot{v}_t$	Flow rate of raw material entering the process system at time step *t*, in MB/hr.
ρ_b	Cold start fuel cost of boiling unit *b*, in $.
ρ_g	Cold start fuel cost of generator *g*, in $.
$	Logical IF symbol.

ACKNOWLEDGEMENTS

The author wishes to express his sincere thanks and deserved appreciation to those that always supported this effort. This work could not be completed without the guidance and patience of Professor Richard D. Christie and the financial support provided by Saudi Aramco. The author extends his thanks to the utility and process facility representatives for providing the data needed to accomplish this work.

DEDICATION

This dissertation is fondly dedicated to my wife, Sumaiah Alhumaidi. Her continuous love and support have helped me achieve this great accomplishment.

Chapter 1. INTRODUCTION

In 2001, the Gulf Cooperation Council Interconnection Authority (GCCIA) was established for the purpose of constructing the GCC interconnection project, operating and maintaining the interconnection grid, and facilitating GCC regional electricity trading market. Bahrain, Kuwait, Saudi Arabia and Qatar interconnected in 2009 while the United Arab Emirates (UAE) hooked up in 2011, with Oman currently connected to UAE via a 220kV link that will be upgraded to 400kV as seen in Figure 1.1 [1]. In 2002, the Electricity and Cogeneration Regulatory Authority (ECRA) was formed in Saudi Arabia. Their mission is to ensure the supplies of electricity and desalinated water products provided to consumers are adequate, reliable, of high quality and fairly priced [2]. This in turn introduced the first step toward deregulation of the electric sector in Saudi Arabia. The discussion and comparison between dynamic pricing scheme and fixed pricing scheme is a hot topic in Saudi Arabia. Recently, major industrial customers started building their own generation facilities which increased the number of potential market participants from the generation side. Table 1.1 lists existing generation companies that are connected to the electric gird in Saudi Arabia which are Saudi Electricity Company (SEC), ARAMCO, Saline Water Conversion Company (SWCC), Water and Electricity Company (WEC), and MARAFIQ.

Electric demand in Saudi Arabia has been increasing 8% annually in the past few years which made it difficult if not impossible to build new electrical infrastructure that can cope with the rapid growth of power consumption [3]. One way to deal with this issue is to implement Demand Response (DR) for consumers who have concentrated load in one place that can easily be controlled, such as large industrial customers. DR can reduce the volatility of energy prices, consumption of fuel and the range of loading. It can also defer capital investment in generation and transmission, improves social welfare, and enables stochastic energy resources that are carbon-free, once it is implemented. Hence, it can spare financial resources on enhancing the overall generation efficiency. The consumption of fossil fuel resources reduces which in turn lowers the cost of energy for consumers. DR can also accommodate stochastic energy resources that are carbon-free, if DR is proven to be economically and technically viable. An existing gas processing facility in the Gulf region produces 1100 MBD of Natural Gas Liquid (NGL)

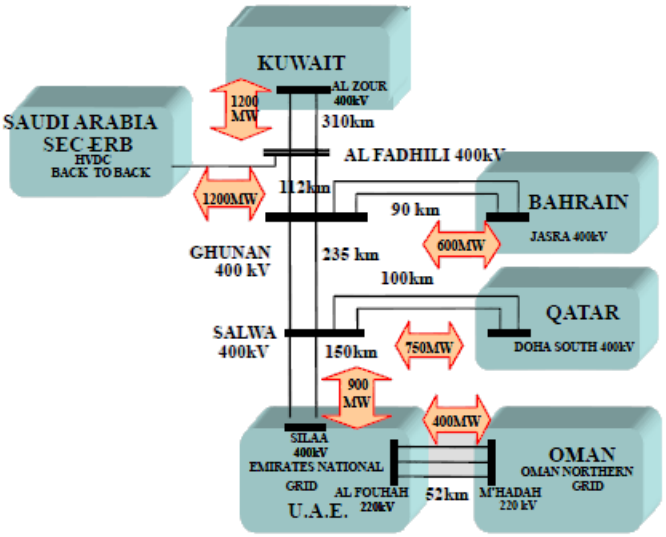

Figure 1.1. Single-line diagram of GCC interconnection project [1].

Table 1.1. Overview of Installed Capacity in Saudi Arabia in 2007 [2]

Production entity	Capacity (MW)	Future Expansion (MW)
SEC	30,670	41,200
SWCC	5,029	-
Tihama Power	1,074	-
MARAFIQ	1,040	2,745
ARAMCO	1,050	300
WEC	2,220	-

products and owns a cogeneration system that produces up to 310 MW of power and 2500 Mlb/hr of steam. The plant's operational philosophy may be impacted when the vertically-integrated utility decomposes to smaller utility companies who participate in an electricity market that allows for real-time pricing of electricity. This proposal examines the potential of implementing DR in this large gas processing facility. The final result of the thesis will assist the plant's management in the decision of implementing a real-time price demand response (RTPDR) program from technical and economical perspectives at the process facility. If the decision is in favor for PBDR program, then it will have a large-scale benefit that increases the social welfare and benefits the whole society.

Industrial facilities that have the ability to adjust their production level in presence of process limitations are good candidates for RTPDR, and technical feasibility needs to be

established. The system-wide impact of RTPDR on the complex power system for a high penetration level of responding loads should be evaluated. Examining the financial and technical feasibility of RTPDR for an industrial facility is the drive for this work, and is the focus of this dissertation. This is done by developing an optimal scheduler for a specific industrial facility to determine the optimal output of the facility as a function of the electricity price and process characteristic.

To that end, the steps taken in this dissertation are as follows: determine the state of the art to first, formulate and solve the instantaneous optimal scheduling problem with variable electricity price for the industrial facility; second, develop a process plant model over a time horizon that accurately represents power and process limitations during load adjustment; third, evaluate a design study of RTPDR at the process facility; fourth, apply the developed model to multiple facilities within a test system to extrapolate the effects of RTPDR on the Saudi Grid System.

1.1 LITERATURE REVIEW

DR and Demand Side Management (DSM) are used in technical papers interchangeably. In the literature, some papers used DR to refer to a load control by the utility. In [4], Asano et al. used DR to refer to load reduction by the utility, which is achieved by controlling air conditioning and lighting in an office space in Tokyo. In [5], Mohagheghi & Raji referred to DR as a demand-side management solution, which targets consumers, for the purpose of reducing or shifting load at a specified time for a specified duration. [4] and [5] referred to load reduction by the utility as DR. However, it is considered in this proposal as DSM because it is utility controlled.

Several papers used a combination of DR and DSM programs and classified them as either DR or DSM [6], [7], [8], [9], [10]. In [6], Torriti et al. shared the experience of DR implementation in the UK, Italy and Spain. DR is initially used to refer to an action at the customer side of the electricity meter. However, the paper referred to interruptible contracts as a DR program in the industrial sector. In [7], Saele and Grande used DR to refer to smart metering, load control, price-based energy combined with TOU tariff. In [8], Lu used DSM to refer to both the direct load control by the utility and indirect load control by consumer. In [9], Wang et al. highlighted that home energy management system (EMS) can control load by either the utility, defined as Direct Load Control (DLC) DR, or by the consumer, defined as indirect load control

DR. In [10], Han et al. classified interruptible loads, TOU, dynamic price, and direct load control as DR models. Smart metering in [7] is classified based on the control strategy. If incentive payment is offered as interruptible load contract and smart metering is controlled by the utility, then they are considered DSM in this proposal. However, if incentive payment is offered thru the price signal of energy such as RTP change and smart metering us controlled by load, then they are considered DR in this proposal. [6], [7], [8], [9], and [10] considered load control by the utility and interruptible loads as DR while it is best suited for DSM since the action is initiated by the utility. [6], [7], [8], [9], and [10] considered price-based energy, TOU, dynamic price, indirect load control, and an action at the customer side of the electricity meter as DR programs which is the proper classification for them in this proposal because the control action is initiated from the consumer side and it is voluntary.

Several papers have classified DR into different categories based on purpose or source of incentive [11], [12], [13], [14]. In [11], Kuroda et al. classified DR as either market based DR (MBDR) program or price-menu based DR (PBDR) program. The MBDR program, in which incentive is provided by a market, is categorized into emergency-based for electric system reliability or economic-based for market price reduction and stability. However, PBDR program incentives are provided by the utility or aggregators. Examples of the PBDR program are TOU, Critical Peak Pricing (CPP), RTP, and peak time rebate. In [12], Albadi and El-Saadany categorized DR programs into incentive-based or price-based programs. Incentive-based programs include typical load control and curtailable programs while market-based programs include demand bidding, emergency DR, capacity market, and ancillary service market. On the other hand, price-based programs are TOU, CPP, and RTP. In [13], Conchado and Linares classified DR programs based on purpose. If DR is used to improve system reliability, then it is usually executed through emergency-based, system-led, load-response, incentive-based, direct-load control programs. However, if DR is used to reduce system costs, then it is usually executed through price-based, market-led, price-response, incentive-based, passive-load control programs. In [15], Tang et al. define DR as change in demand by end users due to a change in energy price over time or due to incentive payments that are designed to lower demand when system reliability is jeopardized. The Department of Energy (DOE) defines DR as “Changes in electric usage by end-use customers from their normal consumption patterns in response to changes in the price of electricity over time, or to incentive payments designed to induce lower electricity

use at times of high wholesale market prices or when system reliability is jeopardized" [14]. [15], [11], [12], [13], and [14] definition of DR is ambiguous and it mixes between DR and DSM definitions in this proposal. Incentive payments in [15] are classified based on the incentive source and control strategy. MBDR program in [11], Incentive-based program in [12], DR to improve system reliability in [13] are referred to as DR programs but they are all examples of DSM in this proposal because they deal with involuntary action by the utility. The provided financial incentives in [14] are based on agreement contracts and it is not from changing load consumption in response to the RTP of electricity. Hence, agreement contracts are classified in this proposal as DSM because load does not have control over changing its energy consumption level.

Only few papers used DR definition consistently to refer to an action from the consumer side [16], [17]. In [16], Hammerstrom et al. highlighted TOU, Real Time Price (RTP) and demand bidding as part of DR programs. In [17], Menniti et al. referred to demand bidding for an energy coalition as a DR program. [16] and [17] stated DR programs that refer to the proper classification of DR in this proposal because all of these program are based on a control action from the consumer side.

Due to the confusion about the use of DR and DSM terms in the literature, DR and DSM should be distinguished from each other. In this proposal, DSM is defined as an agreement between the utility and a customer to curtail load during an emergency with an incentive to lower the energy price for participating customers. Load in this case is utility-controlled and customers do not influence the utility's decision of load curtailment. DR is defined, in this proposal, as the change in electricity consumption, which is decided by the consumer, due to a change in energy price. Customers in this case can decide the amount of load they want to shed based on the current price of electricity and the available financial incentive. In this work, RTPDR is a type of DR that describes a load that can change its power consumption in response to a change in the RTP of electricity, which is the main focus of this research.

In the literature, several papers discussed industrial sector participation in the context of DSM. Other papers discussed DR implementation in the residential sector. However, only few papers discussed DR implementation in the industrial sector.

Several papers have discussed DR benefits, DR wide-implementation issues, and electricity market performance in presence of DR [6], [18], [19], [20], [21]. In [6], Torriti et al. highlighted

the new trend of involving commercial and residential customers in DR. They stated the factors that inhibit the advancement of DR which are the limited knowledge about energy saving capacities, high cost estimate of DR infrastructure, focus on liberalizing the market rather than creating policies to promote DR, and uncertainty of DR performance. The paper claims that policy support for DR is expected, especially with the introduction of smart meters in various European countries. It also highlights the lack of financial incentives to promote DR. In [18], Kirschen showed that DR benefits consumers who participate actively in the electricity market and helps the market to operate more efficiently. He also highlighted that the capital cost of DR deployment might be more than the potential savings if a storage facility is not present. In [19], Singh and J. Ostergaard highlighted some issues associated with DR implementation, especially customer acceptance. They also claim that DR is very valuable to markets relying on more renewable energy resources. In [20], Jidong et al. highlighted an issue of DR that causes high electricity prices to appear when generators are scheduled to minimize the total operating cost. The paper highlighted the need for an evaluation tool of the social benefits of DR. In [21], Yang and Chen discussed market performance in presence of DR and its effects on LMP. They also highlighted the need for studying local and global effects of DR in the electricity market. [6], [18], [19], [20], and [21] overviewed DR program and discussed issues associated with the wide-implementation and deployment of DR. These issues are customer acceptance, quantification of DR benefits to motivate participation, and the cost of DR deployment. A major contribution of this proposal is to quantify DR benefits. Industry is motivated by economics and RTPDR is expected to provide enough financial incentives to motivate industrial customers to accept DR deployment and participate in RTPDR program. An evaluation tool of RTPDR benefits for a large customer, an industrial facility, is suggested and effects of RTPDR in the future Saudi Grid is proposed. A design study for the major parameters that affect RTPDR implementation at the industrial facility is also proposed. The study will evaluate the expansion of the existing raw material storage system at the industrial facility based on a cost-benefit approach for the purpose of RTPDR implementation.

Table 1.2. Overview of DR Classification in the Literature

Reference	Load Variation	Reference	Proposal
Asano et al. [4]	Direct Load Control	DR	DSM
Mohagheghi & Raji [5]		DR	
Saele and Grande [7]		DR	
Lu [8]		DSM	
Wang et al. [9]		DR	
Han et al. [10]		DR	
Tang et al. [15]		DR	
Albadi and El-Saadany [12]		DR	
Torriti et al. [6]	Interruptible Loads	DR	DSM
Han et al. [10]		DR	
Albadi and El-Saadany [12]		DR	
DOE [14]		DR	
Lu [8]	Indirect Load Control	DSM	DR
Wang et al. [9]		DR	
Conchado and Linares [13]		DR	
Han et al. [10]	TOU	DR	DR
Kuroda et al. [11]		DR	
Albadi and El-Saadany [12]		DR	
Hammerstrom et al. [16]		DR	
Han et al. [10]	Dynamic Price	DR	DR
Tang et al. [15]	Real Time Price	DR	DR
Kuroda et al. [11]		DR	
Albadi and El-Saadany [12]		DR	
DOE [14]		DR	
Hammerstrom et al. [16]		DR	

Albadi and El-Saadany [12] Hammerstrom et al. [16] Menniti et al. [17]	Demand Bidding	DR DR DR	DR
Kuroda et al. [11] Albadi and El-Saadany [12]	CPP	DR DR	DR
Kuroda et al. [11] Albadi and El-Saadany [12] Conchado and Linares [13]	Emergency DR	DR DR DR	DSM

Most papers in the literature deals with residential and commercial DR implementation [16], [9], [11], [7], [8], [22], [4]. In [16], Hammerstrom et al. implemented RTPDR in a utility distribution feeder that experiences frequent overloads for the purpose of controlling load during peak period, successfully demonstrating some benefits of RTPDR. In [9], Wang et al. discussed the use of a residential load model for DR that can be implemented in a home Energy Management System (EMS). They suggest incorporating the home EMS into a multi-agent system to quantify the effects and benefits of DR from various aspects. In [11], an evaluation tool for DR programs is presented by Kuroda et al. to extract the benefits of peak load reduction in the residential sector. In [7], Saele and Grande highlighted the potential of cost-effective DR in the presence of automatic meter reading projects. They also claim that an automated DR can achieve flexibility in demand and create a stable response over time. In [8], Lu demonstrated that a 6 MW HVAC load can provide 24 hours of load following or regulation services. She discussed a DSM tool for residential and commercial customers, which can be used for load balancing purposes. In [22], the authors suggested to model DR by utilizing consumer behavior modeling, which uses price elasticity matrices that take consumer rationality into account. In [4], Asano et al. claim that DR can be technically feasible if communication infrastructure is present. A field experiment to control lighting and air conditioning in an office space in Tokyo was conducted using two control strategies that resulted in 10% and 23% reduction in load respectively. The paper emphasized that DR implementation in a market is dependent on customer acceptance. It also highlighted the need for automated DR in a grid with a high penetration of stochastic resources. [4], [7], [8], and [22] discussed DSM for commercial and

residential customers. They highlighted issues associated with DSM implementation which are customer acceptance and automation of DSM. In [8], the author showed that DR can be used for regulation service which is a different application of DR benefits that is not discussed in this proposal. In this proposal, industrial customer participation is a function of the profit obtained from implementing DR. The facility's response is determined by an algorithm based on the expected RTP of electricity which is an automated process. In [16, 9, 11], the authors implemented DR in the residential sector which is different from implementing DR in the industrial sector. DR in the industrial sector involves an associated cost for load reduction and requires compliance with process constraints, which affects profit obtained from DR implementation. In [22], the authors solved the optimization problem for energy settlement in a microgrid system that involves demand bidding. In this proposal, an optimization problem that aims to maximize an industrial facility's profit is modelled and discussed.

Few papers have discussed the quantification of DR benefits [23], [10], [5]. In [23], Kowli and Gross used a statistical model to simulate a large system for planning and policy analysis and to quantify the benefits of DR on an electricity market. In [10], Han et al. used a statistical tool, Support Vector Machine regression algorithm (SVMSA), to create a DR model in order to quantify DR characteristics such as quantity, speed, and load recovery time, etc. The model was analyzed on a TOU program, which demonstrated a significant reduction in peak load. In [5], an intelligent system, fuzzy logic, is proposed to implement a DR program in an industrial site. The system consists of three actions; the first action ensures compliance with the plant constraints; the second action determines candidate load for reduction based on a priority list; and the last action performs an economic analysis for the DR action. While [23] proposed a method to quantify DR benefits, it focused in the load curtailment effects of DR resources in the electricity market for system planning analysis. The accuracy of the model in [10] depends on the proper selection of input attributes for the model which might differ from one application to another. The analysis in [10, 23] lacks quantification of DR benefits, especially financial incentives that motivates consumers to participate in DR programs. The fuzzy system discussed in [5] is burdensome and might be subjective, especially for the classification and creation of priority lists. The financial evaluation module details are not provided. Numerical results and solution time were not reported. Solution time is expected to be longer than a similar size problem since it involves solving three different problems. Hence, it might not suit large-scale implementation.

The authors in [15] discussed the implementation of DR in the industrial sector. In [15], Tang et al. studied the possibility of implementing DR in two types of equipment; medium frequency induction and electrolytic bath machines. The paper suggested an appropriate DR program for each type of equipment based on its operational characteristics and equipment flexibility to change its power consumption. The electrolytic bath machine was found to take long time for adjustment as well as having limited range for power reduction. The medium frequency induction machine showed suitability for dynamic pricing and showed a reduction of around 20% in power consumption. While the paper discusses DR application in the industrial sector, it lacks the quantification of DR benefits for consumers who participate in DR programs. In this proposal, an industrial facility's profit is maximized by an algorithm that quantifies consumer benefit due to RTPDR implementation or loss due to the reduction of the production level, which is not addressed in [15].

DR and Demand Side Management (DSM) are used in technical papers interchangeably. In the literature, some papers used DR to refer to a load control by the utility. In [4], Asano et al. used DR to refer to load reduction by the utility, which is achieved by controlling air conditioning and lighting in an office space in Tokyo. In [5], Mohagheghi & Raji referred to DR as a demand-side management solution, which targets consumers, for the purpose of reducing or shifting load at a specified time for a specified duration. [4] and [5] referred to load reduction by the utility as DR. However, it is considered in this proposal as DSM because it is utility controlled.

1.2 SUMMARY AND RESEARCH DIRECTION

Most of the work in DR literature focuses in the residential sector while the industrial sector is mostly discussed from the utility side control perspective, which is a DSM application that is not covered in this work. Also, it was highlighted that DR in presence of Automatic Meter Reading (AMR) is technically feasible. In addition, several papers emphasized the need for quantifying DR effects and benefits, especially from the consumer side which is part of the contributions of this proposal. Several papers highlighted the main factors that inhibit wide implementation of DR in which customer acceptance is a key factor. Industry is motivated by profit and RTPDR is expected to provide enough financial incentives for industrial customers to participate in RTPDR program.

This proposal examines the feasibility of implementing RTPDR in an industrial facility, a gas process plant, which incurs a cost for changing its production level and has limited product storage. The economic feasibility of DR at the subject facility will be evaluated based on the benefits captured from implementing RTPDR. The proposed work will be conducted on a large industrial facility that has a peak load of 90 MW and owns a cogeneration facility, making it a good candidate for DR implementation. The formulation is suited for automated DR implementation since the optimization algorithm can make a decision about the plant's load level whenever it predicts or receives a real-time price signal. It is proposed to model multiple large responsive loads into a real test case, the Saudi Grid, for the purpose of quantifying the effects of RTPDR in the electrical system.

The application in this research differs from prior work by implementing profit maximization for an industrial facility that has a mix of generators and boilers, and experiences some process constraints. These constraints include storage capacity and process design constraints. Process design limits should be considered such as the minimum flow rate of raw material, which can cause process concerns [24, 25].

The outcome of this research is a RTPDR scheduling tool for a large industrial plant that maximizes its profit in presence of fluctuating RTP and an evaluation tool for the impact of a high penetration level of large RTPDR industrial loads in the Saudi Grid. It will be the first practical RTPDR to appear for an industrial facility with a detailed model that captures process and thermal constraints and dynamics. The research will study the effects of RTPDR on the plant's profit when the electrical system changes from a vertically integrated utility into an electricity market. A design study is introduced which will evaluate the impact of changing the size of the process facility's parameters on RTPDR implementation. The process facility under study and similar RTPDR loads will be connected to a proposed system, the Saudi Grid. The optimal scheduling algorithm will produce a demand curve for each RTPDR load over a possible range of RTP of electricity. The demand curve will be modelled as a dispatchable load for each RTPDR facility in the Saudi Grid DC Optimal Power Flow (OPF). The approximate captured benefits by the RTPDR load in presence of other responding loads can be quantified and evaluated. RTPDR effects on the electricity market performance and policy implementation can be evaluated by looking into the consumer surplus, generation profit, and change in social

welfare. Qualitative results of this work may influence the decision to move to an electricity market and the decision by the plant owner to Participate in a RTPDR program.

Chapter 2. OPTIMAL INSTANTANEOUS SCHEDULING OF A NATURAL GAS PROCESSING FACILITY WITH RTPDR

2.1 INTRODUCTION

This chapter formulates an instantaneous scheduling problem that is solved to find the demand curve of a large industrial load, a gas processing facility. The formulation in this chapter is implemented to test the feasibility and to explore the characteristics of a Real Time Price-based Demand Response (RTPDR) load. This will serve as the first step toward solving the complete RTPDR load scheduling problem.

A RTPDR optimal scheduling is based on reducing load during periods of high electricity price and increasing load during periods of low electricity price. Industrial facilities have a concentrated load in one place, which should have a low cost to control. Hence, industrial facilities could be motivated to participate in a demand response program.

This chapter analyzes a natural gas processing facility with significant generation capability, which can change its output fairly quickly, to explore the effects of RTPDR on the operation of the plant and its profit. The instantaneous scheduling problem is solved and results are discussed in this chapter. This work was published in [26].

2.2 CHOOSING A PLANT

Industrial facilities that own generation units are a good target for RTPDR. As Real Time Price (RTP) increases because of congestion in the electrical system or a shortage of supply, co-generation output can be increased to reduce facility demand or even supply power to the utility [27]. RTPDR may also affect an industrial facility's process to achieve reduction of load. Changing the co-generation system output impacts the amount of steam and electric power available for the process facility. Industrial facilities have the potential to increase their profits by adjusting their load in response to the RTP, motivating participation.

Many processes cannot change their output fast enough to be able to respond to the RTP of electricity. For example, an oil refinery has a long thermal time constant. As a result, it is

difficult to change the production rate of a refinery within a relatively short period of time. Hence, refineries are not good candidates for RTPDR implementation [28, 29]. Other process, however, can respond either because the process has a short thermal time constant or the facility owns cogeneration units that can be quickly rescheduled. A gas processing facility, for example, has a short thermal time constant compared to an oil refinery which makes it a good candidate for RTPDR implementation, especially if the facility owns an internal generation system.

The RTPDR analysis in this chapter have been tailored to a specific gas process plant but can be applied to similar industrial plants by incorporating process and generation constraints and limitations into the model which differs from one plant to another. In this chapter, an optimal scheduling algorithm for an industrial process facility is developed. The algorithm is distinguished by modeling design and process constraints for the gas processing plant, such as raw material storage capacity, minimum flow rate, and energy and steam requirements for the process plant.

2.3 System Description

The system under study is a natural gas facility, which converts raw materials into end products. It consists of two co-generation units with a total capacity of 310 MW of power and 1.5 MMlb/hr of steam at 400 psi and four boilers with a total steam capacity of 1.76 MMlb/hr at 400 psi, which is supplied to the process. The subject facility can supply up to 1,100 thousand Barrels per Day (MBD) of Natural Gas Liquid (NGL) products. The facility's power and steam demands at full capacity are 90 MW and 2.5 MMlb/hr respectively. The process steam supply was the controlling requirement for sizing the generation facility. The excess electric power was originally intended to be wheeled to a neighboring plant.

A cogeneration facility can operate either as electric-load or thermal-load following [30]. The plant under study operates its cogeneration facility in thermal-load following mode, which means that steam is the main product of the co-generation facility and electricity is a by-product.

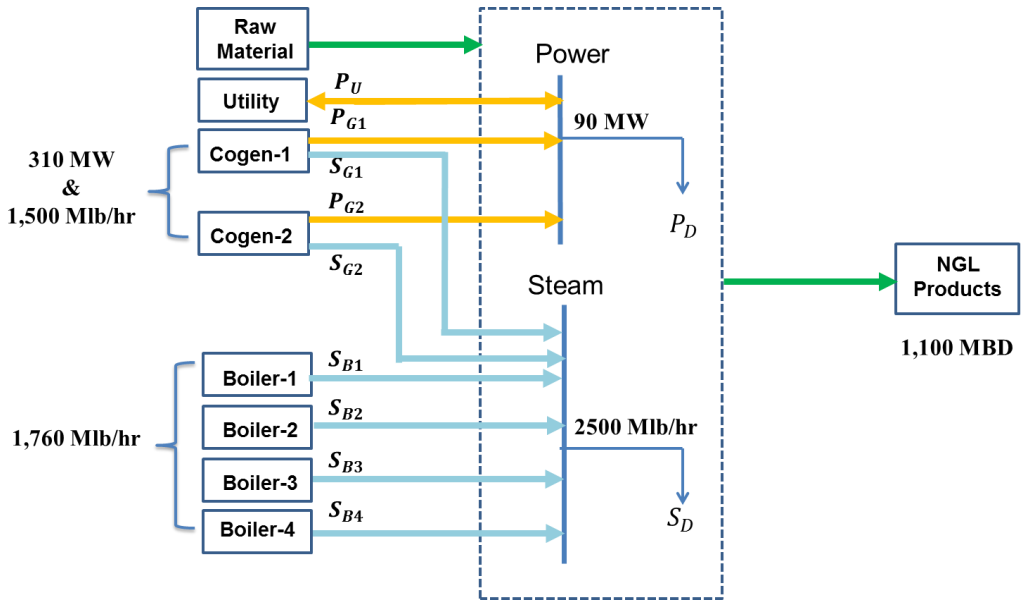

Figure 2.1. Block diagram of the process facility

2.4 PLANT ECONOMICS

The natural gas that comes from a gas well is the raw material for the gas processing facility and it consists of a mix of hydrocarbons. The mix for the plant under study consists of 40% Ethane, 30% Propane, 10% Butane, 10% Iso-Butane, and 10% Natural Gasoline. The processing facility separates these hydrocarbons and sells the different products. An indication of the profitability of an NGL process is referred to as "fractionation spread" (Frac Spread). The Frac Spread represents the value of each component minus the value of the raw material if it is not processed. Table 2.1 shows an example of calculating the frac spread for a process facility for a given price of raw materials and end-products. The price of one barrel of NGL products, which is the weighted average of the NGL content in one barrel of raw materials, is $36.92. The shrink per barrel, which is the value of the raw material before processing, is $15.00. Hence, the Frac Spread, which is the profit obtained from processing one barrel of raw materials, is $21.92.

A process plant can respond to the RTP of electricity for the purpose of maximizing its profit in two ways; partially, by changing the power output level of its co-generation system, or fully, by changing both the co-generation system power output and the production level of the process facility. When the Frac Spread is high, i.e. the natural gas price drops or the NGL products price rises, the optimization process should keep the process output high to capture the

benefit from high NGL prices. However, the optimum generation power output level is anticipated to vary as RTP fluctuates to maximize the process plant's profit. When frac spreads are low or near zero, the optimization process should limit the production level of the facility and also change the generation system power output to maximize the process plant's profit. Hence, the plant implements full RTPDR to capture the benefit from fluctuating RTP. In a few instances, when frac spreads are zero or negative, the optimizer might decide to shut down the processing plant and change only the generation system power output to maximize the processing plant's profit. Hence, co-generation ownership increases the flexibility of the process facility to implement a RTPDR program. It also provides an alternative source of income by selling power to the utility when it is not profitable to process NGL products.

Scenarios for selling NGL products are identified as high, low, and negative revenues. The expected process facility response that maximizes profit for each scenario is identified in Table 2.2.

The plant under study faces factors that may affect its profit beside the frac spread, such as government subsidies and transportation costs. Government subsidies come in the form of control of NGL product prices for local consumers. This affects the frac spread calculation because NGL products are sold at a discounted price to local consumers, which impacts the NGL prices in Table 2.1. In this work, transportation cost is ignored because of the proximity of the process plant to a seaport loading station. Because of the way the process facility operates due to government subsidies and imposed government regulations, the plant may experience low or even negative profits if it cannot reduce its production level during high RTP. The facility is also required to maintain a minimum production level at all times, which affects its profit. This constraint is discussed with more details in Chapter 3, which deals with a time-horizon scheduling of the process facility.

Table 2.1. Frac Spreads for a Typical NGL Process Facility

	Ethane	**Propane**	**Iso-Butane**	**N-Butane**	**Natural Gasoline**	**Composite**
Barrel composition	**40%**	**30%**	**10%**	**10%**	**10%**	**100%**
Price per Barrel	4.84	12.03	5.71	5.33	9.00	36.92
Shrink per Barrel	4.66	4.83	1.75	1.82	1.93	15.00
Margin per Barrel	0.18	7.20	3.96	3.51	7.07	**$21.92**

Table 2.2. Expected Effect of Frac Spread on RTPDR

Scenario	Frac Spread	Process Facility's Expected Response	Justification
Scenario-1	High	Partial RTPDR by the co-generation system, production at full-capacity all the time	Profit obtained from processing NGL products is very high even at a high RTP of electricity
Scenario-2	Low	Full RTPDR	At high RTP, profit obtained from selling energy to the utility might be higher than the profit obtained from processing NGL products
Scenario-3	Negative	Partial RTPDR by the co-generation system, process is shutdown	Processing NGL products results in a loss regardless of the RTP of electricity because Frac Spread in negative

Frac Spread varies with the market price of its content. On rare occasions, Frac Spread was observed to be negative such as in late 2005 and at the beginning of 2009. Frac Spread was also observed to be very low in late 2006 and at the beginning of 2007 [31]. The plant under study is mainly faced with low Frac Spread, so the analysis in this proposal will be carried based on scenario-2 of Table 2.2. An optimization problem to maximize instantaneous profit for a natural gas facility subject to RTP is formulated below.

2.5 Profit Maximization Problem Formulation for a Gas Processing Facility

Objective Function The objective is to maximize instantaneous profit for an NGL processing facility. Profit is revenue minus cost. Revenues are collected from processing NGL products and from selling power to the utility. Costs are incurred from purchasing power from the utility, and operating the co-generation units and boilers. Note that the cogeneration units produce both electric power and process steam while the boilers only produce process steam. The objective function is then:

$$\max_{V,P_g,u_g,S_b,u_b,P_u} \left\{ (Fs * V) - C(P_u) - \sum_{g=1}^{G} u_g * C_g(P_g) - \sum_{b=1}^{B} u_b * C_b(S_b) \right\} \quad (2.1)$$

where Fs is the frac spread obtained from selling one MB of NGL products, V is the production volume in MB/hr, P_u is the amount of power purchased from or sold to the utility in MW, p_u is the energy price in \$/MWh, $C(P_u)$ is the cost of purchasing from or selling power to the utility in \$/hr which is $P_u * p_u$, G is the total number of co-generation units at the natural gas facility, u_g is the status (on, off) of generator g, C_g is the cost function for generator g, the output power of co-generation unit g is P_g, B is the total number of boilers at the natural gas facility, u_b is the status (on, off) of boiler b, C_b is the cost function for boiler b, and the output steam of boiler b is S_b.

The solution to the profit maximization is a set of on and off outputs describing the generator status u_g for all the generators, and the boiler status u_b for all the boilers. The output power of each generator and the output steam of each boiler are problem variables of the optimal scheduling algorithm. Status variables u_g and u_b are integer variables while P_g and S_b are continuous. C_g's are not linear, but they can be easily linearized to permit a mixed integer linear programming (MILP) formulation. In Chapter 3, this work will be extended to include scheduling over a time-horizon. Testing MILP on small and medium size problems, in which optimal scheduling over a time-horizon is part of, showed the suitability of MILP to produce a global optimal solution with much less computational time compared to Lagrangian relaxation (LR) method [32]. Hence, MILP is adopted as a solution method for this work.

2.5.1 *System Constraints*

These constraints are related to how the power and steam systems operate. In this formulation, they include the power balance and steam balance constraints.

a) Electric Power Balance: The power generated by a co-generation unit P_g plus the power purchased from or sold to utility (P_u) must be equal to the power demand (P_D). Mathematically:

$$\sum_{g=1}^{G} P_g + P_u = P_D \quad \forall \ \ 1 \leq g \leq G \tag{2.2}$$

b) Steam Balance: The steam generated by co-generation units S_g plus the steam generated by boilers S_b must be greater than or equal to the steam demand S_D, assuming the excess steam can be vented, if needed, as exhaust heat. The steam balance constraint is then:

$$\sum_{g=1}^{G} S_g + \sum_{b=1}^{B} S_b \geq S_D \quad \forall \ \ 1 \leq g \leq G, 1 \leq b \leq B \tag{2.3}$$

2.5.2 *Thermal Generation Constraints:*

These constraints describe physical limits of the co-generation units which includes the upper and lower power output limits of the co-generation units.

a) Piecewise Linear Generator Cost Curves: a piecewise linear function is used to represent generator cost curves. Each break point in the linear function represents a change in the incremental cost of the generator. For Mixed Integer Linear Programming (MILP) implementation, the cost curve is linearized into three segments closely following the formulation in [33]. Mathematically:

$$C_g = NLC_g + \sum_{\boldsymbol{M_g}=1}^{3} MC_{g,\boldsymbol{M_g}} \cdot P_{g,\boldsymbol{M_g}} \quad \forall \ \ 1 \leq g \leq G \tag{2.4}$$

Where NLC_g is the no-load cost of generator g in \$/hr, $MC_{g,i}$ is the marginal cost of segment i of generator g in \$/MWh, and $P_{g,i}$ is the amount of power in segment i of generator g in MW.

Increasing the number of segments yielded a negligible change in results, specifically profit, and resulted in a solution time increase. Hence, three segments were determined to be an adequate trade-off between accuracy and efficiency. The output of generator g, then, becomes:

$$P_g = P_{g,1} + P_{g,2} + P_{g,3} \quad \forall \ 1 \leq g \leq G \tag{2.5}$$

b) Power Constraints: this constraint represents the minimum and maximum power output for each power segment of the linearized cost curve.

$$P_{g,min} \leq P_{g1} \leq P_{g,min} + \frac{P_{g,max} - P_{g,min}}{M_g} \quad \forall \ 1 \leq g \leq G \tag{2.6}$$

$$0 \leq P_{g,m} \leq \frac{P_{g,max} - P_{g,min}}{M_g} \quad \forall \ 1 \leq g \leq G, 2 \leq m \leq M_g \tag{2.7}$$

$$P_{g,min} \ \leq P_g \leq P_{g,max} \quad \forall \ 1 \leq g \leq G \tag{2.8}$$

Table 2.3. Generation Cost Curve Breakpoints

g	***NLC*** **($)**	***P1*** **(MW)**	***MC1*** **($/MWh)**	***P2*** **(MW)**	***MC2*** **($/MWh)**	***P3*** **(MW)**	***MC3*** **($/MWh)**
1	811.45	50	16.89	85	16.98	120	17.06
2	811.45	50	16.89	85	16.98	120	17.06

2.5.3 *Power and Steam Demand Constraints*

Representative operational data are used for the relationship between the volume of production and the power demand as well as the steam demand of the process facility.

a) Relationship between the power demand and production volume: motors and pumps represent 80% of the facility's electrical load. Hence, we expect the relationship between the production volume and power to be similar to a pump curve relationship which is represented as a quadratic function. Mathematically:

$$P_D(V) = a + b \cdot V + c \cdot V^2 \tag{2.9}$$

Equation (2.9) is linearized into a large number of segments (100) to reduce the artifact effects from the piece-wise linear approximation. This number of segments is found to be a reasonable trade-off between an accurate linear approximation and an acceptable computational time. Mathematically [33]:

$$P_D(V) = NLP + \sum_{i=1}^{100} MP_i \cdot V_i \tag{2.10}$$

where NLP is the no-load power of the process in MW, MP_i is the marginal power for segment i in MW/MB, and V_i is the volume of production in segment i in MB.

b) Relationship between the steam demand and production volume: The relationship between the steam demand and production volume is assumed to be linear. Mathematically:

$$S_D(V) = A_s \cdot V \tag{2.11}$$

2.5.4 *Co-generation System Power & Steam Relationship*

Data were obtained from generators' data sheets and from representative operational data. The relationship between the co-generation system power output and steam output is almost linear. Hence, a linear fit of the relationship between the power and steam is implemented. Mathematically:

$$S_g = A_{s,g} \cdot P_g + B_{s,g} \; \forall \; 1 \leq g \leq G \tag{2.12}$$

where $A_{s,g}$ is the slope of the fitted line which corresponds to the incremental process steam of generator g in Mlb/MW and $B_{s,g}$ is the intercept which corresponds to no-load steam of generator g in Mlb.

2.6 Simulation Results and Discussion

The simulation was conducted on a PC using the Xpress-IVE toolbox, version 1.21.2 [34]. The instantaneous optimal scheduling problem is relatively small in size; hence, the optimizer solved it almost instantaneously.

Three scenarios of operating the gas processing facility subject to changing RTP were identified and examined: the base case scenario, the co-generation response scenario, and the full RTPDR scenario. In the base case, both production volume and cogeneration output are kept constant. Plant profit varies with electricity prices. In the cogeneration response case, production volume is kept constant but cogeneration system status and output is varied as electricity price varies. In the RTPDR case, cogeneration system status and output, boiler system status and output, and production volume vary as electricity price changes.

Simulation results of the co-generation power output, production level, and purchased power from the utility for a RTP range between \$5/MWh and \$350/MWh are shown in Figure 2.2, Figure 2.4 and Figure 2.5 respectively. Corresponding boilers and co-generation units' status are shown in Table II.

At low RTP, less than $5/MWh, purchasing power from the utility is more economical than running the co-generation system. However, the boiler and cogeneration systems operate in order to supply the required steam for the process facility to operate at full capacity. The cogeneration system operates at its minimum power output level of 50 MW for each unit.

At a RTP of $65/MWh, the revenue generated from selling NGL products is less than the revenue generated from selling power to the utility and the avoided cost of operating boiler-1. Hence, boiler-1 shuts down and the optimal production level declines slightly. At a RTP of $85/MWh, the revenue obtained from selling power to the utility and the avoided cost of operating the cheapest boiler, boiler-4, becomes higher than the revenue obtained from selling NGL products. As a result, boiler-4 shuts down and the production level decreases as seen in Figure 2.2. The steam requirement at this production level can be supplied by the co-generation system steam supply without running additional boilers.

Note that the marginal power for each unit of volume (MB) changes as volume changes. As a result, purchased power from the utility at each level changes accordingly which affects the total cost of producing one MB of NGL products. This explains the gradual decline in production level that is seen in Figure 2.2.

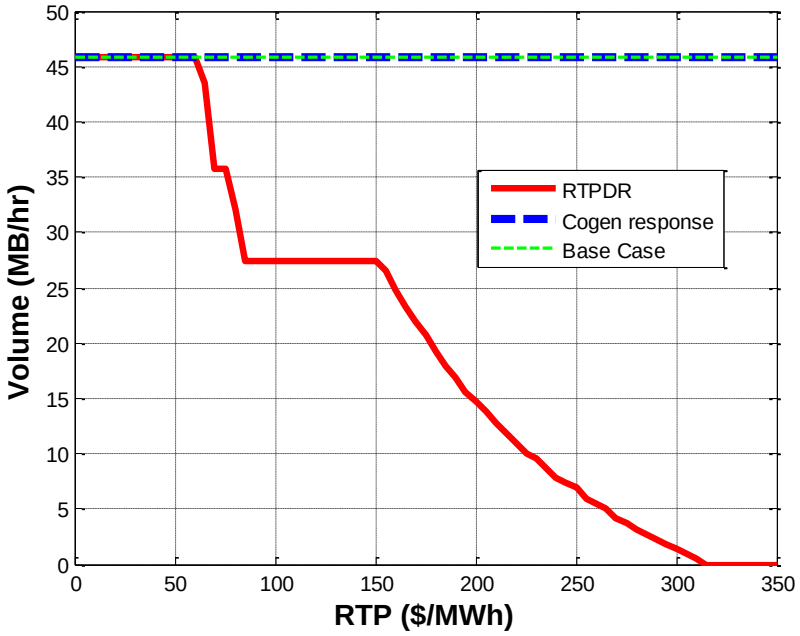

Figure 2.2. Production level of the process facility at different RTP.

Table 2.4. Equipment Status at Critical Production Levels (1: ON, 0: OFF)

Utility Price ($)	Production Level (MBD)	Status					
		G1	G2	B1	B2	B3	B4
0	45.83	1	1	1	1	1	1
5	45.83	0	1	1	1	1	1
10	45.83	1	1	1	0	1	1
65	43.54	1	1	0	0	1	1
70	35.82	1	1	0	0	0	1
85	27.48	1	1	0	0	0	0

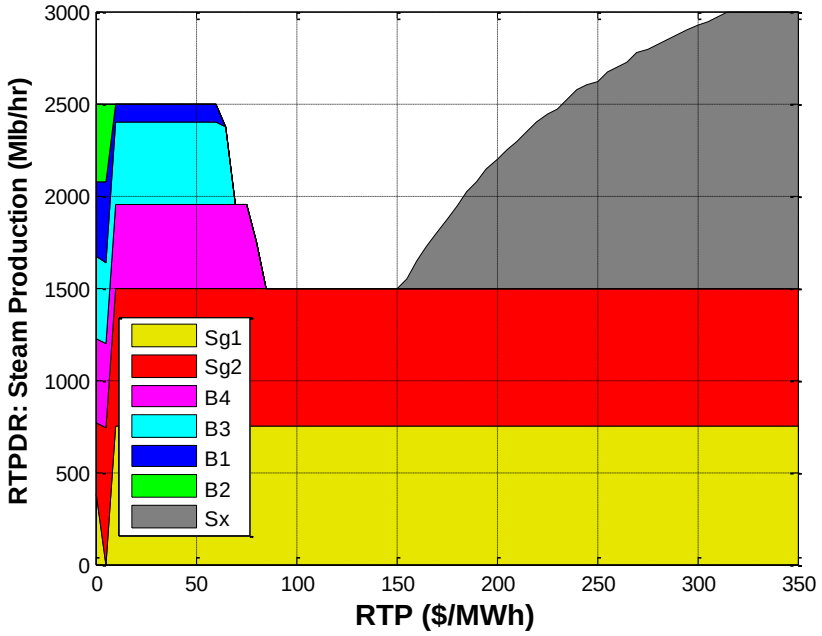

Figure 2.3. Steam production of the process facility at different RTP.

At a RTP of $155/MWh, the production level declines gradually until the plant shuts down completely at a price of $315/MWh. This allows the cogeneration system to export all its power to the utility to generate higher revenues. Note that the production level declines at a price of $155 because the marginal revenue generated from selling power to the utility is higher than the marginal revenue generated from selling NGL products, even if exhaust heat (S_x) is vented, as seen in Figure 2.3.

It is interesting to note that the production level that maximizes the facility's profit is not always the maximum allowed capacity. This result illustrates how RTPDR changes the intuitive solution of producing at full capacity to maximize profit for the process facility. The reason is

that the revenue obtained from selling NGL products can be less than the revenue obtained from selling power to the utility, especially at high RTP.

Figure 2.4 demonstrates the demand curves for different scenarios. The cogeneration response and RTPDR curves show price elasticity of the process facility. At low RTP, the process facility exports 10 MW to the utility. At a RTP of $5/MW, the process facility export power increases to 62.31 MW due to the change of the power output level of cogeneration unit-1 as seen in Figure 2.5. At a RTP of $10/MW, the process facility power export increases to 220 MW and the cogeneration system operates at full capacity. The extra excess electric power is sold to the utility to generate more revenue for the process facility. The abrupt shift in the cogeneration system production level and export to the utility occurs because the incremental cost of producing power from the cogeneration system at this price is less than the combined cost of purchasing power from the utility and running boiler-2 to supply the needed steam for the process facility. The process power demand starts declining at a RTP of $65/MW until it reaches 46.33 MW at a price of $85/MWh as a direct result of the production level adjustment in response to RTP. Exported power increases gradually from 265.5 MW at a price of $155/MWh to the maximum export power of 305 MW at a price of $315/MWh when the plant shuts down completely as seen in Figure 2.4. Note that a positive value represents import from the utility and a negative value represents export to the utility. In the cogeneration response scenario, the process facility always produces at full capacity and the production level is not changed.

Running the co-generation system is less economical than purchasing power from the utility at low RTP, less than $5/MWh but the cogeneration system operates at its minimum production level as seen in Figure 2.5 and Figure 2.6 to supply the required steam to process raw materials at full capacity. Also, at this RTP, the process facility has to export 10MW of power to the utility. At a RTP of $5/MWh, it is more economical to run only one generator at 152.31MW, co-generation unit-2, to supply the required steam for the process and export the remaining power of 62.31 MW to the utility. This is because the cost of running co-generation unit-2 is less than the cost of purchasing power from the utility in addition to the avoided cost of running co-generation

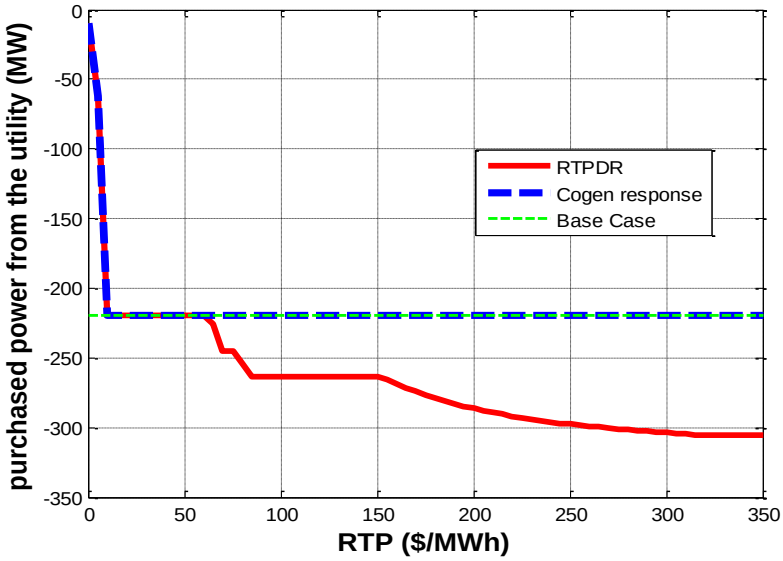

Figure 2.4. Demand curve for the process facility at different RTP

unit-1. The co-generation system operates at full capacity at a RTP of $10/MWh as seen in Figure 2.5 and Figure 2.6. The abrupt shift in generation is experienced because the incremental cost of gas turbines becomes lower than the incremental cost of purchasing power from the utility in addition to the avoided cost of running boiler B-2 which results in a rapid shift of co-generation unit-1 output from off to full capacity.

In the co-generation response scenario, the co-generation system initially produces power at the minimum production capacity even though the marginal cost of cogeneration power is higher than the utility price. The reason for running the cogeneration system at that price is to supply the needed steam to run the gas facility at the required full capacity.

In the full RTPDR scenario, the process facility's profit is $6,380/hr at a RTP of $5/MWh, and it increases at a slow pace as RTP increases. This is higher than the profit of $4,750 obtained from the base case scenario. However, at a RTP of $15/MWh, the RTPDR profit starts increasing rapidly as seen in Figure 2.7. The incremental cost of the co-generation system at that price is lower than the incremental cost of purchasing power from the utility. Hence, the process facility's profit comes from two sources: selling NGL products and selling power to the utility. Hence, the plant's profit increases as RTP increases due to exporting power to the utility, as seen in Figure 2.7. At a RTP of $65/MWh, the full RTPDR scenario profit is higher than the co-generation response scenario profit. At that price, the profit obtained from selling power to the utility is higher than the profit obtained from selling NGL products. The full RTPDR scenario

has the flexibility to adjust the plant's production level to maximize the process facility's profit.

A small profit for the process facility in the full RTPDR and co-generation response scenarios is observed at low RTP because of the over-sized co-generation system at the process facility. In some instances, when there is a high demand for steam, the process facility is forced to start the co-generation system and sell the excess power to the utility at a price that is lower than its production cost. Also, it is worth mentioning that the plant's benefit from implementing RTPDR for the process facility is analyzed by considering only the profit obtained from processing NGL products at the discounted product price, which is controlled by government regulations for local consumers.

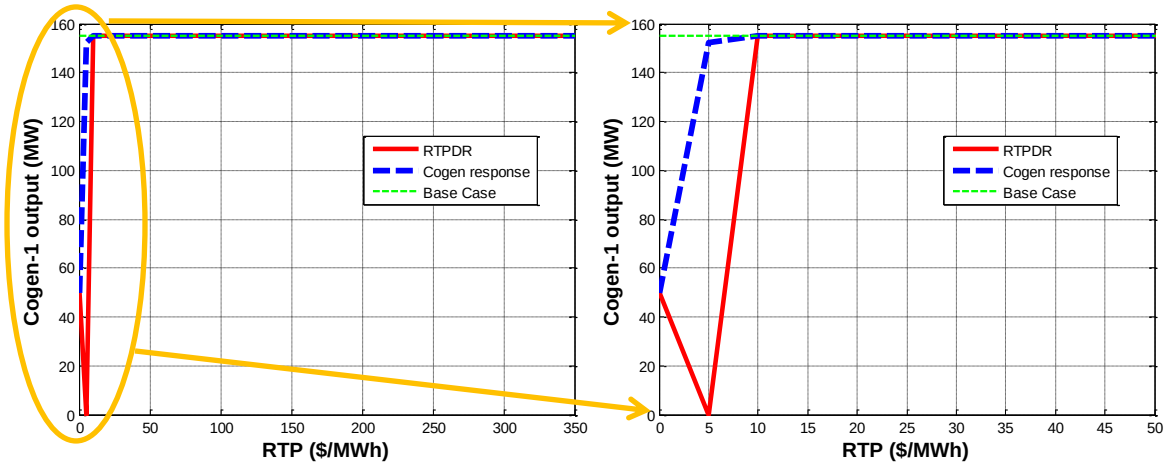

Figure 2.5. Co-generation unit-1 power output at different RTP

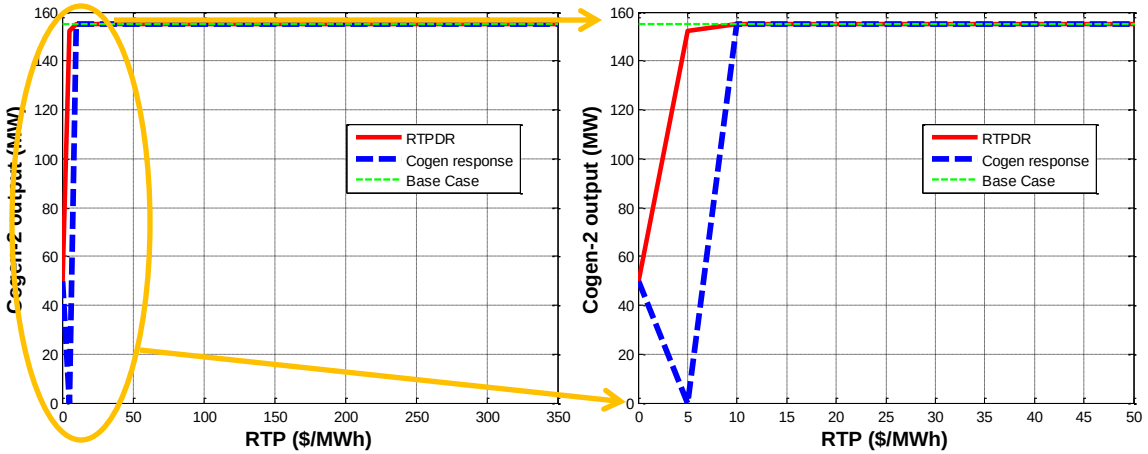

Figure 2.6. Co-generation unit-2 power output at different RTP

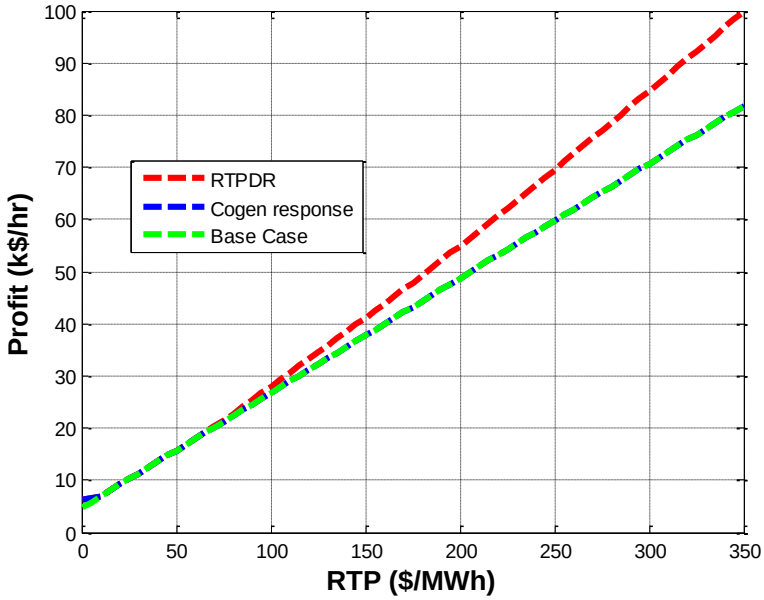

Figure 2.7. The gas facility's profit at different RTP

2.7 Proposed Sensitivity Analysis to the Natural Gas Price

In Saudi Arabia, more than 60% of generators are fueled by natural gas [35]. Hence, it is expected to observe a high correlation between electricity price and natural gas price after complete deregulation of electricity sector in Saudi Arabia. Hence, it is of interest to the facility's owner as well as the system operator to evaluate the effect of fluctuating gas price on both the plant's schedule as well as the utility's scheduled generation since most of the current utility's generators are thermal generators.

It is proposed to study a range of gas prices which reflects two gas pricing schemes: the subsidized gas price and the unsubsidized gas price. Note that the price of gas affects the cost curve of generators as well as the revenue obtained by the process facility, which is reflected in the frac spread calculation. This analysis is discussed with details in Chapter 3.

2.8 Conclusion

A gas processing facility can maximize its profit by implementing a RTPDR program that interacts with the RTP of electricity. This allows the gas facility to select the optimum production level that maximizes profit and decide whether or not to purchase power from or sell power to the utility. Initial results suggest that shutting down the production system completely

and selling power to the grid at a high RTP is more profitable than processing NGL products, although electricity prices high enough to shut down production are not frequently encountered in current electricity markets.

Simulation of the process facility's model indicates that the solution method in this chapter does not work for negative RTP of electricity, which can appear when transmission system congestion is in effect or when market subsidy is offered. Therefore, the scheduling problem is reformulated to accommodate the chosen solution method, which is discussed with details in Chapter 3.

It is evident from the preliminary work that RTPDR can be implemented successfully in a gas processing facility to increase its profit. In the next chapter, this work will be extended to an optimization over a time horizon to provide a more practical schedule. The time-series optimization algorithm will include detailed process constraints such as storage capacity, flow rate constraints, and contractual constraints. The algorithm will also be expanded to model generation and process transition constraints and startup times against a predicted electricity price time-series. The new formulation is similar to expanding an economic dispatch (ED) to a unit commitment (UC) problem.

Chapter 3. TIME-HORIZON SCHEDULING OF A NATURAL GAS PROCESSING FACILITY WITH RTPDR

Chapter 2 demonstrated that a RTPDR program can be successfully implemented in a simple gas processing facility that interacts with an instantaneous RTP of electricity to schedule its optimal production level, co-generation unit status and output level, and boiler unit status and output level. In this chapter, the model is extended to carry the optimization over a time horizon in order to include the effects of time-dependent constraints and provide a more practical schedule. This is due to the use of a better model that incorporates the process and thermal component dynamics at the gas processing facility. In this chapter, a problem formulation that maximizes profit for a large consumer, an industrial facility, that has a mix of generators and boilers in addition to process and flow constraints over a time horizon is proposed and developed. Implementation and testing of the proposed formulation are part of this chapter's contributions.

In order to model the dynamics of the process system at a gas processing facility more accurately, process constraints that limit the facility's ability to respond to the RTP of electricity need to be considered. These constraints include contractual, storage capacity, and flow rate constraints. At the process facility under study, local customers have their own storage system for the process facility's end-products. Hence, an end-product storage limitation does not currently present a concern.

Optimization over a time-horizon requires more parameters and constraints in addition to keeping track of time for each variable. For example, startup time for generators and boilers should be considered. Also, equipment constraints such as minimum up-time, minimum down-time, ramp-up, and ramp-down constraints should also be part of this model.

When considering solution methods for the time-horizon process facility scheduling problem to maximize profit, the facility's generation and process systems are expected to change as the RTP of electricity changes. The nature of these changes resembles the process of a unit commitment (UC). UC is an optimization algorithm whose objective is typically to schedule generation startups and shutdowns to minimize the total operating cost of the utility. Several papers have discussed optimal scheduling of generators and UC implementation. UC can be formulated to minimize the operating cost of generation companies (GENCOs), maximize

GENCOs payout, or maximize GENCOs profit. For example, in [36], cost minimization was introduced to solve a UC problem with wind and energy storage. In [32], the authors solved a priced-based UC with the objective of maximizing payoff for a GENCO that owns a given generation mix.

Although time-horizon optimization is a larger problem compared to instantaneous scheduling, it is similar to but smaller in dimensionality than a typical utility UC. There are examples in the literature for utilities with similar size problems that were solved with MIP. For example, the authors in [36] have solved a UC that consists of 10 generators for a period of one year using a MIP formulation. In [32], the authors have used MILP to solve the scheduling problem for a small, medium, and large system. In the large system, a modified IEEE 118-bus system that has a generation mix of 76 units was presented. It was demonstrated that MILP can reach a more accurate solution compared to a LR-based approach in the expense of computational time. However, testing small and medium size problems, in which optimal scheduling over a time-horizon is part of, showed the suitability of MILP to produce a global optimal solution with much less computational time. Hence, MILP is a good candidate method for solving the gas facility's scheduling problem and is adopted as a solution method for the formulation proposed in this chapter.

This chapter develops an optimal scheduling algorithm for a natural gas processing facility that has significant generation capabilities and can change its production level fairly quickly. The purpose of the algorithm is to explore the effects of implementing a RTPDR program on the operation of the gas processing facility and its profit. The algorithm in this chapter is distinguished from other work in this area by modeling the process dynamics of the gas processing facility. The algorithm also models the incoming raw material storage capacity, generation limits, boilers limits, and energy and steam requirements for the process facility over a time-horizon. The DR analyses in this work have been tailored to a specific process facility but can be applied to similar industrial facilities if process limitations are modeled properly.

3.1 SAUDI GRID LOAD & PRICE PROFILE

The effects of a RTPDR program on a process facility's schedule and its profit can only be analyzed if data for the RTP of electricity are available. Currently, the Saudi Grid tariff structure is a fixed pricing scheme of $32/MWh while the benefits of a RTPDR program are derived from

the volatility of the RTP of electricity. Hence, a mechanism that approximates the expected RTP profile in the Saudi Grid is needed.

The average concentration of industrial and large commercial loads in ERCOT system is observed to be similar to the concentration of industrial and commercial load in the Saudi Grid [37, 38]. Hence, load profile of the ERCOT system is expected to be close to the load profile in the Eastern and Central provinces of the Saudi Grid. Figure 3.1 compares the weather profile between Houston, TX and Manama, Bahrain that is the closest city, which has a published historical weather data, to the Eastern region of the Saudi Grid where the process facility is located, that has a published historical weather data. There is a small difference in temperature between Bahrain and Houston, TX as seen in Figure 3.1. This might result in using more air conditioning units for cooling which consumes more energy. The Generation mix differs between the Saudi Grid and ERCOT, mainly due to the high penetration of renewable resources in the ERCOT system. However, ERCOT data is here considered to be the closest published data to the Saudi Grid, due to the close match of load profile and weather data between the two areas [37, 38]. Hence, the use of ERCOT load data to extract the expected RTP profile for the Saudi Grid is adopted in this analysis because electrical load and price are found to be strongly correlated [39, 40, 41].

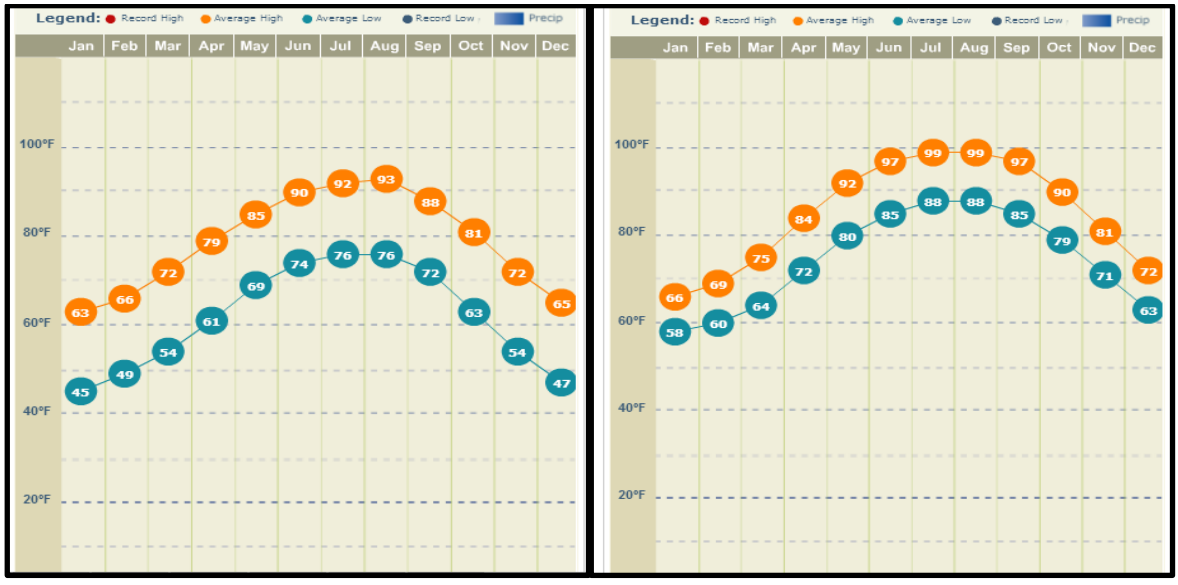

Figure 3.1. Weather profile for Houston, TX (left) and Dammam, Saudi Arabia (right) [42, 43]

Scaled historical load data from the ERCOT system are used in the single-bus DCOPF model of the Saudi Grid. While the single-bus DCOPF model produces similar results to an Economic Dispatch (ED) study, it has been selected for several reasons. One reason is that the single-bus model can be expanded to a multiple-bus model that represents the synthesized Saudi Grid. Another reason is that the utility practice in Saudi Arabia is to run its generation based on a priority list that considers different factors such as season, efficiency, criticality, and availability of fuel, which is difficult to accommodate in a UC study. A DCOPF tool that can be customized to model the Saudi Grid and its dispatchable loads is also available and publically accessible.

The scaling factor was calculated using the ratio between the peak loads of the two systems. Simulation of the DCOPF model determines the RTP of electricity for each load data at time step t. Load data of Houston area between 1/1/2012 and 12/31/2012 is used in this work to develop the load profile for the Saudi Grid. The developed generators cost data for the Saudi Grid, which reflects the fuel subsidy, were used in the DCOPF model. Hence, the closest possible electricity price profile for the Saudi Grid is developed, which is needed for testing and analyzing different scenarios for the price-responsive facility's schedule; the base case, the cogeneration-response case, and the RTPDR case.

The Saudi Grid price profile is extracted from the DCOPF model using two cases; the subsidized fuel case and the unsubsidized fuel case. A comparison between the fixed price, the subsidized fuel, and the unsubsidized fuel cases is listed in Table 3.1. A graphical representation of the load and price profile for different cases is shown in Figure 3.2 and Figure 3.3 respectively. The initial assumption is that the plant is too small for its response to affect the system price.

Table 3.1. Comparison between the Fixed Price, Subsidized Fuel, and Unsubsidized Fuel Cases

Case	Fixed Price	Subsidized Fuel	Unsubsidized Fuel
Average Price ($/MWh)	32	6.23	23.42
Highest Price ($/MWh)	32	4.43	14.00
Lowest Price ($/MWh)	32	34.88	110.66
σ	0	0.86	4.83

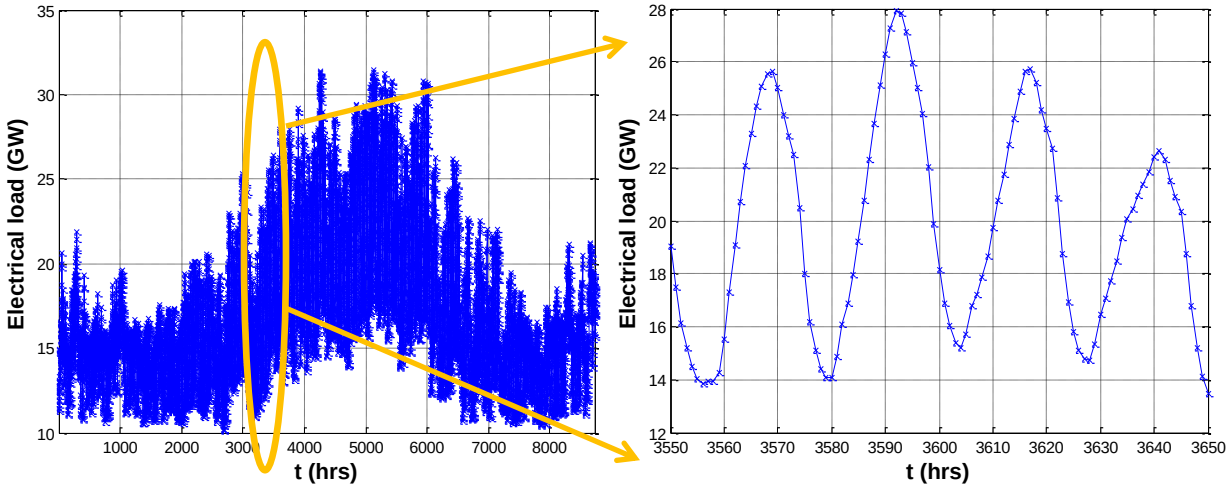

Figure 3.2. Load profile of the Saudi Grid

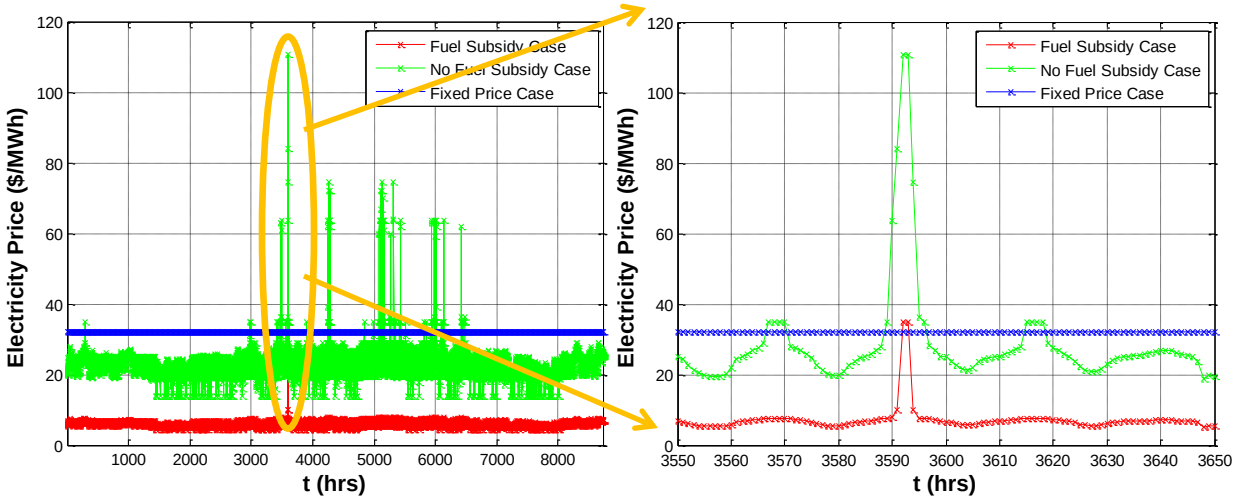

Figure 3.3. Comparison of the price profile between the fixed price, subsidized fuel, and unsubsidized fuel cases

3.2 Profit Maximization for a Gas Processing Facility over a Time-Horizon

An optimization problem to maximize the profit for a natural gas processing facility that faces fluctuating RTPs over a time-horizon is formulated below.

Objective Function The objective of this formulation is to maximize the profit for a NGL processing facility over a time horizon *T*. Profit is defined as the sum over the time horizon of plant production times the Frac Spread (the value increase of the product) less the raw material

loss during processing, minus the cost of the utility power, generator costs and boiler costs, including startup costs for generators, boilers, and the process facility. Revenues are collected from processing NGL products and from selling power to the utility. The problem is to find the values of the process system production level $\dot{v}_t$, process system status $u_{\dot{v}}$, generation units power output P_g, generation units status u_g, boiler units steam output S_b, and boiler units status u_b that maximizes the facility's profit over a time horizon T.

The objective function is divided into three components which are the process system revenue, the energy revenue, and the cost of operation as seen in (3.1), (3.2), and (3.3) respectively. These components are formulated as follows:

$$\text{Process Revenue} = \sum_{t=1}^{T} \left(Fs * \dot{v}_{o,t} - (1-k) * \dot{v}_t * C_{raw}\right) \quad \forall\ 1 \le t \le T \tag{3.1}$$

$$\text{Energy Revenue} = \sum_{t=1}^{T} -P_{u,t} * p_{u,t} \quad \forall\ 1 \le t \le T \tag{3.2}$$

$$\text{Operational Cost} = \text{Generation Cost} + \text{Boiler Cost} + \text{Startup Cost} \tag{3.3}$$

$$\text{Generation Cost} = \sum_{t=1}^{T} \sum_{g=1}^{G} u_{g,t} * C_g\left(P_{g,t}\right) \quad \forall\ \ 1 \le g \le G, 1 \le t \le T \tag{3.4}$$

$$\text{Boiler Cost} = \sum_{t=1}^{T} \sum_{b=1}^{B} u_{b,t} * C_b\left(S_{b,t}\right) \quad \forall\ \ 1 \le b \le B, 1 \le t \le T \tag{3.5}$$

The cost function $C_g\left(P_{g,t}\right)$ is not linear, which is linearized similar to [33]. The cost function $C_b\left(S_{b,t}\right)$ is linear. Due to the operational philosophy of the process facility, boilers are kept operational at all times. Hence, the boilers startup status $u_{b,t}$ becomes one at all times. Hence, the new cost functions formulation become:

$$C_{g,t}\left(P_{g,t}\right) = NLC_g + \sum_{i=1}^{3} MC_{g,i} \cdot P_{g,i,t} \quad \forall\ 1 \le g \le G, 1 \le t \le T \tag{3.4a}$$

$$C_b(S_{b,t}) = A_{s,b} \cdot S_{b,t} + B_{s,b} \qquad \forall \ \ 1 \le b \le B, 1 \le t \le T \qquad (3.5a)$$

Substituting (3.4a) in (3.4) and (3.5a) in (3.5) yields:

$$\text{Generation Cost} = \sum_{t=1}^{T}\sum_{g=1}^{G}(u_{g,t} \cdot NLC_g + \sum_{M_g=1}^{3} MC_{g,M_g} \cdot P_{g,M_g,t}) \qquad \forall\ 1 \le g \le G, 1 \le t \le T \qquad (3.4b)$$

$$\text{Boiler Cost} = \sum_{t=1}^{T}\sum_{b=1}^{B} A_{s,b} \cdot S_{b,t} + B_{s,b} \qquad \forall \ \ 1 \le b \le B, 1 \le t \le T \qquad (3.5b)$$

The startup cost consists of the start-up cost of generation units and the start-up cost of the process system for every time step t. Due to the operational philosophy of the process facility, boilers are not allowed to shut-down. Hence, the boilers startup cost is ignored in this discussion. Hence, the startup cost becomes:

$$\text{Startup Cost} = \sum_{t=1}^{T}\sum_{g=1}^{G} CSU_{g,t} + CSU_{\dot{v},t} \qquad \forall \ \ 1 \le b \le B, 1 \le t \le T \qquad (3.6)$$

The objective function, then, becomes:

$$\max_{\dot{v}_t, u_{\dot{v}}, P_g, u_g, S_b, u_b} \left\{ \sum_{t=1}^{T} \left(\left(Fs * \dot{v}_{o,t} - (1-k) * \dot{v}_t * C_{raw}\right) - \left[P_{u,t} * p_{u,t} + \sum_{g=1}^{G} u_{g,t} * C_g(P_{g,t}) + \sum_{b=1}^{B} u_{b,t} * C_b(S_{b,t}) + \sum_{g=1}^{G} CSU_{g,t} \cdot su_{g,t} + CSU_{\dot{v},t} \cdot su_{\dot{v},t} \right] \right) \right\} \qquad (3.7)$$

where Fs is the Frac Spread obtained from selling one MB of NGL products, $\dot{v}_{o,t}$ is the end product flow rate in MB/hr, k is the process system shrinkage factor, $\dot{v}_t$ is the input material flow

rate in MB/hr, C_{raw} is raw material cost in $/MB, $P_{u,t}$ is the amount of power purchased from or sold to the utility at time step *t* in MW, $p_{u,t}$ is the predicted real-time price of energy at time step *t* in $/MWh, *G* is the total number of co-generation units at the gas processing facility, $u_{g,t}$ is the status (on, off) of generator g at time step *t*, C_g is the cost function for generator g, the output power of co-generation unit g at time step *t* is $P_{g,t}$, *B* is the total number of boilers at the gas processing facility, $u_{b,g}$ is the status (on, off) of boiler *b* at time step *t*, C_b is the cost function for boiler *b*, and the output steam of boiler *b* at time step *t* is $S_{b,t}$, the startup cost of generator g is CSU_g, and $su_{g,t}$ is a binary variable that indicates the startup of generator g at time step *t*, the startup cost of the process system is $CSU_{\dot{v},t}$, and $su_{\dot{v},t}$ is a binary variable that indicates the startup of the process system at time step *t*.

The solution to the profit maximization is a set of values of on and off variables describing the generator status $u_{g,t}$ for all the generators, and the boiler status $u_{b,t}$ for all the boilers, the process system status $u_{\dot{v},t}$ for all time steps in the time horizon *T*. The output power of each generator, the steam output of each boiler, and the production level of the process system are also produced by the plant scheduling algorithm.

3.2.1 *System and Thermal Generation Constraints*

These constraints were discussed in Chapter 2. In this chapter, they are modified to include a time horizon dimension as follows:

a) Power Balance:

$$\sum_{g=1}^{G} P_{g,t} + P_{u,t} = P_{D,t} \qquad \forall \;\; 1 \le g \le G, 1 \le t \le T \qquad (3.8)$$

b) Steam Balance:

$$\sum_{g=1}^{G} S_{g,t} + \sum_{b=1}^{B} S_{b,t} \ge S_{D,t} \;\; \forall \;\; 1 \le g \le G, 1 \le b \le B, 1 \le t \le T \qquad (3.9)$$

c) Piecewise Linear Generator Cost Curve:

$$P_{g,t} = P_{g,1,t} + P_{g,2,t} + P_{g,3,t} \qquad \forall \ \ 1 \le g \le G, 1 \le t \le T \tag{3.10}$$

d) Power Constraints:

$$P_{g,min} \le P_{g,1,t} \le P_{g,min} + \frac{P_{g,max} - P_{g,min}}{M_g} \qquad \forall \ \ 1 \le g \le G, 1 \le t \le T \tag{3.11}$$

$$0 \le P_{g,m,t} \le \frac{P_{g,max} - P_{g,min}}{M_g} \qquad \forall \ \ 1 \le g \le G, 2 \le m \le M_g, 1 \le t \le T \tag{3.12}$$

$$P_{g,t} \ge u_{g,t} \cdot P_{g,min} \qquad \forall \ \ 1 \le g \le G, 1 \le t \le T \tag{3.13}$$

$$P_{g,t} \le u_{g,t} \cdot P_{g,max} \qquad \forall \ \ 1 \le g \le G, 1 \le t \le T \tag{3.14}$$

3.2.2 *Cogeneration System Dynamic Constraints*

a) Ramp Rate Constraints:

The power output of generators does not change instantly. The maximum rate that the power output of a generator can change is mathematically expressed as:

$$P_{g,t} - P_{g,t-1} \le RU_g \qquad \forall \ \ 1 \le g \le G, 2 \le t \le T \tag{3.15}$$

$$P_{g,1} - P_{g,ini} \le RU_g \qquad \forall \ \ 1 \le g \le G, t = 1 \tag{3.16}$$

$$P_{g,t} - P_{g,t-1} \ge -RD_g \qquad \forall \ \ 1 \le g \le G, 2 \le t \le T \tag{3.17}$$

$$P_{g,1} - P_{g,ini} \ge -RD_g \qquad \forall \ \ 1 \le g \le G, t = 1 \tag{3.18}$$

where RU_g is the ramp rate up limit (MW/h) of generator g, and RD_g is the ramp rate down limit (MW/h) of generator g, and $P_{g,ini}$ is the initial power output of generator g.

b) Startup Cost:

The available plant data does not support a detailed startup cost model, a simplified model is used in this work. First the detailed model is developed, then, the simplification is explained.

The value of the startup cost depends on the startup status and the last time the unit is shut down. A detailed startup cost of a thermal generator is modeled using an exponential function [27] that depends on the thermal time constant and the startup cost of generator g which are formulated in (3.19). The exponential function comes from the input fuel that is burned to compensate for the cool down effect that is characterized as an exponential curve from Newton's law of cooling. The startup cost is then:

$$K_{g,t} = \left[\kappa_g - \rho_g \left(1 - e^{\frac{t_g^{off}}{\zeta_g}}\right)\right] \quad \forall\, 1 \le g \le G, 1 \le t \le T \tag{3.19}$$

Where κ_g is the fixed cost of starting-up generator g, ρ_g is the cold start fuel cost of generator g, ζ_g is the thermal time constant of generator g, t_g^{off} is the number of hours that a generator g has been off up to time period *t-1*.

The startup cost can be discretized into hourly periods which can be represented as a stair-wise function that becomes more accurate as the number of interval increases. Also, the initial status for each generator is assumed to be known and is denoted as IS_g. The MIP formulation for the startup cost is [44]:

$$CSU_{g,t} \ge \begin{cases} K_{g,t-IS_g} \cdot \left(u_{g,t} - \sum_{n=1}^{t} u_{g,t-n}\right) \ \forall\, 1 \le g \le G, 1 \le t \le T, IS_g < 0 \\ K_{g,t} \cdot \left(u_{g,t} - \sum_{n=1}^{t} u_{g,t-n}\right) \quad \forall\, 1 \le g \le G, 1 \le t \le T, IS_g > 0 \end{cases} \tag{3.20}$$

$$CSU_{g,t} \ge 0 \qquad \forall\, 1 \le g \le G, 1 \le t \le T \tag{3.21}$$

A MILP formulation is used to take advantage of binary variables and the exponential characteristic of the startup cost. Table 3.2 illustrates different scenarios for the startup cost of (3.20) evaluated at *t=4* for a unit that is initially *ON*. The startup constraints for generator *g* are as follows:

Table 3.2. A Generator Startup Cost Constraint Example

$t = 4$					
$\boldsymbol{u_{g,ini}}$	$\boldsymbol{u_{g,1}}$	$\boldsymbol{u_{g,2}}$	$\boldsymbol{u_{g,3}}$	$\boldsymbol{u_{g,4}}$	$\boldsymbol{CSU_{g,4}}$
1	0	0	0	1	$K_{g,3}$
1	1	0	0	1	$K_{g,2}$
1	1	1	0	1	$K_{g,1}$
1	1	1	1	1	0
1	1	1	1	0	0
1	0	0	1	1	0
1	0	1	0	1	$K_{g,1}$

$$CSU_{g,4} \geq K_{g,1}\left(u_{g,4} - \sum_{n=1}^{1} u_{g,4-n}\right)$$

$$CSU_{g,4} \geq K_{g,2}\left(u_{g,4} - \sum_{n=1}^{2} u_{g,4-n}\right)$$

$$CSU_{g,4} \geq K_{g,3}\left(u_{g,4} - \sum_{n=1}^{3} u_{g,4-n}\right)$$

$$CSU_{g,4} \geq 0$$

Note that generation units' data that are needed for the detailed startup cost formulation such as the cold start-up cost and the thermal time constant are not publically available, so the dynamic start-up cost is not considered in this work. Should data become available in the future, the formulation in this section can be used to improve the accuracy of the process facility's model. Hence, a fixed start-up cost is used in this work and the

selection is justified by the turbine type that is used in the industrial facility under study, which is a gas turbine. The start-up time for a gas turbine unit is on the order of 10 minutes, which makes the impact of the simplification of the start-up cost very small and hence negligible in this work. The start-up cost, then, is formulated using (3.21) in addition to the following [36]:

$$su_{g,t} - \ sd_{g,t} \ = \ u_{g,t} - u_{g,t-1} \ \ \forall \ 1 \le g \le G, 2 \le t \le T \tag{3.22}$$

$$su_{g,t} - \ sd_{g,t} \ = \ u_{g,t} - u_{g,ini} \ \ \forall \ t = 1 \tag{3.23}$$

$$su_{g,t} + \ sd_{g,t} \ \le \ 1 \qquad \forall \ 1 \le g \le G, 1 \le t \le T \tag{3.24}$$

$$CSU_{g,t} = \ su_{g,t} \cdot \kappa_g \qquad \forall \ 1 \le t \le T \tag{3.25}$$

c) Minimum Up/down Time Constraint:

The minimum down time reflects the time needed to start up a generator while the minimum up time is related to a generation unit's thermal stress. These constraints represent machine limits for startup and shutdown times which are represented as follows [45]:

$$UT_{g,ini} = 0, if \ u_{g,ini} = 0 \ \ \forall \ 1 \le g \le G \tag{3.26}$$

$$DT_{g,ini} = 0, if \ u_{g,ini} = 1 \ \ \forall \ 1 \le g \le G \tag{3.27}$$

$$L_g^{up} = max\left\{0, min\{T, \left(MUT_g - UT_{g,ini}\right) \cdot u_{g,ini} \}\right\} \tag{3.28}$$

$$L_g^{down} = max\left\{0, min\{T, \left(MDT_g - DT_{g,ini}\right) \cdot \left(1 - u_{g,ini}\right) \}\right\} \tag{3.29}$$

$$u_{g,t} = u_{g,ini} \quad \forall \ \ g \le G, t \le L_g^{up} + L_g^{down} \tag{3.30}$$

$$\sum_{tt=t-MUT_g+1}^{t} su_{g,tt} \le u_{g,t} \ \ \forall \ \ t > \ L_g^{up} \tag{3.31}$$

$$\sum_{tt=t-MDT_g+1}^{t} sd_{g,tt} \leq 1 - u_{g,t} \;\; \forall \;\; t > L_g^{down} \tag{3.32}$$

The enforcement of the minimum up time and minimum down time constraints in (3.26)-(3.32) is illustrated in Table 3.3 and Table 3.4. (3.26) and (3.27) are used to reset the initial condition for the up-time/down-time respectively. For example, if a unit is shut down, then the initial condition resets the initial up-time to zero. (3.28)-(3.30) enforces the minimum up-time/down-time constraints in the presence of an initial condition $UT_{g,ini}/\ DT_{g,ini}$. Examples of how (3.28)-(3.30) work are illustrated in Table 3.3 and Table 3.4 respectively. (3.31) & (3.32) enforces the minimum up-time/down-time beyond the initial enforcement period. These constraints do not allow the unit status $u_{g,t}$ to change till the minimum up-time/down-time is met. For example, if a unit starts up, then it will not be allowed to shut down till the minimum up-time is met, as per (3.31). An example of this constraint is illustrated in Table 3.5.

If the initial generation unit status is one and the unit has been in operation for two hours prior to the study period, then L_g^{up} calculates the remaining enforcement period as seen in Table 3.3, case-1. As per (3.29), L_g^{down} is forced to be zero. Hence, the unit has to be in operation for additional three hours to satisfy the minimum up-time of the generation unit, as per (3.30). In case-2 of Table 3.3, if the initial condition meets the *MUT* requirement, then no enforcement is needed for the up-time constraint. In case-3, if the initial condition exceeds the *MUT* requirement, L_g^{up} becomes zero as per (3.28). Similar analysis is conducted for the *MDT* and results are tabulated in Table 3.4. Table 3.5 shows the enforcement of the *MUT* for any period beyond the initial enforcement period. If a generation unit starts up at *t=2*, then the left hand side of (3.31) becomes one. As a result, the generation unit status is forced to be one till *t=6*, which satisfies the *MUT* requirement.

Table 3.3. A Minimum Uptime Constraint Example ($MUT = 5$)

Case	$u_{g,ini}$	$UT_{g,ini}$	L_g^{up}	L_g^{down}	$u_{g,t}$	$L_g^{up} + L_g^{down}$
1	1	2	3	0	1	3
2	1	5	0	0	1	0
3	1	7	0	0	1	0

Table 3.4. A Minimum Downtime Constraint Example (*MDT = 4*)

Case	$u_{g,ini}$	$UT_{g,ini}$	L_g^{up}	L_g^{down}	$u_{g,t}$	$L_g^{up} + L_g^{down}$
1	0	2	0	2	0	2
2	0	4	0	0	0	0
3	0	7	0	0	0	0

Table 3.5. Enforcement of the Minimum Uptime ($t = 6, MUT = 5, su_{g,2} = 1$)

L_g^{up}	$t - MUT_g + 1$	t	$u_{g,2}$	$u_{g,3}$	$u_{g,4}$	u_{g5}	$u_{g,6}$	$u_{g,7}$
3	2	6	1	1	1	1	1	0*

*$u_{g,7}$ can be either zero or one

3.2.3 *Boiler Constraints*

a) Steam Constraints:

$$S_{b,t} \geq S_{b,min} \qquad \forall \;\; 1 \leq b \leq B, 1 \leq t \leq T \tag{3.33}$$

$$S_{b,t} \leq S_{b,max} \qquad \forall \;\; 1 \leq b \leq B, 1 \leq t \leq T \tag{3.34}$$

b) Ramp Rate Constraints:

The steam output of boilers does not change instantly. The maximum rate that the steam output of a boiler can change is mathematically expressed as:

$$S_{b,t} - S_{b,t-1} \leq RU_b \qquad \forall \;\; 1 \leq b \leq B, 2 \leq t \leq T \tag{3.35}$$

$$S_{b,1} - S_{b,ini} \leq RU_b \qquad \forall \;\; 1 \leq b \leq B, t = 1 \tag{3.36}$$

$$S_{b,t} - S_{b,t-1} \geq -RD_b \qquad \forall \;\; 1 \leq b \leq B, 2 \leq t \leq T \tag{3.37}$$

$$S_{b,1} - S_{b,ini} \geq -RD_b \qquad \forall \;\; 1 \leq b \leq B, t = 1 \tag{3.38}$$

where RU_b is the ramp rate up limit (Mlb/h) of boiler b, and RD_b is the ramp rate down limit (Mlb/h) of boiler b, $S_{b,ini}$ is the initial steam output of boiler b.

Note that boilers at the process facility under study operate on a "banking" mode for reliability purposes. Hence, boiler status $u_{b,t}$ for all boilers in the process facility is forced

to be one at all times. As a result, the minimum up and down times for boilers are not considered in this simulation. The start-up cost formulation is also ignored in this case. However, if the facility's operational philosophy changes, the start-up cost for boilers can be formulated similar to (3.22)-(3.25). The minimum up and down time constraints for boilers can also be formulated similar to (3.26)-(3.32).

3.2.4 *Power and Steam Demand Constraints*

a) Power Demand Constraint:

The relationship between the demand power and production level is quadratic as discussed in Chapter 2. The relationship was initially linearized similar to Chapter 2 with the inclusion of a time dimension as follows:

$$P_{D,t}\left(\dot{v}_t\right) = NLP + \sum_{M_{\dot{v}}=1}^{100} MP_{M_{\dot{v}}} \cdot \dot{v}_{M_{\dot{v}},t} \;\; \forall \;\; 1 \le t \le T, \;\; 1 \le M_{\dot{v}} \le 100 \qquad (3.39)$$

$$\dot{v}_t = \sum_{M_{\dot{v}}=1}^{100} \dot{v}_{M_{\dot{v}},t} \quad \forall \;\; 1 \le t \le T, \;\; 1 \le M_{\dot{v}} \le 100 \qquad (3.40)$$

Simulation of the process facility's model indicates that the formulation in (3.39) does not work for negative RTP of electricity. The electricity market may experience negative prices due to a high penetration level of renewables in the presence of a market subsidy or even when transmission system congestion is in effect. The future Saudi Market is not expected to provide a renewable energy subsidy in the near future. However, with the rapid growth of the Saudi Grid electrical load, the Saudi Grid may experience transmission congestion in the near future, especially at the low voltage level transmission lines. Hence, negative RTPs might appear in the future Saudi market, which is discussed with details in Chapter 5 for a three-bus test case.

When the convex cost function of generators is linearized, the piece-wise linear approximation consists of several segments with rising slope, e.g. rising marginal cost, for each filled power segment. Similarly, when the convex power demand function is linearized, the piece-wise function consists of several segments with rising slope, e.g. rising marginal power, for each filled processed material flow rate segment, $\dot{v}_{i,t}$. The plant

scheduling algorithm maximizes the process facility profit by reducing the total cost of operation. The formulation in (3.39) assumes a monotonic relationship between the power demand and cost of operation. When the RTP of electricity is positive, then increasing the power demand increases the total cost of operation, which follows the assumption for the formulation in (3.39). When a negative RTP of electricity is considered, then the process facility is rewarded for consuming more energy. In this case, increasing the power demand reduces the total cost of operation, which violates the assumption for the formulation in (3.39). Hence, a different linearization technique that mitigates the issue of negative RTPs of electricity is, then, formulated as follows [36, 46]:

$$BP_1 = \dot{v}_{min} \qquad \forall \quad M_{\dot{v}} = 1 \tag{3.41}$$

$$BP_{M_{\dot{v}}} = BP_{M_{\dot{v}}-1} + \frac{\dot{v}_{max} - \dot{v}_{min}}{100} \qquad \forall \quad 2 \le M_{\dot{v}} \le 100 \tag{3.42}$$

$$P_{D,t}(\dot{v}_t) = \sum_{M_{\dot{v}}=1}^{100} P(BP_{M_{\dot{v}}}) \cdot Z_{M_{\dot{v},t}} \qquad \forall \quad 1 \le t \le T, \quad 1 \le M_{\dot{v}} \le 100 \tag{3.43}$$

$$\dot{v}_t = \sum_{M_{\dot{v}}=1}^{100} BP_{M_{\dot{v}}} \cdot Z_{M_{\dot{v},t}} \qquad \forall \quad 1 \le t \le T, \quad 1 \le M_{\dot{v}} \le 100 \tag{3.44}$$

Additional constraints are introduced to enforce only one active volume segment at a time for each time step t [36, 46]. These constraints were modified to allow the process system to shut down, if decided by the optimizer. The constraints, then, are:

$$\sum_{M_{\dot{v}}=1}^{99} Y_{M_{\dot{v}},t} = 1 \cdot u_{\dot{v},t} \qquad \forall \quad 1 \le t \le T, \quad 1 \le M_{\dot{v}} \le 99 \tag{3.45}$$

$$\sum_{M_{\dot{v}}=1}^{100} Z_{M_{\dot{v}},t} = 1 \cdot u_{\dot{v},t} \qquad \forall \quad 1 \le t \le T, \quad 1 \le M_{\dot{v}} \le 100 \tag{3.46}$$

$$Y_{100,t} = 0 \qquad \forall \quad 1 \le t \le T \tag{3.47}$$

$$Z_{M_{\dot{v}},t} \le Y_{M_{\dot{v}},t} \qquad \forall \quad 1 \le t \le T, M_{\dot{v}} = 1 \tag{3.48}$$

$$Z_{M_{\dot{v}},t} \leq \ Y_{M_{\dot{v}}-1,t} \ + \ Y_{M_{\dot{v}},t} \qquad \forall \ \ 1 \leq t \leq T, \ \ 2 \leq M_{\dot{v}} \leq 100 \qquad (3.49)$$

b) Steam Demand Constraint:

The relationship between steam demand and production level is linear as discussed in Chapter 2. The relationship is formulated as follows:

$$S_{D,t} = A_s \cdot \dot{v}_t \quad \forall \ \ 1 \leq t \leq T \qquad (3.50)$$

c) Co-generation System Power & Steam Relationship:

$$S_{g,t} = A_{sg} \cdot P_{g,t} + u_{g,t} \cdot B_{sg} \quad \forall \ \ 1 \leq g \leq G, 1 \leq t \leq T \qquad (3.51)$$

3.2.5 *Transmission System Constraints*

These constraints represent the maximum amount of power that can be imported from or exported to the utility. These constraints are formulated as follows:

$$PU_t \leq TL_{max} \qquad \forall \quad 1 \leq t \leq T \qquad (3.52)$$

$$PU_t \geq -TL_{max} \qquad \forall \quad 1 \leq t \leq T \qquad (3.53)$$

3.2.6 *Process System Dynamic Constraints*

These constraints describe the process flow and transition in more details within the planning horizon *T*.

a) Material Balance Constraint:

The raw materials entering the process system plus the raw materials entering the storage tank must equal the incoming raw materials entering the gas processing facility for each time step *t* in the scheduling time horizon.

$$\dot{v}_t + \dot{v}_{s,t} \ = \ \dot{v}_{in,t} \qquad \forall \ \ 1 \leq t \leq T \qquad (3.54)$$

Where $\dot{v}_t$ is the flow rate of raw material entering the process system in MB/hr, $\dot{v}_{s,t}$ is the flow rate of raw material entering the storage tank in MB/hr, $\dot{v}_{in,t}$ is the flow rate of raw material entering the gas processing facility in MB/hr, for every time step *t*.

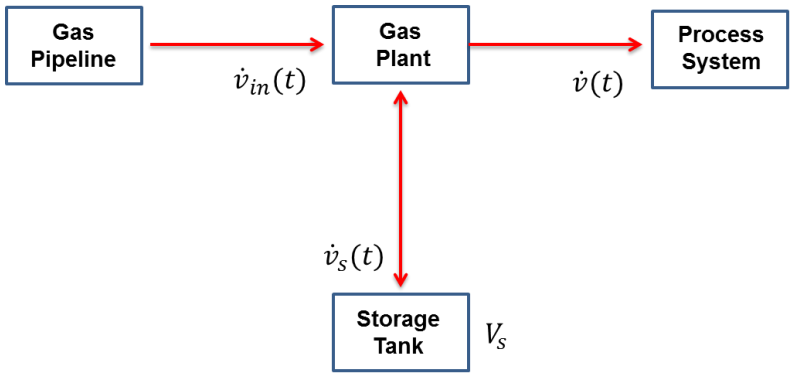

Figure 3.4. Block diagram of the process flow.

b) Total Production constraint:

The amount of processed volume at time step *t* is the sum of the processed volume at time step *t-1* in addition to the flow rate of raw materials entering the process system at time step *t*. The initial volume V_{ini} is assumed to be zero.

$$V_1 = V_{ini} + \dot{v}_1 \qquad \forall \quad t = 1 \tag{3.55}$$

$$V_t = V_{t-1} + \dot{v}_t \qquad \forall \quad 2 \leq t \leq T \tag{3.56}$$

Where V_{ini} is the processed volume at the beginning of the study period in MB, V_t is the amount of processed volume at time step *t* in MB, V_{t-1} is the amount of processed volume in the previous time step in MB, and $\dot{v}_t$ is the flow rate of raw material entering the process system in MB/hr, for every time step *t*.

c) Storage capacity constraint:

Storage capacity of the process facility can be treated similar to hydro scheduling without the complexity of the energy storage process.

Incoming raw material storage: a typical gas processing facility has storage tanks that are capable of storing $V_{s,max}$ of incoming raw materials. For a typical planning study, the initial storage tank level is assumed to be known to be $V_{s,ini}$. The assumption of a half-full tank at the end of the planning period mitigates horizon effects beyond the study horizon. Hence, the storage capacity constraints can be expressed as follows:

$$V_{s,1} = V_{s,ini} + \dot{v}_{in,1} - \dot{v}_1 \qquad \forall \quad t = 1 \tag{3.57}$$

$$V_{s,t} = V_{s,t-1} + \dot{v}_{in,t} - \dot{v}_t \qquad \forall \quad 2 \le t \le T \tag{3.58}$$

$$0 \le V_{s,t} \le V_{s,max} \qquad \forall \ 1 \le t \le T \tag{3.59}$$

$$V_{s,T} = 0.5 \cdot V_{s,max} \tag{3.60}$$

Where $V_{s,t}$ is the amount of raw materials in the storage tank at time step *t* in MB, $V_{s,max}$ is the maximum storage capacity of the gas processing facility in MB, $V_{s,ini}$ is the initial amount of raw materials in the storage tank in MB, $V_{s,T}$ is the amount of raw materials in the storage tank at the end of the study horizon in MB.

End-product Storage: at the process facility under study, local customers have their own storage system for the end products. Hence, an end-product storage constraint is not formulated in this work.

d) Relationship between input and output Volume:

The end-product volume is less than the incoming raw materials volume due to the process system loss and the transformation of the raw material from gas into liquid. Hence, the input raw material flow rate and the end-product flow rate are directly related by the shrinkage factor, which is expressed as follows:

$$\dot{v}_{o,t} = k \cdot \dot{v}_t \qquad \forall \ 1 \le t \le T \tag{3.61}$$

where k is the shrinkage factor which represents the ratio of the input volume to the produced volume. In this work, k is assumed to be 0.99. Note that the shrinkage factor does not account for a reduction in the raw material, natural gas, due to its use in the operation of the process system of the RTPDR facility. The portion of the raw material that is used as a fuel for the process system is already accounted for in the cost part of the objective function.

e) Contractual constraint:

The gas processing facility under study has short-term and long-term contracts to supply a specific amount of NGL products within a specific time frame. The facility under study has contracted $V_{T,min}$ end-products with its local and international customers. The contracted volume is assumed to be delivered within the contracted time frame to avoid

any contract violation penalty. The production volume at the beginning of the time-horizon, V_{ini}, is assumed to be zero. Also, the process facility cannot produce more than its production capacity at any time step *t* within the time-horizon schedule. The subject facility has both long-term, typically yearly, and short-term, typically weekly contracts. The long-term contracts are incorporated into the contracted volume constraint at the end of the time-horizon schedule. Hence, the long-term constraint is formulated as the sum of the weekly target volumes. For the short-term contracts, the contractual constraint is enforced weekly. The contractual constraint can be fixed or adaptive constraint. An illustration about the different between a fixed and adaptive contractual constraint is presented in Figure 3.5. The fixed contractual constraint distributes the total contracted volume over the number of days of the study period equally regardless of the previous schedule results. However, the adaptive contractual constraint is dependent on the previous day schedule. Hence, the minimum allowed volume of production, daily target production level, in the current planning period is determined based on the produced volume in the previous day, the remaining number of days of the target week, and the weekly target volume. So, if the production level in the previous planning period was high, due to low RTP of electricity, then the contractual constraint is more relaxed in the current planning period. On the other hand, if the production level of the previous day is low, due to high RTP of electricity, then the contractual constraint becomes more binding in the current planning period, as seen in Figure 3.5.

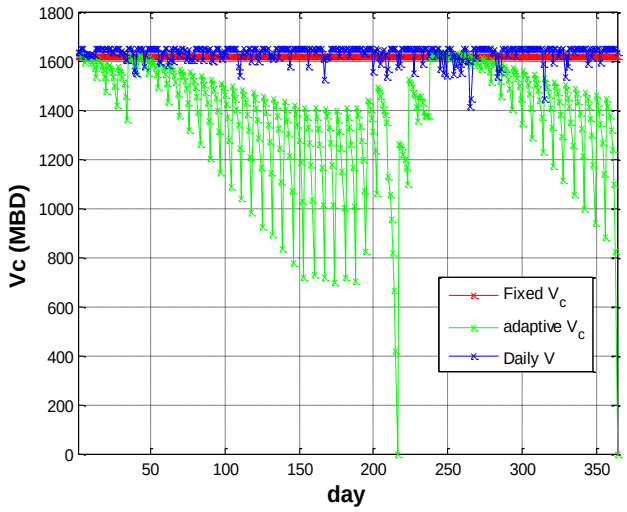

Figure 3.5. Comparison between the fixed and adaptive contractual constraints

Table 3.6. A Contractual Constraint Example

Case	Week	Day	$V_{W,t}$	$V_{tot,ini}$	N_d	R_{TH}	$V_{d,t}$
1	1	1	7,623	0	7	1.5	1,633.5
2	1	2	7,623	1,100	6	1.5	1,630.8
3	2	1	15,246	7,700	7	1.5	1,617.0

The contractual constraint is formulated to be flexible and adaptive. An example of the contractual constraint at different scenarios is shown in Table 3.6. Table 3.6 illustrates the idea of the adaptive contractual constraint. For example, the contractual constraint is relaxed in the second day of week-1 because the production level was high in the first day. The contractual constraint is, then, formulated as follows:

$$V_{tot,d} = V_{tot,d-1} + \sum_{t=1}^{24} \dot{v}_{o,t} \qquad \forall\ 2 \le d \le day, 1 \le t \le 24 \tag{3.62}$$

$$V_{tot,d} = V_{tot,ini} + \sum_{t=1}^{24} \dot{v}_{o,t} \qquad \forall\ d = 1, 1 \le t \le 24 \tag{3.63}$$

$$N_d = floor\left(1 + \frac{day}{7}\right) \cdot 7 - day + 1 \qquad \forall\ 1 \le t \le T, 1 \le d \le 364 \tag{3.64}$$

$$V_{c,target} = \frac{V_{1,t} - V_{tot,ini}}{N_d} * R_{TH} \qquad \forall\ 1 \le t \le T, d = 1, w = 1 \tag{3.65}$$

$$V_{c,target} = \frac{V_{w,t} - V_{tot,d-1}}{N_d} * R_{TH} \qquad \forall\ 1 \le t \le T, 2 \le d \le 363, \quad 1 \le w \le 51 \tag{3.66}$$

$$V_{c,target} = V_{52,t} - V_{tot,d-1}\ \forall\ 1 \le t \le T, d = 364,\ w = 52 \tag{3.67}$$

$$V_{c,target} \le \sum_{t=1}^{24} \dot{v}_{o,t} \qquad \forall\ 1 \le t \le 24, 1 \le d \le day \tag{3.68}$$

f) Process Ramp Rate Constraints:

The process facility under study is designed to change its production level fairly quickly. However, from historical operational data, the maximum ramp-up and ramp-down limits

of the process system were extracted from real operational data. These constraints are formulated similar to generator's ramp-up and ramp-down constraints in (3.15) - (3.18). These constraints, then, are:

$$\dot{v}_t - \dot{v}_{t-1} \leq RU_V \quad \forall \quad 2 \leq t \leq T \tag{3.69}$$

$$\dot{v}_1 - \dot{v}_{ini} \leq RU_V \quad \forall \quad t = 1 \tag{3.70}$$

$$\dot{v}_t - \dot{v}_{t-1} \geq -RD_V \quad \forall \quad 2 \leq t \leq T \tag{3.71}$$

$$\dot{v}_1 - \dot{v}_{ini} \geq -RD_V \quad \forall \quad t = 1 \tag{3.72}$$

g) Process System Raw Material Flow Rate Constraint:

Two scenarios are considered. The first one considers a continuous change of the incoming raw materials flow rate and the other one considers a limited change for the incoming raw materials flow rate.

Scenario-1: the flow rate of the raw material entering the process system $\dot{v}_t$ fluctuates over time. However, a typical gas processing facility is designed to have a minimum flow rate of 25% of the process system capacity for operational considerations [24, 25]. The constraint is, then, formulated as follows:

$$\dot{v}_t \geq 0.25 \cdot \dot{v}_{max} \quad \forall \ 1 \leq t \leq T \tag{3.73}$$

Where $\dot{v}_{max}$ is the maximum production flow rate in MB/hr.

Scenario-2: the flow rate of the raw material entering the process system $\dot{v}_t$ also fluctuates over time similar to scenario-1. However, it is not practical, from operation point of view, to change the flow rate of the incoming raw material continuously because of the needed extensive coordination, personnel, and change in operational status of related equipment which imposes higher operational and maintenance costs. Hence, the process facility is assumed to incur a startup cost when it is forced to shut down due to the drop of the flow rate of the raw material entering the process system below the minimum allowed design

limit. It is also assumed that any change between the minimum flow rate limit and the maximum design capacity incurs a small cost that is negligible in this work because the process system is designed to operate within these limits and the facility's personnel are trained to deal with flow rate fluctuations within the acceptable operational limits. Constraints for this scenario are discussed subsequently.

h) Minimum up/down time constraint:

When the process system starts up, there is a time delay and cost associated with running additional utilities to prepare the process system to receive the raw material again. The flow rate of the raw material entering the process system is a semi-continuous variable in which it can be either a zero or a value between 25% and 100% of its rated design capacity. Hence, it falls in the category of MIP formulation. Hence, the formulation in (3.74)-(3.80) is similar to the formulation of the minimum up/down time of thermal generators [45]. Even though the *MUT* for the process system is formulated in this work, the minimum up time constraint is not enforced in the process facility's scheduling algorithm for several reasons. One reason is that it is easier to adapt an existing formulation than developing a new formulation from scratch. Another reason is that the formulation in this work might be used for other industrial facilities that have different process dynamics. In this case, a minimum up time constraint might be needed when coordinating a facility's shutdown. The plant scheduling algorithm is small in dimensionality compared to a typical UC problem. Hence, the problem is not expected to suffer from a long computational time. Hence, the *MUT* value is set to one for the process facility under study.

The *MUT/MDT* constraints represent process system limits for startup and shutdown times which are similar to *MUT/MDT* of thermal generation in (3.26)-(3.32). These constraints are, then, formulated as follows:

$$UT_{\dot{v},ini} = 0, if\ u_{\dot{v},ini} = 0 \tag{3.74}$$

$$DT_{\dot{v},ini} = 0, if\ u_{\dot{v},ini} = 1 \tag{3.75}$$

$$L_{\dot{v}}^{up} = max\left\{0, min\{T, \left(MUT_{\dot{v}} - UT_{\dot{v},ini}\right) \cdot u_{\dot{v},ini}\}\right\} \tag{3.76}$$

$$L_{\dot{v}}^{down} = max\left\{0, min\{T, \left(MDT_{\dot{v}} - DT_{\dot{v},ini}\right) \cdot \left(1 - u_{\dot{v},ini}\right)\}\right\} \tag{3.77}$$

$$u_{\dot{v},t} = u_{\dot{v},ini} \quad \forall \quad t \leq L_{\dot{v}}^{up} + L_{\dot{v}}^{down} \tag{3.78}$$

$$\sum_{tt=t-MUT_{\dot{v}}+1}^{t} su_{\dot{v},tt} \leq u_{\dot{v},t} \ \forall \ \ t \geq \ \ L_{\dot{v}}^{up} \tag{3.79}$$

$$\sum_{tt=t-MDT_{\dot{v}}+1}^{t} sd_{\dot{v},tt} \leq 1 - u_{\dot{v},t} \ \forall \ \ t \geq \ \ L_{\dot{v}}^{down} \tag{3.80}$$

Note that the minimum down time considers the time needed to start up the process system while the minimum up time considers the time needed to coordinate the process system shut down, which is very short for the process facility under study. The current facility's operational philosophy is to have the process system on auxiliary load when the production level becomes zero to allow a fast restart for the process system when needed. Hence, any change in the production level of the process system is automated and $MUT_{\dot{v}}$ is, then, set to one. However, if the facility's operational philosophy changes in the future or a RTPDR program is implemented in a facility that requires coordination time before shutdown, then the $MUT_{\dot{v}}$ can be set to the appropriate value. The process system of the facility under study rarely shuts down, which makes the computational time impact of the added constraint very small and hence negligible.

i) Startup cost:

The value of the startup cost depends on the startup status and the last time the process system is shutdown. A detailed discussion about the startup cost for thermal generators is stated in section 3.2.2-b. The startup cost for the process system is chosen to be a fixed startup cost. The startup cost here considers the cost of running boilers and generators

until the process system begins delivering end-products. The startup cost also considers the cost of personnel who are needed to coordinate the process system startup procedure. The startup constraint is, then, formulated as follows:

$$su_{\dot{v},t} - sd_{\dot{v},t} = u_{\dot{v},t} - u_{\dot{v},ini} \quad \forall\ t = 1 \tag{3.81}$$

$$su_{\dot{v},t} - sd_{\dot{v},t} = u_{\dot{v},t} - u_{\dot{v},t-1} \quad \forall\ 2 \le t \le T \tag{3.82}$$

$$su_{\dot{v},t} + sd_{\dot{v},t} \le 1 \qquad \forall\ 1 \le t \le T \tag{3.83}$$

$$CSU_{\dot{v},t} = su_{\dot{v},t} \cdot \kappa_{\dot{v}} \quad \forall\ 1 \le t \le T \tag{3.84}$$

The formulation in (3.81)-(3.84) formulates the startup cost of the process system similar to the startup cost of thermal generators. The only difference is the inclusion of the cost of personnel involvement and process system preparation in the fixed startup cost of the process system. (3.82) formulates the detection of the startup status of the process system. The process system cannot startup and shutdown simultaneously, which is reflected in (3.83). (3.84) calculates the startup cost of the process system only if the process system is starting up. An example of how the startup constraint works is illustrated in Table 3.7. If the process system is *OFF*, then $su_{\dot{v},t}$ is forced to be zero as per (3.82). Hence, the startup cost is zero as per (3.84). If the process system is shutting-down, then $u_{\dot{v},t} - u_{\dot{v},t-1}$ becomes -1 which forces $su_{\dot{v},t}$ to be zero and $sd_{\dot{v},t}$ to be one, hence the start-up cost is zero as per (3.84). However, if the process system is in operation, then, the right hand side of (3.82) becomes zero. The left hand side of (3.82) can only be zero if both the $su_{\dot{v},t}$ and $sd_{\dot{v},t}$ are one or zero. $su_{\dot{v},t}$ and $sd_{\dot{v},t}$ cannot be one simultaneously, as per (3.83). Hence, the start-up cost becomes zero, as per (3.84). If the process system is starting-up, then $u_{\dot{v},t} - u_{\dot{v},t-1}$ becomes one which forces $su_{\dot{v},t}$ to be one and $sd_{\dot{v},t}$ to be zero. Hence, the startup cost of the process system becomes $\kappa_{\dot{v}}$ as per (3.84).

Table 3.7. An Example of the Startup Constraint for the Process Facility

Process System Status	$u_{\dot{v}}^{t}$	$u_{\dot{v}}^{t-1}$	$u_{\dot{v}}^{t} - u_{\dot{v}}^{t-1}$	$su_{\dot{v}}^{t}$	$sd_{\dot{v}}^{t}$	$su_{\dot{v}}^{t} - sd_{\dot{v}}^{t}$
OFF	0	0	**0**	0	0	**0**
ON	1	1	**0**	1	1	**0***
Shut down	0	1	**-1**	0	1	**-1**
Start up	1	0	**1**	1	0	**1**

*not allowed

j) Production Level Constraints:

These constraints formulate the lower and upper limits for the process system production flow rate. The constraints, then, are:

$$\dot{v}_t \geq u_{\dot{v},t} \cdot \dot{v}_{min} \qquad \forall \ \ 1 \leq t \leq T \tag{3.85}$$

$$\dot{v}_t \leq u_{\dot{v},t} \cdot \dot{v}_{max} \qquad \forall \ \ 1 \leq t \leq T \tag{3.86}$$

3.3 ROLLING TIME-HORIZON SCHEDULING

The developed optimization algorithm schedules and maximizes profit for the process facility under study for a whole year, which might not be practical. Conducting a rolling time-horizon study with short generation planning periods has been adopted in several papers for various reasons [45, 47, 48]. One reason is that the forecast accuracy improves significantly as the planning horizon decreases. Looking into error calculation in time-series modeling, forecast error and uncertainty increase as the horizon length increases, as seen in Figure 3.6 [49, 50, 51]. Hence, dividing the planning horizon into smaller periods improves the accuracy of load and price forecasts in the short-term. Computational time reduction can also be achieved due to the use of smaller planning periods [48]. Other reasons include the reduction of horizon effects and the flexibility of changing the generation system schedule in a daily basis. The horizon effects can be decreased by solving for N days and using only N-M days as the result.

Due to the aforementioned reasons, the yearly time-horizon profit maximization algorithm is divided into 364 periods and each period consists of 36 hours. However, data for the first 24 hours

are used in this analysis to avoid horizon effects, as seen in Figure 3.7. Also, for the first planning period, initial conditions are assumed to be known. For the subsequent planning periods, the facility's schedule of hour "24" in the previous planning period is used as the new initial condition for the current planning period, as seen in Figure 3.7.

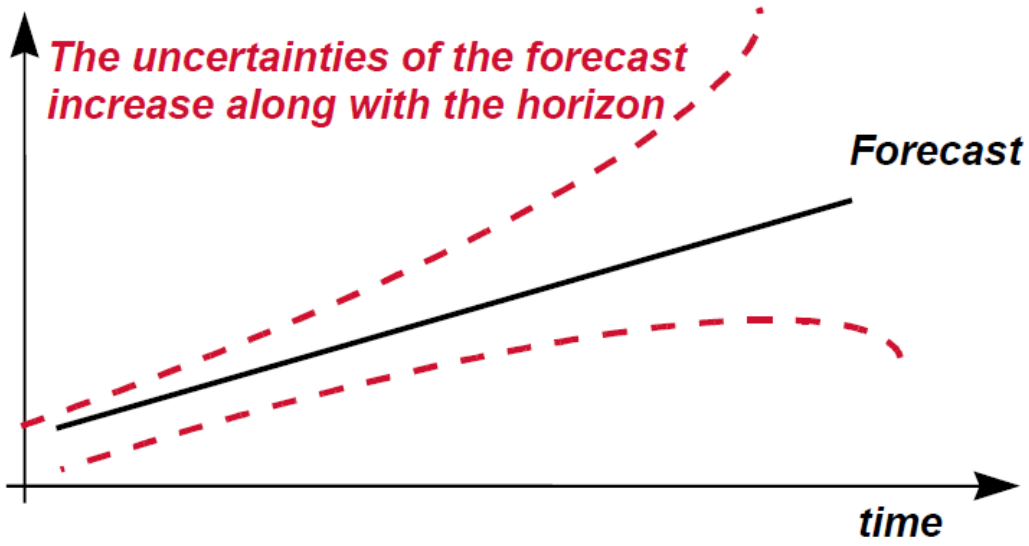

Figure 3.6. Forecast accuracy as a function of horizon length; [50] re-produced from [51]

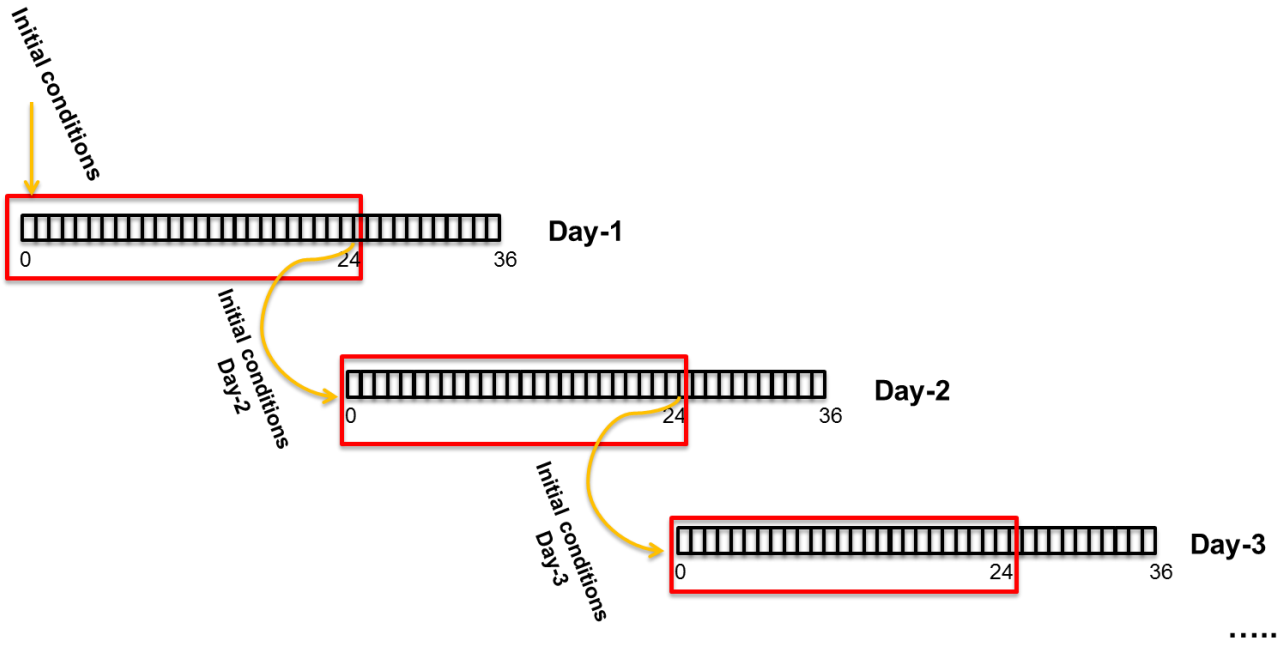

Figure 3.7. Rolling time-horizon scheduling showing initial conditions carry-over

Table 3.8. Computational Time as a Function of the Horizon Length

Horizon	Computational Time (s)	Profit ($)
Yearly	926	77,119,982
Daily (rolling)	302	77,119,848

The main advantage of the rolling time-horizon scheduling is that it uses a daily price forecast, which can be predicted with reasonable error compared to a yearly price forecast. Hence, the optimization algorithm generates a more practical schedule for the process facility compared to scheduling the process facility for the whole year due to the inclusion of look-ahead prices and the accuracy of the forecast. Also, the rolling time-horizon algorithm takes into account the previous schedule results and adapts its future schedule based on the new initial conditions for each planning period. The new initial conditions are the status and production level of the process system, generation units' status and output level, boilers output level, the storage system level, the previous cumulative processed volume, the duration of time since a generator is started up or shut down, and the duration of time since the process system is started up or shut down. A computational advantage arises from using a daily rolling time-horizon study, which is a function of the problem size. The computational advantage is noticeable and the time needed to reach a solution for a daily rolling time-horizon study is reduced by more than 65% compared to the time needed to schedule the process facility for a whole year, as seen in Table 3.8. The difference in the final objective function value is very small and hence negligible.

The formulation of the daily rolling time-horizon study carries the same formulation for the yearly time-horizon study that is discussed earlier in this chapter. However, additional formulations are needed for initial conditions update for each planning period. This is achieved by the following:

3.3.1 *Co-generation System*

$$P_{g,ini} = P_{g,24} \; \forall \; 1 \leq g \leq G \tag{3.87}$$

$$u_{g,ini} = u_{g,24} \; \forall \; 1 \leq g \leq G \tag{3.88}$$

$$UT_{aux_{g,t}} = \begin{cases} t-1, if\ su_{g,t} > 0 \\ 0, \quad if\ su_{g,t} = 0 \end{cases} \qquad (3.89)$$

$$\forall\ 1 \le g \le G, 1 \le t \le 24$$

$$UT_{g,ini} = UT_{g,ini}\ \$\left\{\sum_{t=1}^{T} su_{g,t} = 0\right\} + 24 - smax\left\{UT_{aux_{g,t}}\right\} \qquad (3.90)$$

$$\forall\ 1 \le g \le G, 2 \le t \le 24$$

$$DT_{aux_{g,t}} = \begin{cases} t-1, if\ sd_{g,t} > 0 \\ 0, \quad if\ sd_{g,t} = 0 \end{cases} \qquad (3.91)$$

$$\forall\ 1 \le g \le G, 1 \le t \le 24$$

$$DT_{g,ini} = DT_{g,ini}\ \$\left\{\sum_{t=1}^{T} sd_{g,t} = 0\right\} + 24 - smax\left\{DT_{aux_{g,t}}\right\} \qquad (3.92)$$

$$\forall\ 1 \le g \le G, 2 \le t \le 24$$

where $ is a logical IF symbol.

An example of initial conditions calculation for the up-time and down-time constraints is illustrated in Table 3.9 and Table 3.10. If a unit does not start-up during the current planning horizon, then $UT\_aux_{g,t}$ is zero for all time steps *t*. Hence, as per (3.90), the new initial condition becomes the previous initial condition in addition to the current planning period of 24 hours, as seen in case-1 of Table 3.9. On the other hand, if a unit starts up at *t=10* during the current planning horizon, then $UT\_aux_{g,t}$ is zero for all time steps *t* except $UT\_aux_{g,10}$, which gets a value of nine as per (3.89). Hence, the new initial condition becomes the time difference between the duration of the planning period and the passed time since a generation unit has started up, which becomes 15 as per (3.90). Similar analysis is conducted for the down-time initial condition and results are tabulated in Table 3.10.

Table 3.9. An Example of the MUT Initial Condition Calculation

Case	***Startup***	***Previous*** $UT_{g,ini}$	$smax\left\{UT_{aux_{g,t}}\right\}$	$UT_{g,ini}$
1	None	10	0	34
2	$su_{g,10}$	10	9	15

Table 3.10. An Example of the MDT Initial Condition Calculation

Case	*Shutdown*	*Previous* $DT_{g,ini}$	$smax\left\{DT_{aux_{g,t}}\right\}$	$DT_{g,ini}$
1	None	5	0	29
2	$sd_{g,15}$	5	14	10

3.3.2 *Boiler System*

$$S_{b,ini} = S_{b,24} \; \forall \; 1 \le b \le B \tag{3.93}$$

3.3.3 *Process System*

$$\dot{v}_{ini} = \dot{v}_{24} \tag{3.94}$$

$$u_{\dot{v},ini} = u_{\dot{v},24} \tag{3.95}$$

$$UT_{aux_{\dot{v},t}} = \begin{cases} t-1, if \; su_{\dot{v},t} > 0 \\ 0, \quad if \; su_{\dot{v},t} = 0 \end{cases} \quad \forall \; 1 \le t \le 24 \tag{3.96}$$

$$UT_{\dot{v},ini} = UT_{\dot{v},ini} \; \$\left\{\sum_{t=1}^{T} su_{\dot{v},t} = 0\right\} + 24 - smax\left\{UT_{aux_{\dot{v},t}}\right\} \tag{3.97}$$

$$\forall \; 1 \le t \le 24$$

$$DT_{aux_{\dot{v},t}} = \begin{cases} t-1, if \; sd_{\dot{v},t} > 0 \\ 0, \quad if \; sd_{\dot{v},t} = 0 \end{cases} \quad \forall \; 1 \le t \le 24 \tag{3.98}$$

$$DT_{\dot{v},ini} = DT_{\dot{v},ini} \; \$\left\{\sum_{t=1}^{T} sd_{\dot{v},t} = 0\right\} + 24 - smax\left\{DT_{aux_{\dot{v},t}}\right\} \tag{3.99}$$

$$\forall \; 1 \le t \le 24$$

3.3.4 *Storage System*

$$V_{s,ini} = V_{s,24} \tag{3.100}$$

3.4 DISCUSSION AND ANALYSIS

The profit maximization algorithm was simulated on a quad-core i7 computer with a speed of 2.4 GHz speed and 6 GB of RAM using GAMS, version 24.0.2 with CPLEX solver [52]. It took around 302 seconds to simulate a daily rolling-time horizon scheduling of a gas processing facility for one year. The start-up cost has been carried using a fixed start-up cost because the co-generation units are rarely shut-down due to the use of the co-generation system steam in the process system. Also, the start-up of combustion turbines takes around 10 minutes or less and hence the assumption of a fixed start-up cost is justified. Also, the operational philosophy of the process facility is to have the boiler system in operation "banking" all the time, for reliability purposes.

The analysis was carried on two cases; the subsidized fuel price and the unsubsidized fuel price for the Saudi Grid generators. Three scenarios were considered for each case; the base-case scenario, the co-gen response scenario, and the full RTPDR scenario.

3.4.1 *Subsidized Fuel Price Case*

In the base case scenario, the captured profit was lower than the profit obtained from the co-generation response and the RTPDR scenarios, as seen in Table 3.11. This is attributed to the flexibility of the cogeneration system to change its output level in response to fluctuations in the RTP of electricity, as seen in Table 3.13. In the full RTPDR scenario, the profit is higher than the profit obtained from the co-generation scenario because the process system can also change its production level in response to fluctuations in the RTP of electricity as seen in Table 3.14. Varying the process system in response to the RTP of electricity, beyond the first planning period, does not add more benefit to the process facility while varying the cogeneration system captures more benefit to the process facility under study. Hence, the profit obtained from the cogen response scenario is expected to be close to the profit obtained from the full RTPDR scenario.

Table 3.11. Profit Comparison for Different Scenarios (subsidized fuel case)

Scenario	Profit ($)	Profit Change ($)	% Change
Base case	72,536,862	0	0
Cogen response	77,119,837	4,582,975	6.32
Full RTPDR	77,119,848	4,582,985	6.32

Table 3.12. Cost and Revenue Allocation for Different Scenarios (subsidized fuel case)

Scenario	NGL revenue ($)	Energy Revenue($)	Cost of operation($)
Base case	142,833,067	11,965,032	82,261,238
Cogen response	142,833,067	3,402,741	69,115,971
Full RTPDR	142,832,822	3,403,035	69,116,010

Table 3.13. Total Generated Power for Different Scenarios (subsidized fuel case)

Scenario	Generated Power (MW)	cogen-1 (MW)	cogen-2 (MW)	Δ cogen-1 (MW)	Δ cogen-2 (MW)
Base case	2,708,160	1,354,080	1,354,080	0	0
Cogen response	1,331,170	671	1,330,499	(1,353,409)	(23,581)
Full RTPDR	1,331,220	620	1,330,600	(1,353,460)	(23,480)

Table 3.14. Total Production for Different Scenarios (subsidized fuel case)

Scenario	total Volume (MB)	Δ Volume (MB)
Base case	400,400	0
Cogen response	400,400	0
Full RTPDR	400,399	(1)

The end-product revenue in the RTPDR scenario is slightly lower than the end-product revenue in the base case and cogen response scenarios, as seen in Table 3.12. The energy revenue in the cogen response and RTPDR scenarios are much lower than the energy revenue in the base case scenario. Due to the ability of the process system to respond to the RTP of electricity in the RTPDR scenario, the energy revenue in the RTPDR scenario is slightly higher than the energy revenue in the cogen response scenario, as seen in Table 3.12. The cost of operation is high in the base case scenario due to the inability of the process facility to respond to the RTP of electricity. The cost of operation was low in the cogen response and RTPDR scenario due to the ability of the cogeneration system to change its power output in response to the RTP of electricity. The slight

increase in the cost of operation in the RTPDR scenario compared to the cogen response scenario is due to the slight increase in the power output of the cogeneration system in the RTPDR scenario, as seen in Table 3.13.

The total generated power for the base case is fixed. In the co-gen response and RTPDR scenarios, the co-generation system reduces its power production when the RTP of electricity becomes lower than the cost of running the cogeneration system. Hence, the generated power in these scenarios is lower than the base case scenario, as seen in Table 3.13. In the full RTPDR scenario, the process facility reduces its production level when the RTP of electricity is high enough to generate more revenue to the process facility compared to the revenue obtained from selling NGL products. Hence, the co-generation system has more flexibility to reduce its power output or even shut down completely, especially if the co-generation facility is not required to be operational to provide the needed steam for the process system. As a result, the generated power in the full RTPDR scenario is slightly higher than the co-gen response scenario, as seen in Table 3.13.

The total production of the process system is fixed for the base case and the co-gen response scenarios. However, in the full RTPDR scenario, the process facility reduced its production level slightly in the first hour of the study period to maximize profit, as seen in Table 3.8. Note that Boiler B-3, the second cheapest boiler, was not able to increase its production level to full capacity in the first hour due to its ramp-up constraint, which influenced the process system to slightly reduce its production level to maximize profit for the process facility, as seen in Table 3.14.

The total exported power to the utility has reduced in the co-gen response scenario compared to the base case scenario due to the ability of the generation system to reduce its power output during low RTP of electricity to maximize profit for the process facility. Hence, the total generated power has reduced which resulted in a lower total power export to the utility compared to the base case scenario, as seen in Table 3.15. Also, the total power export has slightly increased in the full RTPDR scenario compared to the co-gen response scenario. This can be explained by the total increase of the generated power in the RTPDR scenario in addition to the slight reduction of the process system production level compared to the co-gen response scenario. Hence, the combined effect resulted in a slight increase in power export to the utility compared to the co-gen response scenario, as seen in Table 3.15.

The total steam production of Boilers B-1, B-2, and B-3 has increased in the co-gen response and full RTPDR scenarios compared to the base case scenario, as seen in Table 3.16. The total steam production of Boiler B-4 has reduced slightly in the co-gen response and RTPDR scenarios compared to the base case scenario. Steam production from boilers B-1, B-2, and B-3 has increased mainly due to the reduction of the co-generation system power output during low RTP of electricity, which in turn reduced the total steam production from the cogeneration system. Hence, boilers B-1, B-2, and B-3 were dispatched at full capacity to compensate for the lost steam from the co-generation system. Also, steam production from the cheapest boiler B-4 has reduced slightly in the co-gen response and RTPDR scenarios, as seen in Table 3.16. The reduction of the steam output from the cheapest boiler is related to the fluctuation of the RTP of electricity. In particular, when the RTP of electricity became low, the co-generation system decided to shut down one of its generators to maximize profit. In order to achieve that without affecting the process system, boilers are prepared to compensate for the expected lost steam. Hence, boilers that have limited flexibility due to their binding ramp-up constraints such as B-2 and B-3 begin raising their production level ahead of time. Hence, the process facility decided to reduce the output level of the cheapest boiler B-4 during the transition period in order to reduce the amount of the vented steam.

Table 3.15. Total Power Export to the Grid for Different Scenarios (subsidized fuel case)

Scenario	Total Export to the Utility (MW)	Total change in Power export (MW)
Base case	1,921,917	0
Cogen response	544,926	(1,376,990)
Full RTPDR	544,978	(1,376,938)

Table 3.16. Steam Production for Different Scenarios (subsidized fuel case)

Scenario	Boiler-1 (Mlb)	Boiler-2 (Mlb)	Boiler-3 (Mlb)	Boiler-4 (Mlb)
Base case	436,800	611,520	3,724,412	3,974,880
Cogen response	3,798,620	3,711,593	3,887,196	3,974,865
Full RTPDR	3,798,620	3,711,593	3,887,196	3,974,865

The analysis in this section suggests that the main source of the added profit to the process facility comes from reducing the co-generation system output and purchasing power from the utility instead. This result is highly influenced by the generators' fuel subsidy in the Saudi Grid, which is expected to reduce over time or even disappear in the near future. Hence, a similar analysis is conducted using the unsubsidized fuel price for generators to understand the expected behavior of the process facility in presence of unsubsidized fuel price in the Saudi Grid. It is predicted that the RTP of electricity will be higher. Hence, a change in the cogeneration system power output is limited. On the other hand, a more frequent change in the production level of the process system is expected to occur. Hence, the RTPDR case is expected to show more benefit to the RTPDR facility.

3.4.2 *Unsubsidized Fuel Price Case*

When fuel subsidy is reduced or eliminated, the RTP of electricity is expected to increase because fuel cost is directly related to the incremental cost of generators, which sets the price in the marginal price market. In the Saudi Grid, the fuel price is fixed and the amount of subsidy depends on the fuel type. The unsubsidized fuel price data, international fuel prices, were obtained from [53, 54, 55] using the closing price of 3/2/2015 and conversion rates from [55]. A comparison between the subsidized and unsubsidized fuel prices for the Saudi Grid is shown in Table 3.17.

In the unsubsidized fuel price case, the power system generators are expected to react differently. For example, generators, who used to receive a high fuel subsidy, might reduce their power output or even shut down completely. Generators, who used to receive a low fuel subsidy, might increase their power output or even get dispatched, if they were previously shut down.

In the cogen response scenario, the cogeneration system never reduces its power output and is dispatched at full capacity due to the high RTP of electricity. Hence, the base case and cogen

Table 3.17. Comparison between Fuel Prices in the Subsidized and Unsubsidized Fuel Cases

Case	Subsidized Fuel ($/MMBTU)	Unsubsidized Fuel ($/MMBTU)	% Subsidy
Gas	0.75	2.79	73.12
Oil	0.74	10.63	93.04
Diesel	0.63	13.95	95.48

response scenarios have similar behavior and profit. In the RTPDR scenario, the captured profit is higher than the profit obtained from the base case and co-gen response scenarios, as seen in Table 3.18. The process system in the RTPDR scenario has the flexibility to change its production level in response to fluctuations in the RTP of electricity, as seen in Table 3.21. Hence, the process facility maximized its profit by reducing its production level during an event of high RTP of electricity because the benefit obtained from selling power to the utility exceeded the benefit obtained from selling NGL products at full production capacity.

The end-product revenue in the RTPDR scenario is slightly lower than the end-product revenue in the base case and cogen response scenarios because the production level of the process system in the RTPDR scenario is lower than the other two scenarios, as seen in Table 3.19 and Table 3.21. The energy revenue in the RTPDR scenario is higher than the energy revenue in the base case and cogen response scenarios. This is due to the ability of the process system to respond to the RTP of electricity in the RTPDR scenario, which allows the process facility to sell more power to the utility taking advantage of the high RTP of electricity, as seen in Table 3.22. The cost of operation is high in the base case and cogen response scenarios due to the inability of the process facility to respond to the RTP of electricity. The cost of operation was low in the RTPDR scenario due to the ability of the process system to change its production level in response to the RTP of electricity, as seen in Table 3.19 and Table 3.21. Hence, the process system consumes less power and steam during events of high RTP of electricity, which allows the cogeneration system to sell more power to the utility, as seen in Table 3.22.

In the unsubsidized fuel price case, the RTP of electricity is high enough to schedule the co-generation system to dispatch at full capacity at all times for all scenarios, as seen in Table 3.20. Even though the cogeneration system can change its power output in the co-gen response and RTPDR scenarios, the cogeneration system decided to dispatch at full capacity. In this case, the incremental cost of running the co-generation system is lower than the combined cost of purchasing power from the utility and generating steam from the boiler system.

Table 3.18. Profit Comparison for Different Scenarios (unsubsidized fuel case)

Scenario	Profit ($)	Profit Change ($)	% Change
Base case	96,718,038	0	0
Cogen response	96,718,038	0	0
Full RTPDR	114,475,218	17,757,180	18.36

Table 3.19. Cost and Revenue Allocation for Different Scenarios (unsubsidized fuel case)

Scenario	NGL revenue ($)	Energy Revenue($)	Cost of operation($)
Base case	142,756,400	44,986,612	91,024,974
Cogen response	142,756,400	44,986,612	91,024,974
Full RTPDR	142,095,481	54,423,650	82,043,913

Table 3.20. Total Generated Power for Different Scenarios (unsubsidized fuel case)

Scenario	Generated Power (MW)	cogen-1 (MW)	cogen-2 (MW)	Δ cogen-1 (MW)	Δ cogen-2 (MW)
Base case	2,708,160	1,354,080	1,354,080	0	0
Cogen response	2,708,160	1,354,080	1,354,080	0	0
Full RTPDR	2,708,160	1,354,080	1,354,080	0	0

Table 3.21. Total Production for Different Scenarios (unsubsidized fuel case)

Scenario	total Volume (MB)	Volume change (MB)
Base case	400,400	0
Cogen response	400,400	0
Full RTPDR	398,332	(2,068)

Table 3.22. Total Power Export to the Grid for Different Scenarios (unsubsidized fuel case)

Scenario	Total Export to the Utility (MW)	Total change in Power export (MW)
Base case	1,921,917	0
Cogen response	1,921,917	0
Full RTPDR	1,926,816	4,900

Table 3.23. Steam Production for Different Scenarios (unsubsidized fuel case)

Scenario	Boiler-1 (Mlb)	Boiler-2 (Mlb)	Boiler-3 (Mlb)	Boiler-4 (Mlb)
Base case	436,800	611,520	3,724,412	3,974,880
Cogen response	436,800	611,520	3,724,412	3,974,880
Full RTPDR	436,800	617,988	3,669,827	3,934,579

The total production of the process system is fixed for the base case and the cogen response scenarios. However, in the full RTPDR scenario, the process facility reduced its production level to maximize profit, as seen in Table 3.21. Note that the total volume reduction is small but higher than the total reduction observed in the subsidized fuel price case. Occasions of high RTP of

electricity high enough to reduce the production level of the process system are rarely encountered. An example of this situation will be discussed in detail using ERCOT system historical price profile in the next section.

The total power export to the utility has increased in the RTPDR scenario compared to the base case and co-gen response scenarios due to the ability of the process system to reduce its production level during high RTP of electricity to maximize profit for the process facility, as seen in Table 3.21 and Table 3.22. Hence, the total power export to the utility is higher in the RTPDR scenario compared to the base case and cogen response scenarios.

The total steam production did not change between the base case and co-gen response scenarios, as seen in Table 3.23. Steam production of Boiler B-1, the most expensive boiler, did not change in the RTPDR scenario. Steam production of boilers B-3 and B-4, cheap boilers, has slightly reduced in the RTPDR scenario compared to the base case and cogen response scenarios, as seen in Table 3.23. The total steam production of Boiler B-2, the second expensive boiler, has slightly increased in the RTPDR scenario compared to the other scenarios. The increased steam production from boiler B-2 and the reduction of the steam output from the cheapest boilers B-3 and B-4 is related to the fluctuation of the RTP of electricity. For example, when the RTP of electricity is high, the process system decides to reduce its production level ahead of time to prepare for the event, due to the ramp down constraint of the process system. Since boilers have different ramp down capabilities, the optimal steam dispatch changes for different production levels. Hence, boilers that have limited flexibility due to their binding ramp-down constraints such as B-3 begin reducing their steam output ahead of time. Hence, the optimization algorithm decided to reduce the output level of the cheapest boilers B-3 and B-4 during the transition period while avoiding any possible vented steam. An example of the boiler system steam output for the RTPDR scenario during a high RTP of electricity event is shown in Table 3.24.

The analysis in this section suggests that the source of the added profit to the process facility comes from reducing the process system output in order to sell more power to the utility. This behavior occurs during events of high RTP of electricity, which is rarely encountered in the system under study. Looking into the process facility's schedule over a range of prices, more than 99% of the time the Saudi Grid price falls in a RTP range that does not introduce any change in the cogeneration system power output and allows a limited maneuver of the production level of the process system. In the RTPDR scenario, it is observed that the marginal benefit for the process

facility in the unsubsidized fuel case is higher than the marginal benefit obtained from the subsidized fuel case. For the above reasons, a further analysis is suggested, which requires the use of an actual price profile, to show the effects of RTP volatility and uncertainty. The analysis will be discussed in detail in the next section.

Table 3.24. Steam Production for Different Boilers during a High RTP Event (day-150)

	t_{14}	t_{15}	t_{16}	t_{17}	t_{18}	t_{19}	t_{20}
RTP ($/MWh)	63.67	84.00	110.66	110.66	74.66	36.27	34.875
V (MB/hr)	45.83	42.74	31.40	34.49	42.05	45.83	45.83
B1 (Mlb/hr)	50.00	50.00	50.00	50.00	50.00	50.00	50.00
B2 (Mlb/hr)	70.00	70.00	70.00	70.00	103.50	173.74	70.00
B3 (Mlb/hr)	426.33	320.74	45.00	50.58	186.58	322.58	426.33
B4 (Mlb/hr)	455.00	391.84	48.84	212.00	455.00	455.00	455.00

3.5 Effects of Real Time Price Volatility and Price Forecast Accuracy

There are two factors that can significantly influence the process facility's profit which are the accuracy of the price forecast and the price profile or volatility. If the process facility can predict the RTP of electricity accurately, then it can increase its realized profit because the schedule of the process facility is planned based on the outcome of the profit maximization algorithm, which has the RTP of electricity as a main input. The price profile affects the process facility's profit because the benefit obtained from the participation in a RTPDR program is realized the most during electricity market events such as a high RTP of electricity and a low (or negative) RTP of electricity. Hence, the developed price profile for the Saudi Grid neither takes into account a price forecasting error nor considers RTP volatility such as price spikes during electrical system events. Hence, testing a price profile from an existing market would show the effects of price volatility and price forecast accuracy. Therefore, historical price data from the ERCOT system were used in this analysis due to close match of weather and load data between the ERCOT system and the Saudi Grid, which is discussed in detail in section 3.1.

3.5.1 *Effects of RTP Volatility*

To study the effects of RTP volatility, historical RTP data of Houston area were obtained from the ERCOT market for one year between 12/1/2009 and 11/30/2010 [56]. Table 3.25 lists statistical differences between the ERCOT price data and the price data obtained from the single-bus DCOPF model of the Saudi Grid. The ERCOT market experiences a higher price volatility compared to the subsidized and unsubsidized fuel cases. The ERCOT market experiences negative RTPs and price spikes, which are not present in the Saudi Grid price data. The single-bus model does not have transmission lines and hence does not experience transmission congestion effects. Negative RTPs might appear in an electricity market when transmission system congestion is in effect, which is discussed in detail in Chapter 5 for the three-bus test case. Price spikes appear during power system abnormalities such as loss of generation or transmission lines. Loss of transmission lines might cause some transmission lines to become congested, which raises the RTP at the congested side of the transmission line. Hence, the ERCOT price data is used to understand the behavior of the RTPDR facility during system events. Hence, the effects of the RTP volatility on the process facility profit can be analyzed.

In the base case scenario, the captured profit was slightly lower than the profit obtained from the cogen response scenario due to the flexibility of the cogeneration scenario to change the power output of the cogeneration system in response to fluctuating RTP of electricity, as seen in Table 3.26 and Table 3.28. In the full RTPDR scenario, the profit of the RTPDR facility is much higher than the profit obtained from the cogen response scenario because the process system can also change its production level in response to fluctuations of the RTP of electricity, as seen in Table 3.29.

Table 3.25. Comparison between the Subsidized Fuel, Unsubsidized Fuel, and ERCOT Cases

Case	Subsidized Fuel	Unsubsidized Fuel	ERCOT
Average Price ($/MWh)	6.23	23.42	37.10
Lowest Price ($/MWh)	4.43	14.00	-25.54
Highest Price ($/MWh)	34.88	110.66	1,257.91
σ	0.86	4.83	42.12

The end-product revenue in the RTPDR scenario is lower than the end-product revenue in the base case and cogen response scenarios, as seen in Table 3.27. However, the energy revenue in the RTPDR scenario is higher than the energy revenue in the cogen response scenario. This is due to the ability of the process system to reduce its production level during high RTP of electricity and sell power to the utility instead, as seen in Table 3.29 and Table 3.30. Due to the ability of the generation system to respond to the RTP of electricity in the cogen response scenario, the energy revenue in the cogen response scenario is slightly higher than the energy revenue in the base case scenario, which is counter-intuitive since the cogeneration system produced more power in the base case scenario, as seen in Table 3.27 and Table 3.28. Upon further analysis, it has been found that during events of low or negative RTP of electricity, the cogeneration system was able to reduce its power output or even shut down completely to maximize profit for the process facility. This is due to ability of the cogeneration system to reduce its power output when the incremental cost of purchasing power from the utility becomes lower than the incremental cost of the cogeneration system. A negative RTP of electricity can occur when a high penetration of renewables that receive subsidies is part of the electricity market or when transmission system congestion is in effect, which is discussed in detail in Chapter 5. Hence, shutting down the cogeneration system in this case saves the process facility an extra payment to the load that consumes its electricity in addition to the cost of operation of the cogeneration system. Hence, due to the ability of the cogeneration system to avoid load payment in the cogen response scenario, the energy revenue becomes higher than the energy revenue in the base case scenario. The cost of operation was the highest in the base case scenario due to the inability of the process facility to respond to the RTP of electricity. The cost of operation in the cogen response scenarios is slightly lower than the cost of operation in the base case scenario due to the ability of the cogeneration system to adjust its power output to reduce load payment during negative RTP of electricity. Hence, the energy revenue of the cogen response scenario becomes higher than the energy revenue of the base case scenario. The cost of operation was the highest in the base case scenario due to the inability of the process facility to respond to the RTP of electricity. The cost of operation in the cogen response scenarios is slightly lower than the cost of operation in the base case scenario due to the ability of the cogeneration system to reduce its power output during low or negative RTP of electricity, which is rarely encountered. The cost of operation was the lowest in the RTPDR scenario due to the ability of the process facility to change its process system

production level and cogeneration system power output in response to fluctuations of the RTP of electricity, as seen in Table 3.27, Table 3.28, and Table 3.29.

Table 3.26. Profit Comparison for Different Scenarios (ERCOT System)

Scenario	Profit ($)	Profit Change ($)	% Change
Base case	123,063,352	0	0
Cogen response	123,144,542	81,190	0.07%
Full RTPDR	133,290,178	10,226,827	8.31%

Table 3.27. Cost and Revenue Allocation for Different Scenarios (ERCOT system)

Scenario	NGL revenue ($)	Energy Revenue($)	Cost of operation($)
Base case	142,756,400	71,331,925	91,024,974
Cogen response	142,756,400	71,378,886	90,990,744
Full RTPDR	140,960,959	73,897,339	81,568,119

Table 3.28. Total Generated Power for Different Scenarios (ERCOT system)

Scenario	Generated Power (MW)	cogen-1 (MW)	cogen-2 (MW)	Δ cogen-1 (MW)	Δ cogen-2 (MW)
Base case	2,708,160	1,354,080	1,354,080	0	0
cogen response	2,700,175	1,350,090	1,350,085	(3,990)	(3,995)
Full RTPDR	2,696,470	1,348,203	1,348,267	(5,877)	(5,813)

Table 3.29. Total Production for Different Scenarios (ERCOT system)

Scenario	total Volume (MB)	Volume change (MB)
Base case	400,400	0
Cogen response	400,400	0
Full RTPDR	395,152	(5,248)

Table 3.30. Total Power Export to the Grid for Different Scenarios (ERCOT system)

Scenario	Exported Power (MW)	Change in Exported Power (MW)
Base case	1,921,917	0
cogen response	1,913,931	(7,985)
Full RTPDR	1,922,957	1,041

Table 3.31. Steam Production for Different Scenarios (ERCOT system)

Scenario	Boiler-1 (Mlb)	Boiler-2 (Mlb)	Boiler-3 (Mlb)	Boiler-4 (Mlb)
Base case	436,800	611,520	3,724,412	3,974,880
cogen response	450,906	627,571	3,722,004	3,974,880
Full RTPDR	458,484	657,244	3,560,447	3,869,716

The total generated power in the base case scenario is fixed. However, in the co-gen response scenario, the co-generation system reduces its power production when the RTP of electricity becomes lower than the cost of running the cogeneration system. Hence, the generated power in the cogen response scenario is lower compared to the base case scenario, as seen in Table 3.28. In the full RTPDR scenario, the process facility has the ability to reduce its production level when the RTP of electricity is high enough to generate more revenue to the facility compared to the revenue obtained from selling NGL products. Hence, the cogeneration system becomes more flexible to reduce its power output or even shut down the generation facility compared to the limited flexibility in the cogen response scenario. Note that the cogeneration system can only shut down if it is not required to operate in order to provide the needed steam for the process system. Occasions of RTP of electricity that is high enough to reduce the production level of the process system are rarely encountered. Hence, the generated power in the full RTPDR scenario is slightly lower than the cogen response scenario, as seen in Table 3.28.

The total production of the process system is fixed for the base case and the co-gen response scenarios. However, in the full RTPDR scenario, the facility was able to reduce its production capacity by more than 1%. Reducing the production level or shutting down the process system during a high RTP of electricity can maximize the profit for the gas processing facility and allow it to sell more power to the utility instead, as seen in Table 28 and Table 3.30.

The total power export to the utility has reduced in the co-gen response scenario compared to the base case scenario because the generation system has the ability to reduce its production level during low RTP of electricity. Hence, the gas processing facility purchases power at cheap price from the utility to maximize profit. As a result, the total generated power has reduced even though the production level of the process facility did not change. This in turn resulted in a lower total power export to the utility compared to the base case scenario, as seen in Table 3.30. The total exported power in the full RTPDR scenario is slightly higher than the total exported power in the base case scenario. The reduction in the process system production level resulted in a higher

power export compared to the reduction in the generated power from the cogeneration system. Hence, the net effect is a slight increase in exported power to the utility compared to the base case scenario, as seen in Table 3.30.

The total steam production from boilers B-1 and B-2 has increased in the cogen response scenario and a further increase was noticed in the full RTPDR scenario. The total steam production from boiler B-3 has slightly reduced in the co-gen response scenario compared to the base case scenario. A further decrease in steam production from boiler B-3 was noticed in the full RTPDR scenario. The total steam production from boiler B-4 has reduced in the RTPDR scenario compared to the base case and cogen response scenarios, as seen in Table 3.31.

The steam production from the expensive boilers, B-1 & B-2, has increased mainly due to the reduction of the cogeneration system power production during events of low RTP of electricity, which in turn reduces the steam production from the cogeneration system. Hence, steam compensation came instead from running the most expensive boilers. On the other hand, the steam production from the cheapest boilers, B-3 & B-4, has reduced slightly in the full cogen response scenario compared to the base case scenario. The steam production has further decreased in the RTPDR scenario due to the reduction of the production level of the process system, which resulted in less demand for steam in the process system. Hence, it resulted in less steam production from boilers B-3 and B-4. Also, a trade-off between cheap and expensive boilers during transition stage of events of high RTP of electricity is expected, which is similar to the event demonstrated in Table 3.24.

From the results of the simulation of the ERCOT system, it has been noticed that the process facility responds more frequently to the RTP of electricity for several reasons. One reason is that the ERCOT system price profile reflects a high RTP volatility, which results in a more frequent change of the process facility's schedule. The process facility's profit from the ERCOT system is higher the profit obtained from the Saudi Grid using the subsidized fuel price. This is expected due to the use of the unsubsidized fuel price for the ERCOT system. However, the process facility's profit from the ERCOT system is lower than the profit obtained from the Saudi Grid using the unsubsidized fuel price, which is affected by the difference in fuel mix between the two systems, different shapes of the price profile, and the consideration of transmission system congestion in the ERCOT system. A high penetration of renewable energy is expected to reduce the RTP of electricity in an electricity market, which is the case for the ERCOT system. As a

result, the expected profit for a price-responsive load is expected to be less, which is an observed result in the ERCOT system. The price profile for the Saudi Grid derives the RTP of electricity from a direct relationship between electrical load and price, which does not account for RTP volatility. However, the ERCOT system price profile inherits RTP volatility, which is expected to increase the expected profit for the price-responsive load.

Negative RTPs and price spikes are occasionally encountered in the ERCOT system and they tend to have opposite effects. Hence, the net benefit obtained from these events is limited in the ERCOT system. The RTP profile for the Saudi Grid is derived from a single-bus model, while the RTP profile for the ERCOT system is derived from a real system that models the transmission system. The RTP of electricity changes in the whole grid when transmission system congestion is in effect. It is expected that the receiving end of a congested transmission line to experience a high RTP of electricity and the remaining parts of the electrical system are affected by different degrees depending on their sensitivity to the congested transmission line, which is discussed with details in Chapter 5. The aforementioned reasons have caused a net reduction of the profit obtained by the price-responsive facility compared to the unsubsidized fuel case of the Saudi Grid. Hence, the results of the Saudi Grid analysis are not conclusive without building a price profile for the Saudi Grid and deriving RTP data from a system that models the transmission system of the Saudi Grid.

Events Analysis

To demonstrate the actual response of the process facility for different scenarios, two events from the ERCOT system were analyzed. These events are representative examples of the expected behavior of the process facility when it participates in a RTPDR program.

The first event represents a strong RTP volatility, as seen in Figure 3.8. The production level of the process facility was not affected by the price volatility because the RTP of electricity was not high enough to influence the production level of the process system, as seen in Figure 3.9. Hence, the cogen response scenario and the RTPDR scenario are expected to have similar behavior. The cogeneration system units changed their power output in response to the change in RTP of electricity, as seen in Figure 3.10 and Figure 3.11. When the RTP of electricity is higher than the marginal cost of the cogeneration system, the cogeneration system units produce power at maximum capacity and sell the excess power to the utility. When the RTP of electricity is lower

than the marginal cost of the cogeneration system, the cogeneration system units reduce their power output to the minimum allowed limit, as seen in Figure 3.10 and Figure 3.11. The cogeneration system does not shut down because the boiler system cannot supply the total steam demand when the process facility operates at full production capacity. Hence, the cogeneration system operates at its minimum power output to supply the remaining steam demand for the process system. The total power export to the utility is directly related to the cogeneration system power output, especially when the production level of the process system is constant. Hence, the total exported power to the utility increases when the RTP of electricity increases and reduces when the RTP of electricity reduces, as seen in Figure 3.12. The boiler system steam output is inversely related to the cogeneration system output level. When the cogeneration system reduces its power output, the steam output from the cogeneration system reduces. Hence, the boiler system increases its steam production to compensate for the reduced steam from the cogeneration system. Therefore, the boiler system increases its steam production when the RTP of electricity is low and reduces its steam output when the RTP of electricity is high, as seen in Figure 3.13. The profit for the process facility is higher in the cogen response and RTPDR scenarios compared to the base case scenario, as seen in Figure 3.14. The profit for the process facility comes from two sources; NGL revenue and energy revenue. Hence, the profit of the process facility reduces when the RTP of electricity reduces and increases when the RTP of electricity increases, as seen in Figure 3.14.

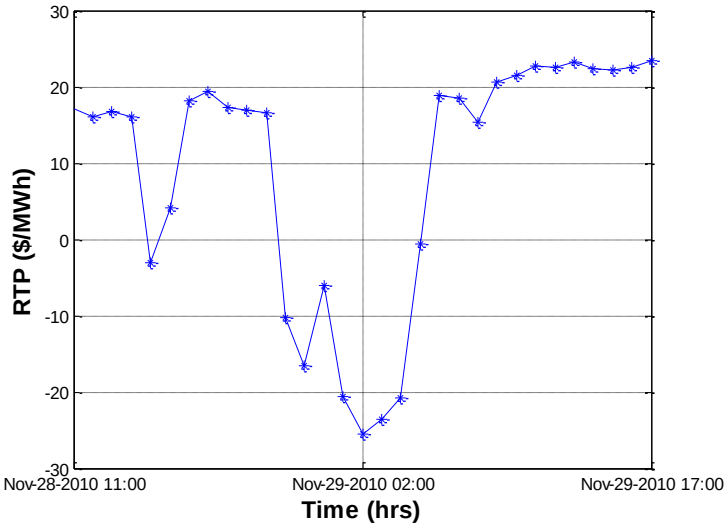

Figure 3.8. RTP profile for event-1

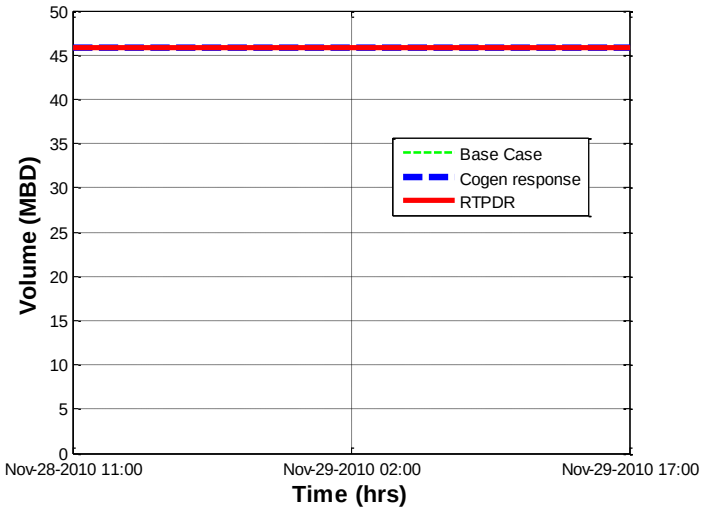

Figure 3.9. Production level during event-1

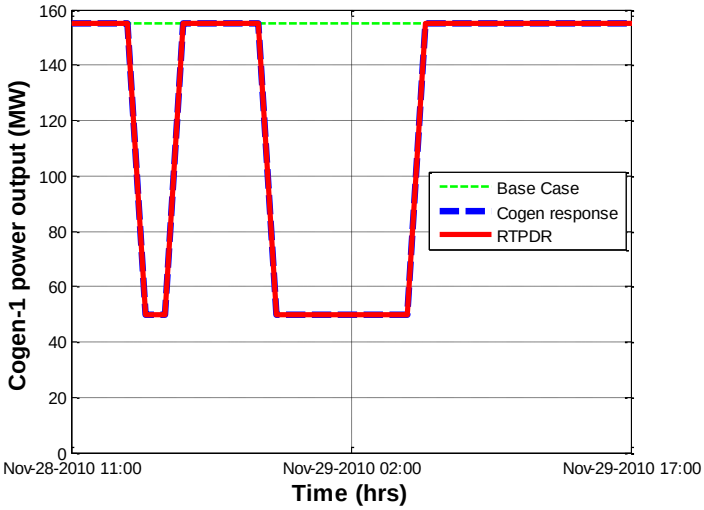

Figure 3.10. Cogen-1 power output during event-1

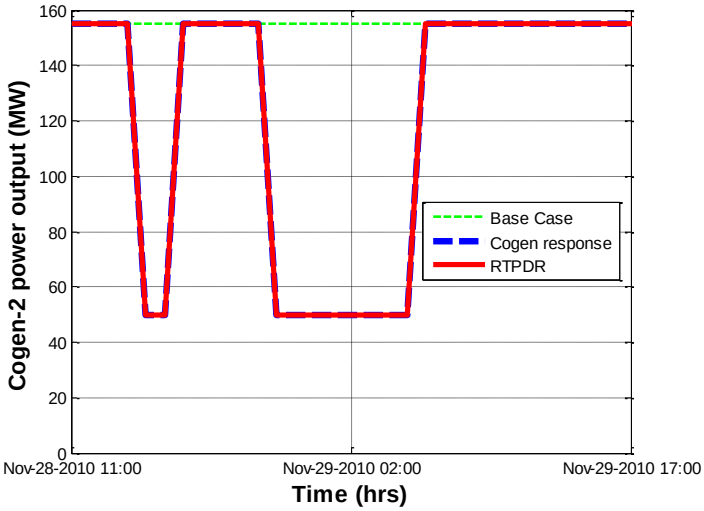

Figure 3.11. Cogen-2 power output during event-1

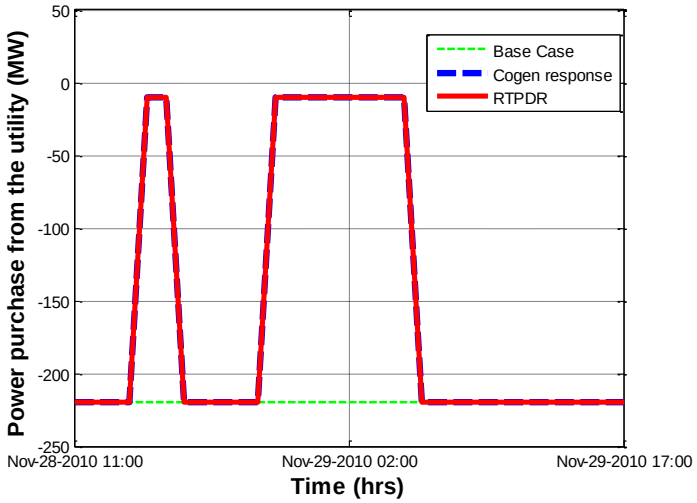

Figure 3.12. Purchased power from the utility during event-1

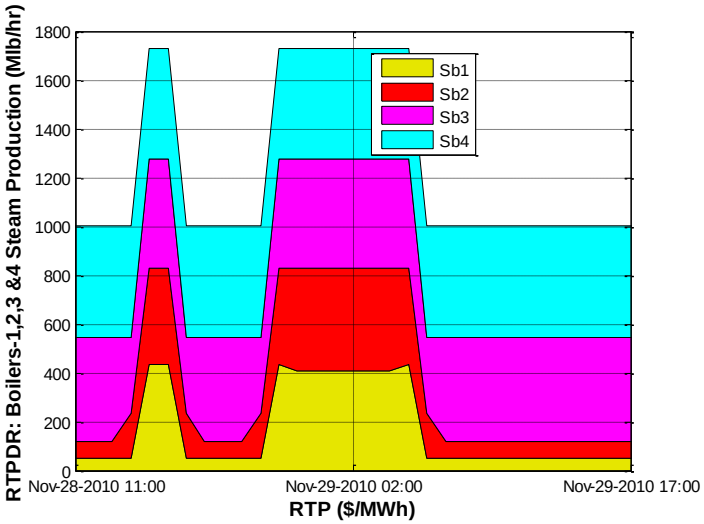

Figure 3.13. Boiler system steam output during event-1

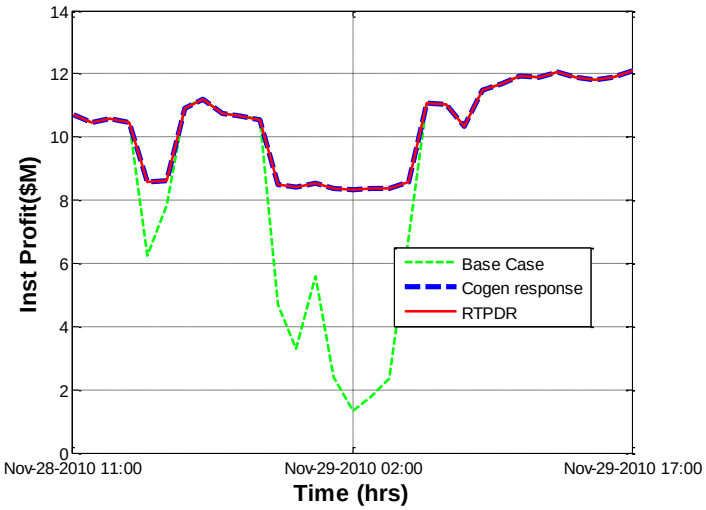

Figure 3.14. Instantaneous profit of the process facility during event-1

The second event represents price volatility with an associated price spike, as seen in Figure 3.15. The production level of the process system reduced sharply till it shut down completely when the RTP of electricity become very high. When the RTP of electricity became lower than the benefit obtained from selling NGL products, the process system was started up. As the RTP of electricity gradually decreased after the price spike, the production level of the process system gradually increased till it reached full capacity again, as seen in Figure 3.16.

The cogeneration system power output did not change during event-2 because the RTP of electricity is higher the marginal cost of the cogeneration system, so the cogeneration system produced at full capacity and exported its excess power to the utility to make more profit, as seen in Figure 3.17 and Figure 3.18. Power export to the utility has increased during very high RTP of electricity due to the decreased production level of the process system to allow the process facility to sell more power to the utility and make more profit, as seen in Figure 3.16 and Figure 3.19. The boiler system steam output is directly related to the production level of the process system. When the production level of the process system reduces, the steam output of the boiler system reduces and vice versa, as seen in Figure 3.16 and Figure 3.20. Hence, the steam production of the boiler system increases when the RTP of electricity is low and reduces when the RTP of electricity is high, as seen in Figure 3.20. The profit of the process facility is higher in the RTPDR scenario compared to the base case and cogen response scenarios. The profit of the process facility reduces when the RTP of electricity reduces and increases when the RTP of electricity increases following the shape of the price profile, as seen in Figure 3.15 and Figure 3.21.

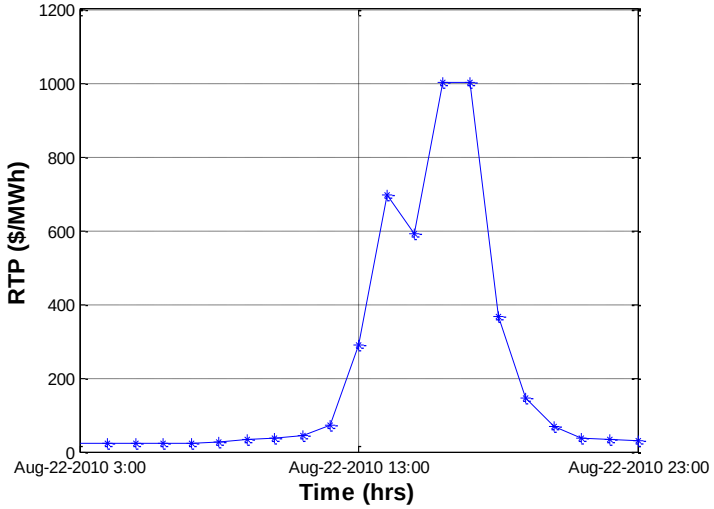

Figure 3.15. RTP profile for event-2

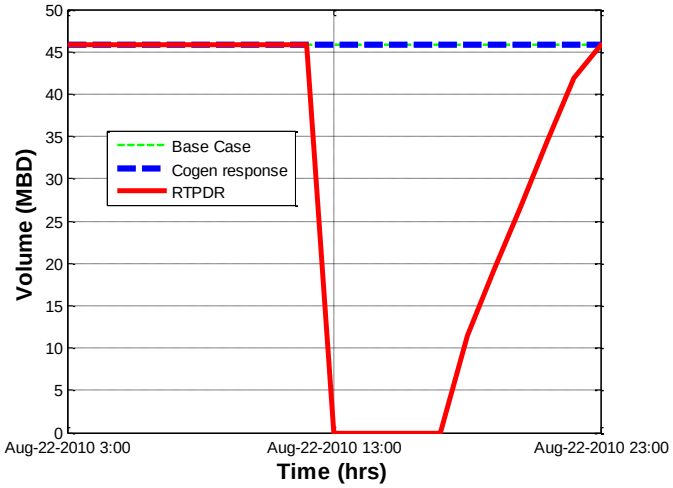

Figure 3.16. Production level for event-2

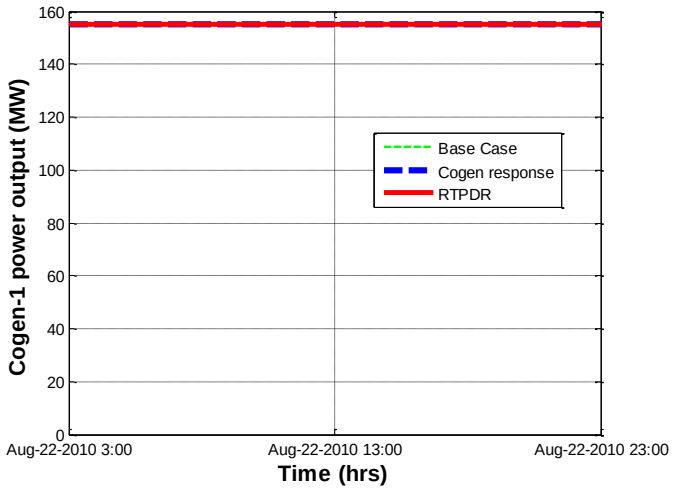

Figure 3.17. Cogen-1 power output for event-2

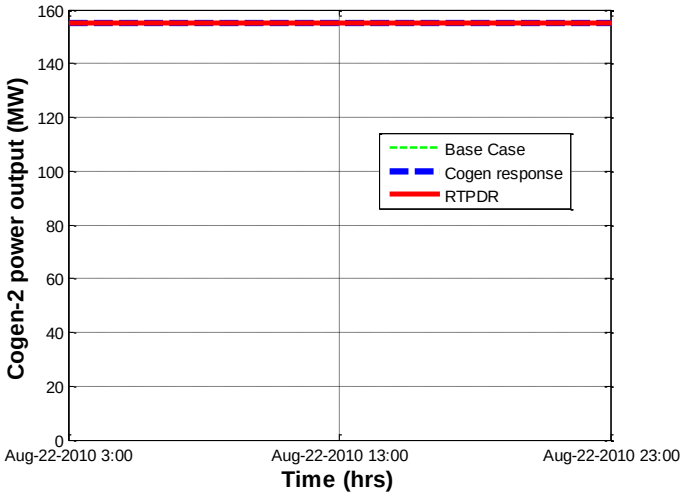

Figure 3.18. Cogen-2 power output for event-2

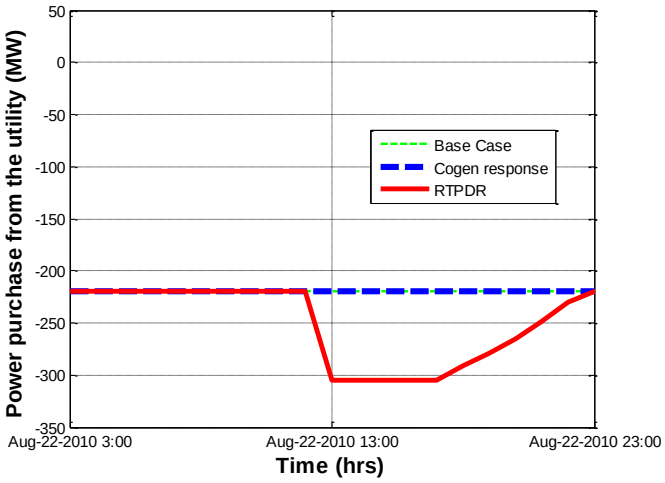

Figure 3.19. Purchased power from the utility for event-2

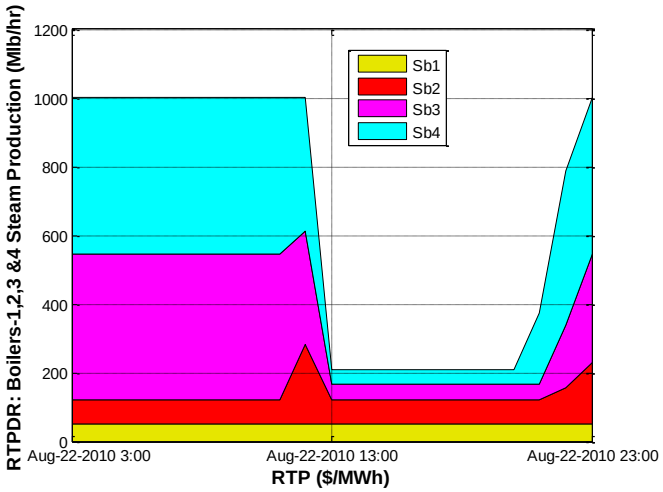

Figure 3.20. Boiler system steam output for the RTPDR scenario in event-2

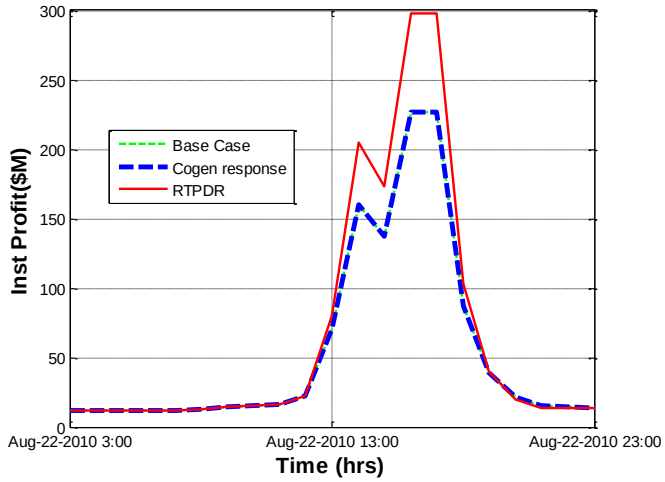

Figure 3.21. Instantaneous profit of the process facility for event-2

From the results of the above events, especially event-2, it has been noticed that the process facility responds to a known future price which is not the current practice in the electricity market due to technical limitations such as the accuracy of the price forecast, and the process system limitations such as ramp up/ramp down and minimum up/minimum down constraints. This is another justification for the impracticality of scheduling the process facility for a full-year. Using a daily rolling time-horizon scheduling, as discussed in a previous section, can reduce the effects of these limitations and improve the accuracy of the short-term price forecast.

The analysis in this section suggests that the source of the added profit to the process facility comes from reducing both the cogeneration system output and the process system output. When the RTP of electricity becomes high, the process system decides to reduce its production level and sell power to the utility instead. When the RTP of electricity becomes low, the cogeneration system decides to reduce its power output to allow the process facility to purchase cheap power from the utility instead. The analysis in this section suggests that while system events are rarely encountered and difficult to predict, they represent a considerable portion of the RTPDR benefits to the process facility. Hence, an accurate forecast for the RTP of electricity is very important to any RTPDR facility in order to extract the full benefit from its participation in the electricity market. Hence, a further analysis is needed to show the effects of RTP uncertainty, which will be discussed in detail in the next section.

3.5.2 *Effects of Price Forecast Accuracy*

An accurate price forecasting tool is very important for any RTPDR facility because it will allow the facility to maximize its profit when it reacts to the RTP of electricity. For example, if an industrial facility is able to predict a high RTP of electricity during the forecasted horizon, it might decide, based on economics, to reduce it production level or even shut down the process system completely. Likewise, if the RTPDR facility is able to predict a low RTP of electricity during the forecasted horizon, then it might decide to increase its production level to take advantage of the low RTP of electricity. Because electricity price profile and price forecast accuracy are important factors in determining a RTPDR facility's profit, the industrial facility under study is tested using ERCOT system data, specifically Houston area due to the reasons mentioned in section 3.1.

Price Forecasting Methods

Several price forecasting methods were examined in this work such as similar-day forecast, ARMA fitting, ANN, and historical DAM price from the ERCOT system. In general, price forecasting is consistent throughout the year with an error averaging around 10% except in two situations. The first situation is when the forecasting tool predicts a high RTP while the actual RTP is low. The second situation is when the RTP price experiences a price spike due to an event in the electricity system, which is not predictable in real-time. Mean Absolute Percentage Error (MAPE) and Symmetrical Mean Absolute Percentage Error (SMAPE) were used for error measurement of the tested price forecasting methods and results are tabulated in Table 3.32. The main contributor to the price forecasting error is the high penetration of stochastic resources in the ERCOT system, in particular wind generation, which significantly influenced the price forecast accuracy. SMAPE is used in this work for error measurement because it is less sensitive to discrete errors. SMAPE error does not exceed 200% by definition while MAPE error does not have an upper bound, which might influence the average MAPE percentage if a bad forecast is part of the sample, as seen in Table 3.32.

Similar-day Price Forecasting Tool

The similar-day price forecasting method is conducted by taking the weighted average of similar days in the past two years. For example, the forecasted first Sunday of this year is the average of the first Sunday of the previous two years. The accuracy of this method is improved when more weight, 75%, is given to the recent year. For example, the forecast of the first Sunday of this year becomes 75% of the price of the first Sunday from the previous year and 25% of the price of the first Sunday two years ago.

Table 3.32. Error Calculation for Different Price Forecasting Methods

Price Forecasting Method	MAPE	SMAPE
ECROT DAM price	26.93%	18.20%
ANN	87.30%	28.98%
Similar day method	109.07%	32.43%
ARMA model	37.49%	25.52%

Price Forecasting ANN

A price forecasting ANN was tested on historical electricity prices from the ERCOT system. Hourly, daily, weekly, and monthly historical price data were used as the input neurons for the price forecasting ANN to mimic the ANN structure provided in [57]. The number of hidden neurons is selected to be 50 which found to yield a reasonable trade-off between computational time and accuracy. The number of training epochs is selected to be 1000. The scaled conjugate gradient algorithm was selected for the ANN training. Initially, the price forecasting ANN is selected to be similar to the ANN provided in [57]. However, input neurons for the ANN were tested for statistical significance of correlation coefficients based on the criteria specified in [58]. According to [58], a correlation coefficient, for a large sample, is considered to have a statistical significance if its value is equal to or greater than 0.05 with a 95% confidence level. Hence, any input parameter that did not show a statistical significance was removed from the input neurons. Also, additional input parameters were tested for statistical significance and only two new input parameters were used in the ANN to improve the price forecasting accuracy. Results of the statistical significance test are tabulated in Table 3.33.

The updated ANN is shown in Figure 3.22 and it has the 6 input neurons; the previous hour *t-1*, the previous hour of the previous hour *t-2*, the same hour of the previous day *t-24*, the previous hour of the previous day *t-25*, the same hour of the previous year *t-8760*, and the previous hour of the previous year *t-8761*. There is only one output neuron for the ANN, which is the forecasted price for the current hour. The price forecasting ANN is performed daily for each hour of the forecasted day. Hence, the output of the ANN is the price forecast for the next 24 hours.

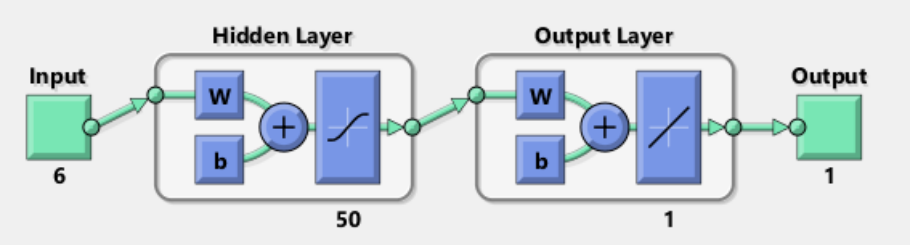

Figure 3.22. ANN structure for the price forecasting algorithm

Table 3.33. Correlation Coefficients for the Input Neurons of the price forecasting ANN

	Original Input Parameters						Additional Input Parameters			
p(t)	**p(t-1)**	**p(t-2)**	**p(t-24)**	**p(t-25)**	**p(t-168)**	**p(t-169)**	**p(t-720)**	**p(t-721)**	**p(t-8760)**	**p(t-8761)**	**p(t-8784)**	**p(t 8785)**
0.485	0.177	0.072	0.055	0.041	0.028	0.026	0.020		0.100	0.074	0.044	0.041

Time-series Price Forecasting Tool

A time-series model fit is examined on the historical electricity price data from the ERCOT system. To make the data more stationary, a square transformation was performed on the data after adding a constant to shift the lowest electricity price to zero. The historical electricity price data is updated daily to reflect the recent electricity price data before the daily ARMA forecast is performed. The output data from the ARMA model are then back-transformed and the constant is removed to get the forecasted electricity price. An ARMA (3, 1) was selected based on the LSE criteria and found to yield the lowest MAPE and SMAPE compared to other orders of ARMA.

ERCOT Historical DAM Price

The most accurate method is found to be the DAM price from ERCOT system. The historical DAM price from the ERCOT system is used as the forecasted daily electricity price. The method can predict the RTP accurately, with less than 10% error, more than 90% of the time. This method has a lower MAPE and SMAPE compared to other tested price forecasting methods, as seen in Table 3.32. Hence, historical DAM price data is used in this work to study the impact of the RTP forecast accuracy in the process facility's profit [56]. The plot in Figures 3.23 shows the forecasted price and actual price for the whole year. The zoomed one week time frame shows that the RTP forecast closely matches the actual RTP except on two occasions. The first occasion reflects an over-estimate of the price forecast while the RTP is lower, as seen in left bottom graph of Figure 3.23. In the second event, the price forecasting tool was not able to predict a price spike, so the forecasted price was much lower than the actual RTP of electricity, as seen in the right bottom graph of Figure 3.23.

Negative RTPs are occasionally observed in the ERCOT system due to high penetration of wind energy and the availability of production tax credit. The Saudi electricity market does not currently face fluctuating RTPs nor experience a negative RTP of electricity. However, fluctuating RTP of electricity is expected to appear when the Saudi Electricity Grid transforms from a vertically integrated utility to an electricity market in the near future with an increased focus on renewable energy resources [38]. Negative RTPs of electricity occur in the ERCOT market if the energy supply is more than the energy demand in presence of production tax credit for renewable energy. However, if energy demand is less than the energy supply in a typical electricity market, then the RTP of electricity should go as low as zero, if renewable energy sets

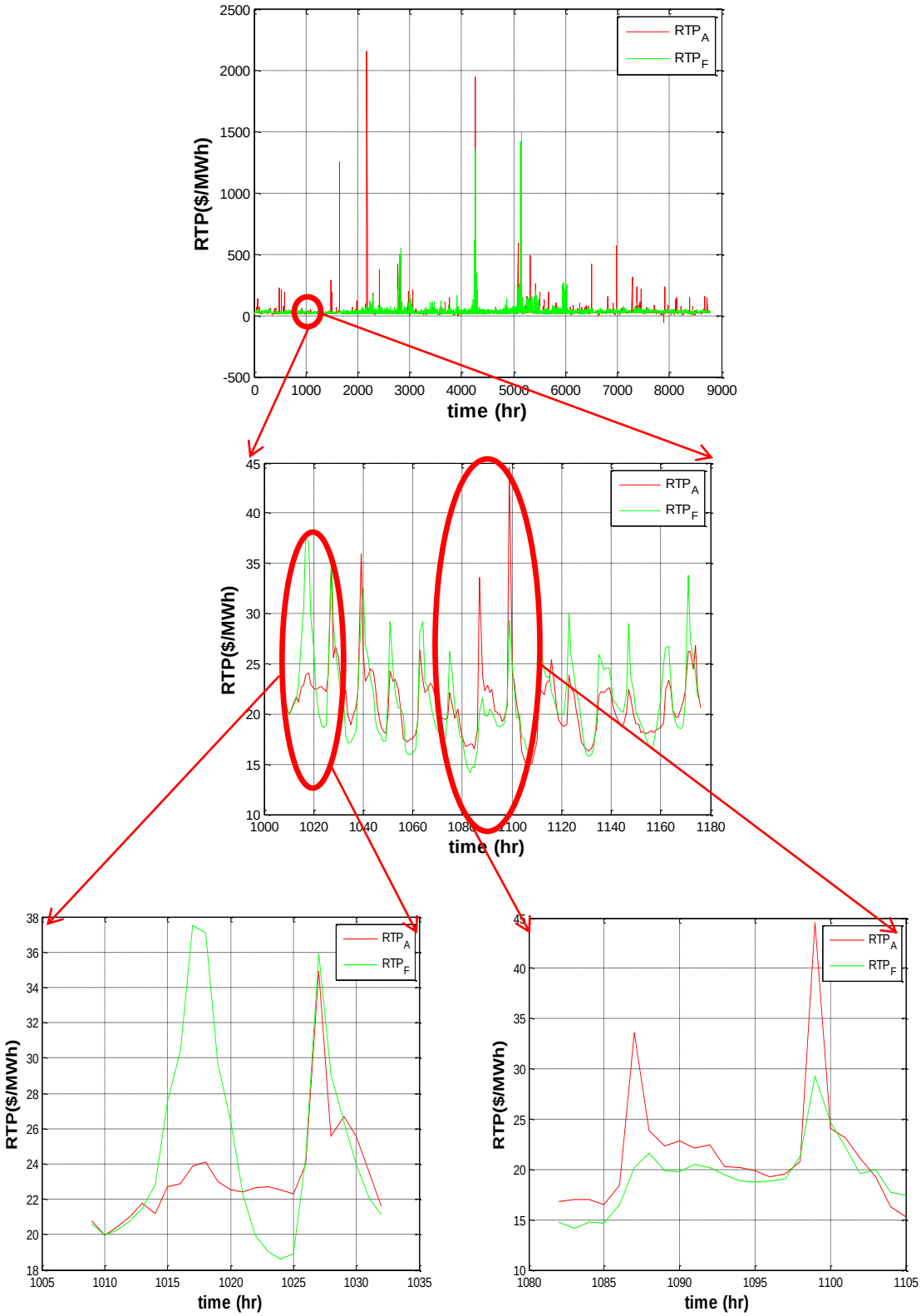

Figure 3.23: Historical forecasted and actual price from ERCOT system for year 2012

the price for the electricity market and the incremental cost of renewables is assumed to be zero. This in turn promotes price-responsive loads to consume more energy to take advantage of the situation, low RTP of electricity, and maximize their profit. In practice, the ISO, for system security purposes, will order some generators to reduce their dispatch to reach a balance between energy supply and demand. The future Saudi electricity market is not expected to offer a tax credit or feed-in-tariff for renewable energy. Hence, negative RTPs are not expected to appear due to a high penetration of renewable energy. However, negative RTPs might appear in the Saudi Grid if transmission system congestion is in effect, which will be discussed in detail in Chapter 5.

There are several limitations of using ERCOT historical prices for the price-responsive load analysis because the RTPDR load is sensitive to the price profile and shape. The Saudi Grid currently offers different levels of fuel subsidy, dependent on the fuel type. Hence, the use of ERCOT price data will not reflect the current condition of the Saudi electricity market because the incremental cost of peaker generators, which is influenced by the fuel cost, determines the market price in a typical marginal-price electricity market, which is the dominant market scheme worldwide.

Price forecasting in this research is mainly used to represent the actual scheduling mechanism of a RTPDR load. In this example, a natural gas processing facility schedules its process and generation systems based on the forecasted price of electricity. However, the realized facility's profit is determined by the actual RTP of electricity rather than the forecasted RTP. Hence, the use of ERCOT price profile is justified for the reasons discussed in this section and for the purpose of this analysis. Hence, ERCOT DAM price forecasting method is adopted for the analysis of the price forecast accuracy.

Effects of Price Forecast Accuracy on the RTPDR Load Profit

The analysis of the price forecasting accuracy was carried using ERCOT historical price data from [59] to show the effects of the RTP volatility on the process facility's profit. The analysis was carried using historical prices for years 2011 and 2013 and results are tabulated in Table 3.34.

The results in Table 3.34 suggest that the higher the RTP volatility, the less accurate the price forecasting tool can predict RTP of electricity. Hence, the difference between the forecasted process facility's profit and the realized process facility's profit becomes larger, as seen in Table 3.34. It should be noted that price spikes are difficult to predict in practice because they represent

Table 3.32. Effects of High RTP Volatility on the Process Facility's Profit

Data Set	ERCOT 2011	ERCOT 2013
σ	153.30	45.31
μ ($)	43.15	31.50
Forecasted Profit ($)	154,599,971	123,805,176
Realized Profit ($)	147,396,678	121,033,654
Difference ($)	7,203,293	2,771,522
% Difference	-4.66%	-2.24%

events in the electricity market that are not predictable. It should also be noted that a change in the process facility's schedule due to a price forecasting error is not frequently encountered, around 5% of the time, because the process facility's response is noticed to be flat over a price range, which is acceptable for the purpose of this research. The demand curve of the process facility is discussed in detail in Chapter 5.

3.6 CONCLUSION

In this chapter, scheduling generators, boilers, and process system over a time horizon has been formulated to synthesize a real-time process facility model. A descriptive model of a gas processing facility that can capture thermal equipment and process system dynamics is provided when considering an implementation of a price-based demand response program that interacts with the RTP of electricity. The model is improved by the inclusion of time dependence, and transition constraints. These constraints are the ramp-up and ramp-down capabilities of generators, minimum uptime and downtime of generators, startup cost of generators, ramp-up and ramp-down capabilities of boilers, ramp-up and ramp-down capabilities of the process facility, minimum downtime of the process facility, and the startup cost of the process facility. Constraints that limit the flexibility of a process facility to respond to the RTP of electricity are also considered in this Chapter. These constraints are storage tank capacity, flow rate limitation, and contractual constraints.

The optimal scheduling algorithm is tested using different cases; the subsidized fuel price case, the unsubsidized fuel price case, and the ERCOT system case. The first case analyzed the

expected behavior and profit of a price-responsive facility that is connected to the existing Saudi Grid. The second case analyzed the expected behavior and profit of the price-responsive facility when fuel subsidy is not offered in the Saudi Grid, which is expected to happen soon. The process facility added benefit comes mainly from rescheduling the cogeneration system in the subsidized fuel case while the process facility added benefit comes from varying the production level of the facility's process system in the unsubsidized fuel case.

The Saudi Grid price data from the subsidized and unsubsidized fuel cases do not consider RTP volatility due to a power system event such as transmission congestion, loss of generation, and high penetration of renewable energy during light loading condition. The ERCOT system price profile considers all of these effects and is derived from a real system price data and hence is used for the analysis of the price-responsive facility's behavior and profit.

The process facility's profit from the ERCOT system is lower than the profit obtained from the Saudi Grid using the unsubsidized fuel price, which is affected by the difference in fuel mix between the two systems, different shapes of the price profile, and the consideration of transmission system congestion in the ERCOT system. Hence, the results of the ERCOT system price profile are used for understanding the expected behavior of the price-responsive facility during high RTP volatility and uncertainty as well as during system events, such as a negative RTP of electricity or a price spike.

The qualitative analysis in this chapter can be generalized to any other electricity market that allows RTPDR load participation and calculates energy cost based on the RTP of electricity. However, quantitative results and the magnitude of benefit to the RTPDR facility may vary in magnitude from one system to another depending on accurate price information of specific systems. The results of the Saudi Grid analysis are not conclusive without building a more realistic price profile for the Saudi Grid that includes the effects of the transmission system and RTP volatility.

The ERCOT DAM tool was found to be the best price forecasting tool among other tested tools. Hence, it was adopted for the analysis of the ERCOT system. Once the Saudi Grid transforms completely from a vertically integrated utility to an electricity market in the near future, RTP data are expected to become available and accessible. The price forecasting tools that are discussed in this chapter can be tested against the RTP data to select the best price forecasting tool that yields the lowest forecast error.

In the next chapter, a design study for the gas processing facility is proposed using the problem formulation in this chapter. In particular, the main design features that affect RTPDR implementation in an industrial facility are considered. Hence, generation capacity, storage tank size, and production capacity are evaluated using a cost-benefit approach to determine the optimal size for each parameter of the gas processing facility.

Chapter 4. OPTIMAL DESIGN STUDY OF A NATURAL GAS PROCESSING FACILITY FOR RTPDR IMPLEMENTATION

4.1 INTRODUCTION

This chapter develops a design study for a natural gas processing facility that has significant generation capabilities, which can change its output fairly quickly, to explore the effects of RTPDR on the operation of the plant and its profit. The analysis is distinguished by the inclusion of some process constraints such as storage system, minimum flow rate, and contractual constraints to quantify the RTPDR benefits captured by the process facility. The design study in this work has been tailored to a specific process plant but can be applied to similar industrial plants by incorporating process constraints and limitations into the model which differs from one plant to another. These constraints can impact an industrial facility's profit.

In Chapter 2, an instantaneous optimal scheduling algorithm that maximizes profit for a RTPDR process facility facing fluctuating RTP of electricity is presented. In chapter 3, an optimal scheduling algorithm that models equipment and process dynamics over a time horizon for a process facility is proposed. This chapter deals with designing a process plant to facilitate RTPDR implementation. In this chapter, the formulation in Chapter 2 and historical RTP from ERCOT are used to determine the design parameters that contribute to an incremental benefit that is greater than the incremental cost of capital equipment when expanded. Once the design parameters are determined, then they will be formulated into a multi-variable objective function that can be analyzed to determine the optimal level for each design parameter. Note that the formulation proposed in Chapter 2 does not include generation and process constraints such as the generator ramp-up and ramp-down, the minimum uptime and downtime, startup cost of generators, flow rate limits, and startup cost of the process. Hence, the study will be expanded to use the formulation in Chapter 3 that incorporates operational scheduling over a time horizon. Hence, the question becomes whether the added operational profit pays for the extra capital cost or not.

A motivation for this work comes from the economy of scale in new equipment purchase, which is very apparent in the capital cost of constructing a new NGL facility. According to [60],

building a NGL plant that is twice the capacity can reduce the capital cost of Metric Ton Per Annum (MTPA) of NGL by 25%. This means that building an NGL plant that has twice the capacity of NGL products will result in an increase of 50% in capital cost to build up that plant. These factors make the gas processing plant suitable and economically attractive for RTPDR implementation.

In this chapter, a cost-benefit approach for the design study of a gas processing facility is proposed for the implementation of a RTPDR program that interacts with the RTP of electricity. Adding more flexibility to the process facility for RTPDR implementation might result in a negative profit when the cost of the added flexibility outweighs the benefit captured from the flexibility. So, the key parameters that effectively contribute to the flexibility of the process facility, for the purpose of RTPDR implementation, will be selected for a detailed design study. These parameters are the generation system size, the storage capacity, and the production capacity of the process facility. Generation system expansion allows the process facility to generate more power to supply the process facility's load during high RTP of electricity and even sell power to the utility. Storage system expansion allows the facility to reduce its production level during high RTP of electricity and store the raw material into the storage system of the facility. Production capacity expansion allows the facility to reduce its production level during high RTP of electricity and compensate for production loss during low RTP of electricity to meet the facility's obligations such as contracts, government requirements, etc. The outcome of the study will highlight the benefits captured from changing these design parameters. The ultimate goal is to include all parameters, which contribute to a positive net benefit when expanded, into a multi-variable formulation that can be analyzed to decide the optimal value for each design parameter.

The analysis in this chapter is tailored toward testing major design parameters that affect the implementation of RTPDR in the process facility. Results are not conclusive without the inclusion of the detailed model of the equipment and process transition constraints that are discussed in Chapter 3. Using Chapter 3 model for the design study is part of the proposed work in this chapter.

4.2 PARAMETERS THAT AFFECT PROCESS FACILITY'S RTPDR PROFIT

The main features that affect RTPDR implementation are generation capacity, storage tank size, and production capacity. Each feature will be evaluated using RTP from ERCOT market.

Marginal profit will be extracted and compared to the marginal cost of increasing the size of each feature. The assessment in this chapter is mainly based on the idea proposed in [61]. The author in [61] argues that utilities are willing to expand their transmission system even if they share the benefit with adjacent utilities only if the incremental benefits exceed the transmission investment cost, which is referenced in this proposal as the cost-benefit approach. In the context of this proposal, the process facility is only willing to expand its production capacity, storage tanks, and co-generation system if the incremental cost of expanding these parameters is less than the incremental benefit observed from increasing the size of the subject parameters. In the next section, each parameter will be analyzed and discussed using the cost-benefit approach when sizing or expanding the value of the aforementioned parameters.

Based on results, all parameters that contribute to a positive net benefit, when expanded, will be combined into one objective function. Then, multiple scenarios will be evaluated to show the effects of design on RTPDR profit. The analysis will also determine the optimal value for each parameter that maximizes profit for the process facility.

4.3 CO-GENERATION DESIGN STUDY AND SIZING

The facility's internal generation consists of two co-generation units. Each generator is rated 155 MW with a steam output of 749 Mlb/hr. It should be noted that when the process facility is upgraded, generators can be upgraded or replaced with a larger size unit. Another option is to add a third generator to the existing generation plant. The design analysis might become different between upgrading a plant versus building a new plant even though the same design concept applies. For example, in upgrading a plant, it is more practical to add another generator instead of replacing the existing generator unit. However, in a new plant design, the number of units and the size of each unit are less limited. Also, an economy of scale appears for the larger size units in terms of operational efficiency.

Table 4.1. Expansion Cost of the Process Facility's Co-generation System [64]

Cost Type	**Cost ($/MW)**
O&M cost	$12,760.00
Capital cost	$984,000.00

Table 4.1 shows the cost of increasing the size of the cogeneration system at the gas processing facility. (4.1) is used to calculate the annualized cost of expanding the co-generation system [62] :

$$AE(i) = PW(i) \cdot (A/P, i, N) \tag{4.1}$$

where *i* is the interest rate at 7.5%, N is the number of years which reflects the life-cycle of the cogeneration facility, *AE(i)* is the annualized cost of co-generation system expansion in $/year, *PW(i)* is the capital cost of co-generation system expansion in $, and A/P is the capital recovery.

It is worth mentioning that generation system size does not come in incremental units but rather in standardized sizes. This means that if the optimizer determines a co-generation unit size that is not a standard unit size. Then, the closest standard unit size from the result should be selected.

Once the annualized cost of the co-generation system expansion is calculated, the maintenance cost is added to the annualized cost as follows:

$$TAC = AE + M \tag{4.2}$$

Where *TAC* is the total annualized cost in in $/yr, *AE* is the annualized cost of the co-generation system expansion in $/year and, and *M* is the annual maintenance cost in $/year.

Table 4.2. A Cost-benefit Analysis of the Co-Generation System Expansion

Unit size (MW)	**Total Size (MW)**	**Facility's Profit ($/year)**	**Annualized Cost ($/year)**	**Facility's Net Profit ($/year)**
155	310	134,494,000	0 (base case)	134,494,000
160	320	137,007,000	960,765	136,046,235
170	340	142,166,000	2,882,295	139,283,705
190	380	152,227,000	6,725,355	145,501,645
220	420	167,281,000	12,489,945	154,791,055
230	460	172,266,000	14,411,475	157,854,525
240	480	177,368,000	16,333,005	161,034,995
245	490	179,707,000	17,293,770	162,413,230
250	500	179,701,000	18,254,535	161,446,465

Analysis of the effect of increasing the generation system size on the plant's profit is shown in Table 4.2. These data were generated from the MIP solver by changing the co-generation system size using historical real-time prices from the ERCOT system for one year [56]. The annualized cost of expanding the co-generation system is calculated using data from Table 4.1 and is tabulated in Table 4.2. Also, the net profit obtained from increasing the co-generation system size is reflected in Table 4.2. It is used for co-generation system sizing decision based on the cost-benefit approach stated in [61].

From Table 4.2, it is recommended to increase the size of the co-generation system at the process facility up to the transfer capacity limit between the utility and the process facility. Note that increasing the size of the co-generation system beyond this point will not result in additional profit which creates a loss to the process facility coming from the capital cost of expanding the generation system size. The facility should not increase the generation system size when the incremental benefit from increasing the size of the cogeneration system becomes lower than the incremental cost of expanding the cogeneration system size. This occurs at 490 MW as seen in Figure 4.1.

Expanding the co-generation system size beyond 490 MW can be economically justified only if the incremental benefit exceeds the incremental cost of expansion the co-generation system in addition to the incremental cost of building a new transmission line. Providing a higher transfer capacity between the utility and process facility can increase its profit. Further expansion to the co-generation system size will increase the profit for the facility from selling energy to the utility and not from production level increase which is a change of business for the process facility. The most important qualitative result from this analysis is that there is no higher limit for generation system size which means that the process facility will become a generation facility instead of a gas processing facility. This is because the profit obtained from selling the added energy is higher than the cost of expanding the generation system at the process facility. Hence, it has been decided that the co-generation system size should not exceed three times the maximum load of the process facility, if it is economically justified, to maintain its core business, which is processing natural gas. This constraint has been determined from surveying the existing gas facilities in the Eastern region of Saudi Arabia and selecting the highest ratio of the generation system size to the peak load of the process facility.

Note that the small negative profit at a co-generation unit size of 250 MW comes from the generator cost curve linearization at a larger range which results in a higher marginal cost per unit of power which in turn results in a higher cost of producing one unit of final product. Table 4.3 shows the incremental cost per unit of power $/MW for a generator size of 245 MW and 250 MW respectively. The profit difference is very small and hence is negligible. However, it should be noted that as unit size becomes lager, the unit should be more efficient. So, it is proposed to include generator cost as a parameter based on unit size and fitting a curve for each generator coefficient based on data available from representative data in addition to data available from [63].

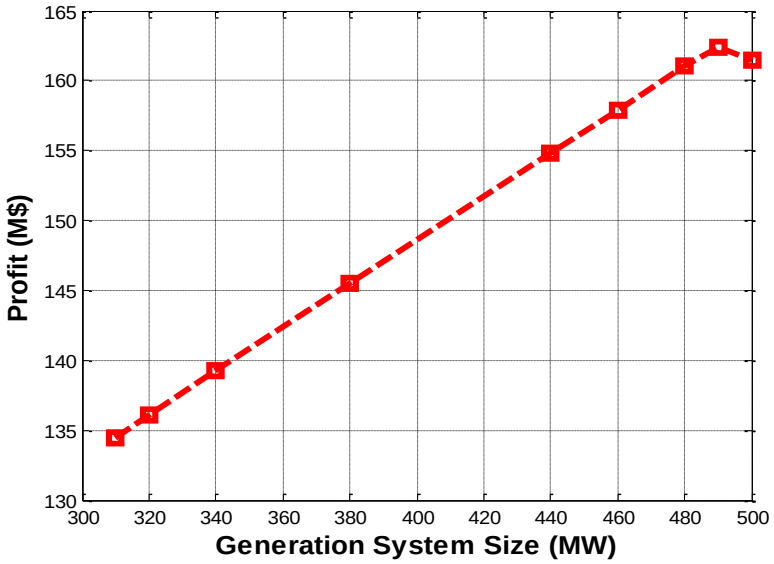

Figure 4.1. Profit of the process facility at different generation system capacities

For the quadratic coefficient of the cost curve of generators, the best fitted curve was found to be an exponential function as seen in Figure 4.2. The curve can be linearized for MIP implementation similar to [33].

Table 4.3. Marginal Costs of 245 MW And 250 MW Generation Units

Power Rating	MC1 ($/MWh)	MC2 ($/MWh)	MC3 ($/MWh)
245 MW	16.926	17.087	17.249
250 MW	16.928	17.094	17.259

Table 4.4. Cost Curve Parameters for Different Generators

P_{max} (MW)	a ($/MW^{2}h)	b ($/MWh)	c ($/h)
12	0.02533	25.5472	24.3891
20	0.01199	37.551	117.7551
76	0.00876	13.3272	81.1364
100	0.00623	18.00	217.8952
155	0.00463	10.694	142.7348
197	0.00259	23.00	259.131
350	0.00153	10.8616	177.0575
400	0.002	7.7169	319.3022

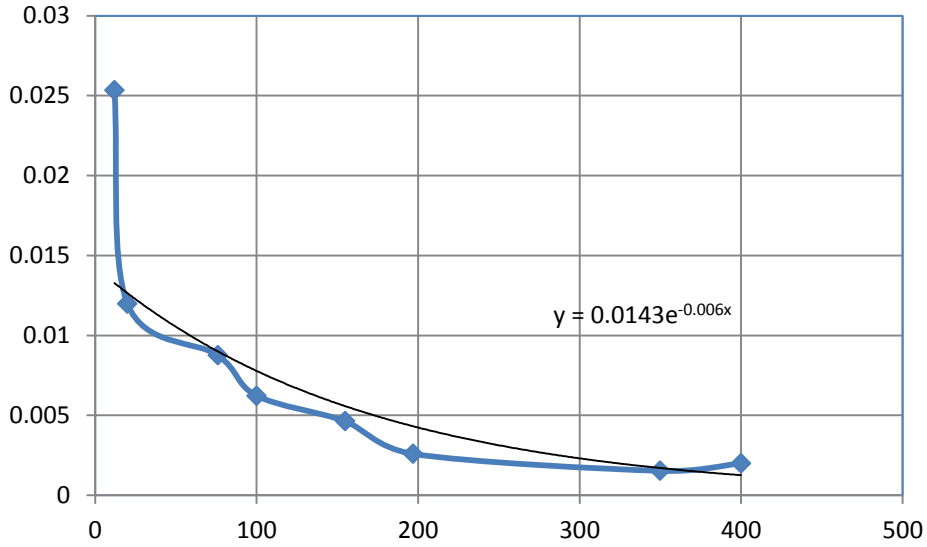

Figure 4.2. Curve fitting for the quadratic coefficient of generator's cost curve

4.4 Production Capacity Economic Evaluation and Sizing

The existing process facility is designed to produce 1,100 MBD of NGL products which is equivalent to 45.83 MB/hr. The cost-benefit analysis can take two different approaches; a new construction approach, and an expansion approach, which assumes that there is an existing infrastructure at the process facility. Table 4.5 shows the cost of two NGL projects in Saudi Arabia; one for new construction and the other for expanding an existing gas processing facility. In this section, the cost of expansion is used because the plant under study is an existing process facility. Also, the cost of expansion is much less than the cost of new construction. This in turn may make the economic analysis more feasible compared to the cost of new construction.

Table 4.5. Capital Cost of Two NGL Plants in Saudi Arabia [65, 66]

Project	Type	Production Capacity (BSCF)	Cost (M$)	Cost ($/SCF)
Wasit gas project	New Construction	2.5	4,600	1.84
Hawiyah NGL	Expansion	0.80	400	0.50

The annualized cost of expanding the production capacity was calculated using (4.1) and is reflected in Table 4.6. Table 4.7 shows the profit obtained from increasing the production capacity at the processing facility as well as the total annualized cost of expanding the existing process facility. Also, the net profit obtained from increasing the production capacity of the process facility is reflected in Table 4.7. It is used for production capacity decision based on the cost-benefit approach stated in [61].

From Table 4.7 results, it is not recommended to increase the production capacity for the process facility for RTPDR applications. Increasing the production capacity will result in a higher marginal cost compared to the marginal benefit captured by the process facility as seen in Figure 4.5. For example, increasing the production capacity by 1 MBD will result in an annual loss of approximately $6M. Expanding the production capacity of the process system beyond 60 MB/hr would require expanding the cogeneration or boiler systems, which results in an additional capital cost to be considered. Other considerations for the co-generation system expansion, beside the RTPDR application, might justify the current system size or even the future expansion cost, i.e. an economic analysis based on the predicted end-product price.

Table 4.6. Cost of Increasing the Production Capacity of the Process Facility

Max V (MB/hr)	Max V (MBD)	Δ V (MBD)	Cost ($)	Δ Cost ($/year)	Δ Maint. Cost ($/year)
45.83	1100	0	0	0	0
46.83	1123.92	23.92	74,080,790	6,272,500	2,222,424

Table 4.7. A Cost-benefit Analysis of the Production Capacity Expansion

Max V (MB/hr)	Profit ($/year)	TAC ($/year)	Net Profit ($/year)
45.83	134,494,000	0 (base case)	134,494,000
46.83	137,007,000	8,494,924	128,512,076

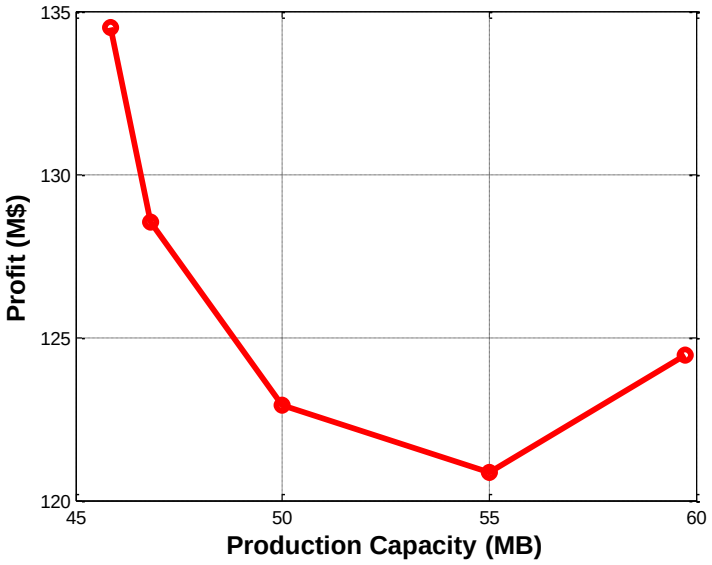

Figure 4.3. Profit of the process facility at different production capacities

4.5 Storage Tank Economic Evaluation and Sizing

The existing facility's storage system for the incoming raw material consists of nine 10,000 barrel bullet tanks and two 8,500 barrel sphere tanks making the total available storage to be 107,000 barrels of storage capacity.

The cost of the base case 107 MB storage tank was calculated using the following equation [67]:

$$A + B \cdot S^n \tag{4.3}$$

The expansion size was calculated using the formula listed in reference [67] as follows:

$$cost_a = cost_b \cdot \left(\frac{S_a}{S_b}\right)^n \tag{4.4}$$

Where S_a is the new equipment size, S_b is the reference equipment size, $cost_a$ is the estimated cost of new equipment, $cost_b$ is the reference equipment cost, n =0.7 for a petro-chemical process.

The annualized cost of expanding the storage system was calculated using (4.1) and is reflected in Table 4.8. Table 4.9 shows the profit obtained from increasing the storage system at the processing facility as well as the total annualized cost of expanding the storage system. Also,

the net profit obtained from expanding the storage system at the process facility is reflected in Table 4.9. It is used for storage system sizing based on the cost-benefit approach stated in [61].

From Table 4.9, it is recommended to increase the size of the storage system to maximize the profit of the process facility when it implements RTPDR. Note that increasing the size of the storage system is recommended until the marginal benefit captured by the process facility is less than the marginal capital cost of the expansion as seen in Figure 4.4 which results in a negative profit.

The outcome of this analysis is that expanding the storage system at the process facility allows selling more energy to the utility by varying the process and modifying the production level when the RTP of electricity is high. Then, compensating the production loss is done in periods of low RTP. This is useful to the process facility when it plans to participate in a RTPDR program. It is also important to consider the facility's response to the RTP of electricity during the design stage for the purpose of sizing the gas facility's storage system.

Table 4.8. Cost of Incoming Product Storage System at the Process Facility

V_s (MB)	V_s (m3)	Capital Cost ($)	Annualized Capital Cost ($/year)	Maintenance Cost ($/year)	TAC ($/year)
107	17,011	1,470,120	124,477	44,104	168,581
200	31,797	2,277,746	192,860	68,332	261,192
300	47,695	3,025,305	256,156	90,759	346,915
500	79,492	4,325,768	366,268	129,773	496,041
650	103,340	5,197,848	440,108	155,935	596,044
700	111,289	5,474,606	463,542	164,238	627,780
705	112,084	5,501,950	465,857	165,058	630,915

Table 4.9. Cost-benefit Analysis of the Storage System Expansion

Storage Tank Capacity (MB)	Facility's Profit ($/year)	Adjusted Total Annualized cost ($/year)	Facility's Net Profit ($/year)
107	134,451,000	0 (base case)	134,451,000
200	134,576,000	92,611	134,483,389
300	134,689,000	178,335	134,510,665
500	134,868,000	327,461	134,540,539
650	134,974,000	427,463	134,546,537
700	135,006,000	459,199	134,546,801
705	135,009,000	462,335	134,546,665

A marginal profit of less than 1% of the process facility's profit was obtained from expanding the storage system size. A contributing factor is the oversized generation capacity that resulted in a limited use for the storage system. A production level expansion was not considered due to its high capital cost, which also limited the use of the storage system. The added benefit from expanding the production level of the process facility due to RTPDR implementation should be considered with other factors such as the expected value of the Frac Spread and the expected future demand. This might influence the decision of expanding the process facility.

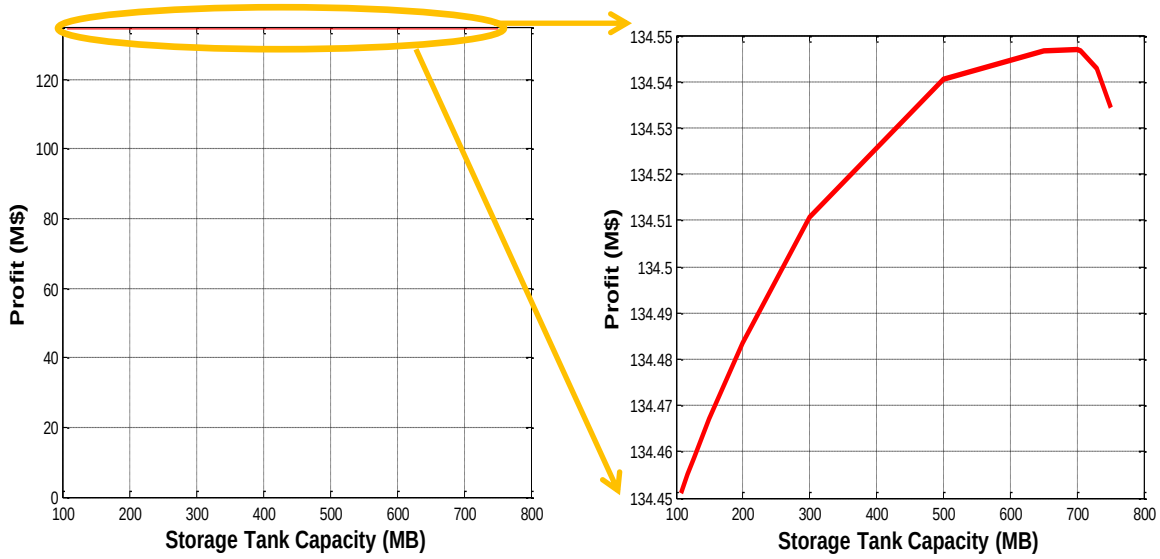

Figure 4.4: Process facility's profit at different storage system capacity

4.6 Optimization over Process Facility's Parameters

4.6.1 *Objective Function*

It has been shown that expanding the process facility's production level for the purpose of maximizing RTPDR profit is not economically feasible. However, cogeneration and storage systems expansion is economically justifiable for the added benefit from RTPDR implementation. Hence, the objective function can be reformulated to include the size of cogeneration and storage systems as follows:

$$\max_{\dot{v}_{p,t},P_g,u_g,S_b,u_b,P_u} \left\{ \sum_{t=1}^{T} \left(\left(Fs * \dot{v}_{o,t}\right) - \left[P_{u,t} * p_{u,t} + \sum_{g=1}^{G} u_{g,t} * C_g\left(P_{g,t}\right) + \sum_{b=1}^{B} u_{b,t} * C_b\left(S_{b,t}\right) + CSU_{g,t} \cdot su_{g,t} + CSU_{b,t} \cdot su_{b,t} \right] \right) - P_{size} * IC_P - V_{s,max} * IC_V \right\} \quad (4.5)$$

The formulation is similar to the formulation discussed in Chapter 3 but the objective function includes the cost of expanding the co-generation and storage systems. Note that P_{size} and $V_{s,max}$ are the process facility's design parameters that should be evaluated at different sizes to determine the effects of changing these design parameters on the net benefit for the RTPDR process facility.

4.6.2 *Discussion*

Multiple scenario evaluation for different generation and storage system sizes showed that there is an optimal storage system size for each generation system size. This suggests that storage system capacity is dependent on the generation system size. As generation system size increases, the optimal storage capacity decreases as seen in Table 4.10. This can be explained by the reduced need to change the process facility's production level in response to an increase in RTP of electricity, especially when the generation system is large and the transfer capacity limit between the process facility and the utility is reached.

The analysis of this work suggests increasing the generation system size up to the transfer capacity between the process facility and the utility after satisfying the facility's electricity demand. So, if the generation system size is 490 MW, there is no need to reduce the production capacity of the process facility because the peak demand of the facility is 90 MW while the transfer capacity is 400 MW. Hence, storage system has not been utilized and there is no added benefit from increasing the storage system capacity. However, if the generation system size is 310 MW, which is the current installed capacity of the process facility's generation system, then it is recommended to expand the storage system to be able to sell energy to the utility by varying the

production level and storing raw materials in the storage system which provides an added flexibility.

The outcome of the study highlights the importance of considering the process facility's response to the RTP of electricity during the design stage, especially for new RTPDR facility. This is due to the added flexibility of selecting design parameters that affects the facility's profit such as generation system size and storage system capacity.

Table 4.10. The Process Facility's Profit at Different Generation and Storage System sizes (K$)

V_s (MB)	$P_{g,max}$ (MW)						
	310	**320**	**340**	**380**	**440**	**490**	**500**
107	134,451	136,046	139,284	145,502	154,791	162,413	161,447
117	134,455	136,050	139,288	145,506	154,794	162,402	161,436
127	134,459	136,054	139,291	145,509	154,797	162,392	161,425
150	134,467	136,061	139,299	145,517	154,802	162,368	161,402
200	134,483	136,079	139,316	145,533	154,812	162,321	161,354
300	134,511	136,106	139,342	145,559	154,821	162,235	161,268
500	134,541	136,135	139,369	145,583	154,818	162,086	161,119
650	134,547	136,140	139,375	145,588	154,802	161,986	161,019
700	134,547	136,140	139,376	145,587	154,794	161,954	160,987
705	134,547	136,140	139,375	145,587	154,794	161,951	160,984

4.7 CONCLUSION

In this chapter, a cost-benefit approach for the design study of a gas processing facility is proposed for the implementation of a price-based demand response program that interacts with the RTP of electricity. A detailed design study for the process facility using three changing design parameters is conducted. Due to the lack of information about the Saudi Grid price profile, a historical DAM price profile from the ERCOT system was used in the design study of the process facility. The output of the study highlights the net benefit captured from changing the generation system size, the storage capacity, and the production capacity for an existing gas processing facility. Initial results recommend expanding the generation system size and the storage system capacity while keeping the production capacity at its current level.

The outcome of the analysis, multiple scenario evaluations, in this chapter recommends expanding the generation system size to sell more energy to the utility to benefit from fluctuation in the RTP of electricity. It independently recommends expanding the storage system capacity to allow for more product storage during periods of high RTP when the production level of the process system reduces or even shuts down completely. The analysis shows that there is an optimal storage system size that changes as the size of the generation system changes. Hence, storage system capacity is dependent on the generation system size. This can be explained by the reduced need to change the process facility's production level in response to an increase in RTP of electricity when the generation system is large and the transfer capacity between the process facility and the utility is reached.

The gas processing facility owner designs the size of the cogeneration system to serve the process system requirement. However, the qualitative analysis in this chapter recommends expanding the cogeneration system size beyond the process system needs. So, what started up as a gas facility with a cogeneration system has turned into a cogeneration system with an attached gas facility. The question is then whether to globally build more independent generation or attach it to a gas facility. This opens the question of whether the gas facility should expand its cogeneration system or the utility generation capacity be expanded, which is decided by social benefit. If the gas facility decides to expand the cogeneration system size, then it will compete with other power generation facilities instead of competing with facilities in similar business, which is a decision that needs to be made by the gas facility's owner.

The qualitative analysis in this chapter is tailored toward testing major design parameters that affect the implementation of a RTPDR program in a gas process facility. The analysis can be expanded to other industrial facilities that have thermal and process constraints. The analysis in this chapter examined each design parameter in isolation. However, initial results indicated an interdependence of the design parameters of the process facility, which suggests room for improvement by formulating a multi-variable design study that can decide the optimal size of each parameter simultaneously. The formulation of the multi-variable design study was found to require a major reformulation and a possible change of the selected optimization technique and solver. In this case, the use of a non-linear solver might be needed.

Initial results of the conducted design study suggest that the captured benefit from varying the aforementioned parameters is influenced by the RTP profile, which is not currently available

for the Saudi Grid. Hence, once RTP data for the Saudi Grid becomes available, then the results of the design study are expected to be more accurate.

In the next chapter, a study of the effects of RTPDR implementation on a small-scale utility system is proposed. Then, several RTPDR loads are modelled into the single-bus Saudi Grid model to study the effects of RTPDR participation in the electricity market. The RTP of electricity is expected to become lower during high RTP of electricity and higher during low RTP of electricity. This in turn improves social welfare of the society and serves the purpose of peak shaving, which can defer the urgent need for upgrading the Saudi Grid to cope with exponentially increasing electricity demand.

Chapter 5. REAL-TIME PRICE DEMAND RESPONSE EFFECTS ON THE ELECTRICITY MARKET AND POWER SYSTEM

5.1 INTRODUCTION

Simulation results from Chapter 2 show that RTPDR can be successfully implemented in a gas processing facility that owns an internal co-generation system. It can respond partially by increasing its co-generation system output to reduce load seen by the utility, and it can respond fully by changing its production level as well.

Chapter 3 proposed an optimal scheduling algorithm over a time horizon for a gas processing facility that implements RTPDR. This chapter proposes to extend this work by studying the effects of RTPDR on the power system to which the plant is connected. Understanding the impact of RTPDR on RTP is very important for industrial participants because it can affect a plant's decision about its optimal production level as well as setting the power output of its generators, which in turn affect its profit. A process facility's profit is influenced by the value and volatility of the RTP of electricity. It is expected that the electricity price becomes lower in presence of several price-responsive loads. The volatility of the RTP of electricity is expected to reduce. Hence, the electricity price is expected to be more stable. Hence, the process facility's profit is expected to reduce in presence of other RTPDR loads that are connected to the same grid.

Chapter 4 performed a design study for a RTPDR load, a gas processing facility. Results of the study suggested that increasing the co-generation and storage systems size might generate more profit for the plant due to the added flexibility. The design study did not recommend increasing the production capacity of the process facility in the context of RTPDR because the annualized cost of the expansion is greater than the observed annual benefit. Also, the study highlighted that the expansion of the storage system yielded a marginal benefit that required a huge investment. Also, a risk analysis that considers fluctuation of the RTP of electricity might be needed. The process facility does not favor the expansion of the storage system due to its internal policy for the minimum allowed annual rate of return on investment.

Several papers highlighted the importance of studying the impact of DR on the power system. However, only a few showed some experimental results. The authors in [23] highlighted the need for a tool to quantify DR effects. The paper used a statistical method to simulate a large system for planning and policy analysis and reflect DR benefits for an electricity market. In [19], the authors stated some issues related to DR implementation such as showing customer benefit and having a DR model. The authors in [20] highlighted the need for an evaluation tool for the social benefits of DR. The authors in [13] discussed some issues associated with quantifying DR benefits. They highlighted the challenge of estimating the change in demand that will be achieved in addition to evaluating these effects on the power system behavior. In [10], a statistical model, Support Vector Machine regression algorithm, is used to come up with a demand response model in order to quantify the DR characteristic. The accuracy of the model depends on the proper selection of input attributes to the model. The authors in [21] discussed market performance in the presence of DR and its effects on LMP. They also highlighted the need to study the local and global effects of DR in the electricity market. The most widely known DR experiment is the Olympic Peninsula Project in which residential customers were allowed to set their zone of comfort that corresponds to a different bidding strategy to deal with a RTP of electricity that changes based on the load level of a distribution feeder. The study showed that RTPDR can change consumer behavior and it solved the issue of an overloaded 13.8KV distribution feeder [16]. However, this experiment did not address wide implementation of RTPDR resources. Another study validated the results of the Olympic Peninsula Project about price-responsiveness of loads. In addition, the paper used model predictive control for the purpose of minimizing power imbalance [68].

RTPDR is expected to have local and global effects on the electricity market performance. Even at a low penetration level, a RTPDR resource might be able to reduce the RTP of electricity when it reduces its consumption as a result of an increase in RTP of electricity, which is likely to happen during transmission congestion or loss of generation. Local effects of RTPDR can be easily analyzed from the relationship between demand and supply at the local node. However, global effects of RTPDR are not easily determined because demand affects power flow and transmission congestion which is dependent on the system topology. So, a change in demand in one bus might result in a change of the RTP at other buses. If a RTPDR load that is located at the receiving end of a congestion transmission line changes its consumption as a result of a change

in the RTP of electricity, it is expected that the RTP of electricity reduces slightly in all buses. The reason for the expected price drop at all buses is that expensive generators are not dispatched which reduces the total cost of generating electricity and hence RTP of electricity reduces. However, expensive generators might be dispatched to satisfy network constraints such as transmission congestion. This in turn results in an increase of the total cost of generating electricity. It can also increase load payment if load concentration is in the area that experienced RTP increase. A numerical example of this scenario is discussed in the three-bus test case [21].

Literature review shows the importance of quantifying the large-scale effects and benefits of DR which emphasizes the importance of this work. It also shows that the field is not well established and more work needs to be accomplished in this area. Hence, the work in this chapter is dedicated to studying the effects of RTPDR on the future Saudi Electricity Market.

This chapter proposes to study the effects of DR implementation on a demonstration utility power system, a single-bus model. Then, the study expands to a small-size test system that has transmission network, the three-bus test case in [69], for further evaluation. A responsive load that constitutes a similar penetration level of DR resources to system load in Saudi Arabia (around 6%) is modeled into the three-bus test case to demonstrate the qualitative effect of RTPDR on an electricity market. The three-bus test case is carefully selected to demonstrate the reaction of a RTPDR load in presence of system events such as the occurrence of negative RTPs of electricity, the limitation of generated power transfer due to transmission system congestion, and the loss of generation. It is then proposed to model and analyze a possible form of the future Saudi Electricity market, which is discussed with details in section 5.3.2.

The analysis introduced in this chapter is expected to show that RTPDR can reduce RTP volatility. Because RTPDR loads react to a change in electricity price, they increase when RTP reduces and they decrease when RTP increases. This in turn serves the purpose of peak shaving. Social welfare of the Saudi Market is expected to improve due to the reduction of the RTP, which decreases generation profit and increases consumer surplus.

Market power effects is expected to reduce because RTPDR load reduces as RTP increases which can expose generation companies to a loss when they increase the price of electricity by having the risk of not being able to find a consumer that is willing to purchase energy. Hence, generators are more motivated to bid their incremental cost which makes the market more efficient and improves the social welfare of society.

The analysis in this chapter advances the existing work in this area by modeling several large price-responsive industrial facilities into the electricity Grid, and the inclusion of a detailed process model of these facilities. Also, the study allows each industrial facility to react to the RTP in a way that maximizes its profit based on the outcome of an optimization algorithm rather than heuristic. This helps to study the impact of RTPDR and quantify its effects not only from the utility side but also from a large consumer's side as well. This in turn helps large industrial facilities that respond to the RTP to capture more benefits from fluctuating electricity prices. If a high penetration level of RTPDR load exists, DR competition might reduce the claimed benefits captured by RTPDR load, which is another motivation for studying the effects of RTPDR on a realistic test case, the Saudi Grid. Results are expected to quantify the approximate benefits captured by RTPDR loads to motivate their participation. RTPDR has also the potential to improve the reliability of the electric grid by relieving congestion and solving the issue of generation shortage, avoiding load shedding and reducing the chance of having a high RTP that can lead to a market failure. In addition, it can defer major transmission and generation system upgrades motivated by the rapid growth in electricity demand.

5.2 DISCUSSION

When the RTP of electricity is applied to industrial facilities, several facilities are expected to participate in a RTPDR program due to the available financial incentive that is captured from reacting to fluctuating electricity prices, which is discussed in detail in Chapter 3. To date, studies have shown that DR is effective in reducing residential load to solve focal issues facing the utility and power system [16]. The integration cost of DR is modest and almost negligible, especially for newly constructed industrial facilities, due to the design practice of having a master central control system at these facilities. However, as DR installations continue their precipitous growth, the scalability of DR might come into question. An increase in the total capacity of responding loads, particularly in close geographic proximity, might require studying the impact of RTPDR loads on the volatility of the market prices in addition to its effects on the power system. The main focus of this research is to study the effect of RTPDR on both the RTP of electricity and the power system. It is motivated by the ability of RTPDR to relieve congestion or mitigate the issue of shortage of generation during peak periods, which might be encountered in the future Saudi electricity market, especially with the current rapid growth of electrical load in Saudi Arabia.

The technological feasibility of DR and its integration has been shown in various researches [16, 8]. However, the adoption of DR as a preferred method of energy cost saving will be based on its economic viability and advantage when compared with other methods. The economic viability should be evaluated with respect to the DR strategy, the electricity market that dictates energy prices and the industrial facility in which production, storage, and internal generation are operated. The cogeneration system at the industrial facility behaves as any other market participant, reacting to market signals for economic gain in addition to increasing the flexibility of the facility's response to the electricity market price.

5.3 THE SINGLE-BUS TEST SYSTEM

To create a general sense of the impact of RTPDR load in the electricity market, two test cases were analyzed. Qualitative analysis from the test cases was used as a guide to understand RTPDR behavior and interpret the results of RTPDR implementation in a more realistic test case, approximating the Saudi Grid.

The single-bus system is used as a theoretical model to illustrate RTPDR effects and guide calculations in the detailed models that are introduced in the subsequent sections. It provides the qualitative analysis for the captured benefits from RTPDR load participation and its local effects on a simple single-bus test system.

The single-bus model consists of 341 generators representing the Saudi Grid generation resources and a lumped load that contains an elastic and inelastic load. It is assumed that all generators bid their incremental cost. The demand curve for the elastic load is assumed to be linear for the theoretical discussion which means that it bids its total load at the lowest price and bids zero load at the highest price. A numerical example that considers the process facility's non-linear bid curve is also discussed in this chapter.

The single-bus model is used for the qualitative analysis of the local effects of RTPDR. It does not analyze system-wide effects of RTPDR because it does not represent the entire system model. This is mainly because the single-bus model does not model the transmission system which impacts the effects of RTPDR when the electrical system constraints are in effect such as transmission usage, generation dispatch, etc.

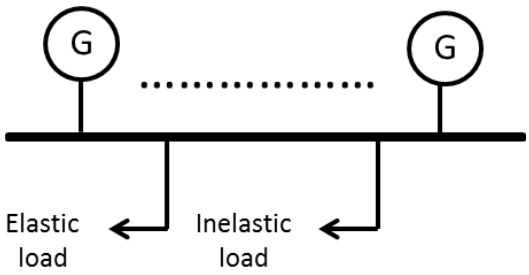

Figure 5.1. The single-bus test system

5.3.1 *Introduction to Social Welfare*

Social welfare is very important to the society and its economics because it provides an indication of the amount of benefit the society gets from paying a cost for a good or service. Worth is the willingness of the society to pay for a good or service which is the area under the demand curve. Figure 5.2 shows the worth of an elastic load and inelastic load. Note that the inelastic load worth is, in theory, infinite. Inelastic demand is willing to pay the energy price even if it is high. This is mainly due to the inability of the demand to change its quantity when the RTP of electricity changes. Elastic load, however, does not face the same situation and its willingness to pay for electricity changes when the energy price changes.

In a perfect competition environment, generators bid their incremental cost. So, the cost is the area under the supply curve. Figure 5.3 shows the cost of serving an elastic load and an inelastic load.

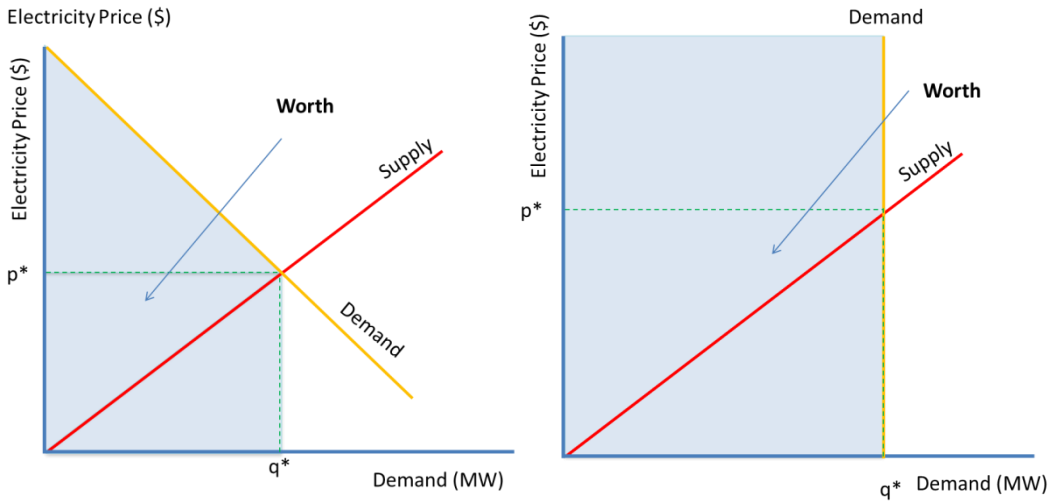

Figure 5.2. The worth of an elastic load (left); the worth of an inelastic load (right)

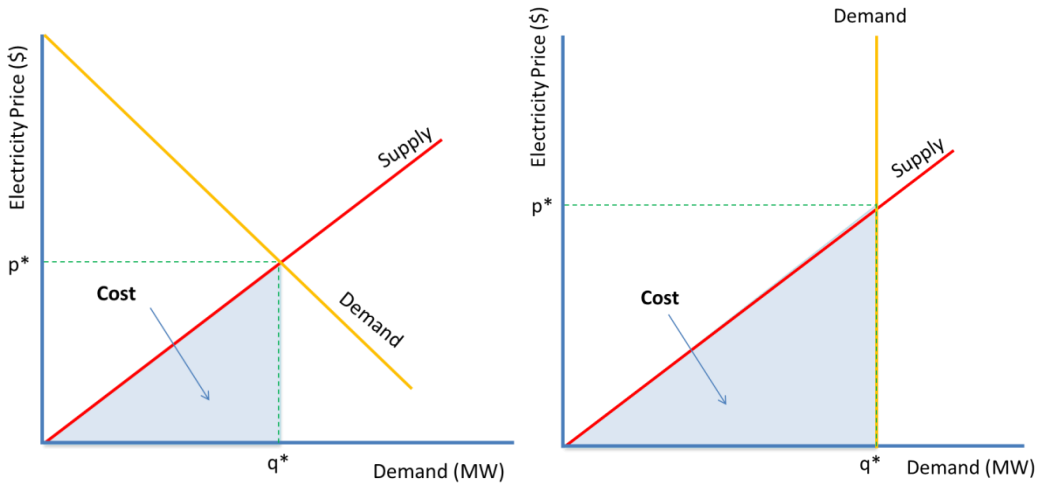

Figure 5.3. The cost of serving an elastic load (left); the cost of serving an inelastic load (right)

Social welfare (SW) is the difference between the worth and the cost which is the highlighted area of the triangle between the supply and demand curves in Figure 5.4. It can be mathematically represented as:

$$SW = Worth - Cost \tag{5.1}$$

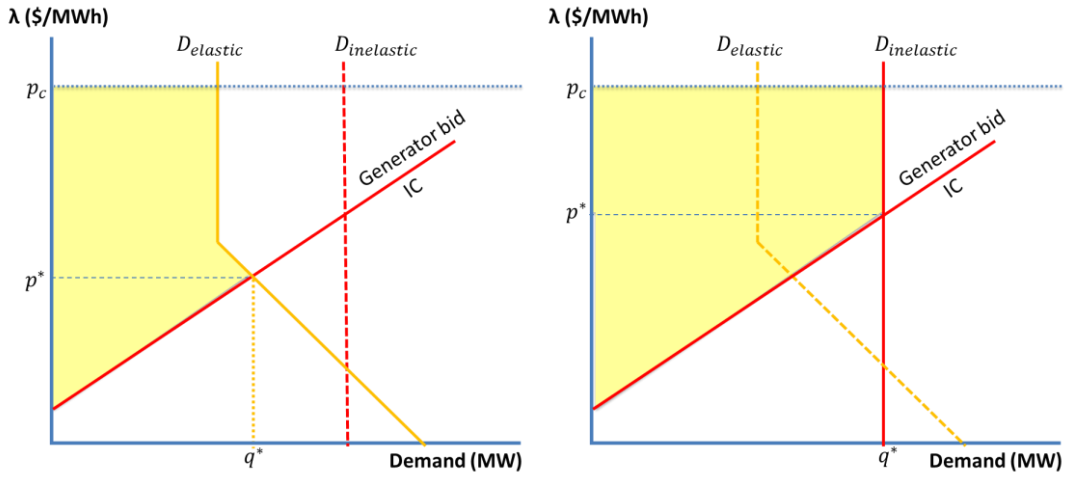

Figure 5.4. Social welfare of an elastic load (left); Social welfare of an inelastic load (right)

Figure 5.4 shows the social welfare of an elastic load and an inelastic load. Note that even though the social welfare of the inelastic load is infinite, a change in social welfare can still be computed by imposing a price cap. The social welfare of an elastic load is represented by the shaded area in the left side of Figure 5.4 while the social welfare of an inelastic load is represented by the shaded area in the right side of Figure 5.4. Figure 5.4 splits social welfare into two parts; consumer surplus (CS) and supplier's profit (SP). Consumer surplus represents the amount of money that consumers saved which is the difference between the market price and their willingness to pay for energy. Supplier's profit represents the extra revenue gained by generation companies which is the difference between the market price and the cost of energy. Hence, it can be mathematically represented as:

$$SW = SP + CS \tag{5.2}$$

To illustrate the idea, a numerical example is provided. If an elastic load has a demand curve that bids its total load when the electricity price is \$10/MWh and shuts down completely when the electricity price is high, \$100/MWh. Generation companies are assumed to bid their incremental cost in the supply curve and market equilibrium occurs when demand equals supply. Assume the equilibrium quantity (q^*) is 50 MW and the equilibrium price (p^*) is \$40/MWh, Then, social welfare is the area of the triangle between the supply and demand curves in figure 5.4, which consists of the supplier's profit and consumer surplus. Supplier's profit is \$1,000/hr and consumer surplus is \$1,500/hr. Hence, social welfare equates to \$2,500 /hr.

RTPDR Effects on Social Welfare: Electrical load is usually partially elastic and partially inelastic load. To examine the theoretical effects of price-responsive loads on social welfare of the society, two cases are introduced when a partially-elastic demand curve is considered. The first case represents a reduction in load for the elastic scenario. The other case represents an increase in load consumption for the elastic scenario. The demand curve for the partially-elastic load represents a RTPDR load that reduces as RTP increases and increases as RTP decreases. In the inelastic scenario, load does not change when RTP fluctuates. Also, a change in social welfare can be measured from either calculating the change in consumer surplus and generation profit or from calculating the change in worth and cost respectively.

In the first case, if a load is treated as an inelastic load while it is believed that it is partially elastic and partially inelastic load, then generation profit increases and consumer surplus

decreases as per Figure 5.5. In Figure 5.5, the partially-elastic consumer, at q, is willing to pay p_1 for the next MWh of energy. However, it is forced to pay p_2^* instead causing the consumer to lose $p_2^* - p_1$. On the other hand, generators at q are willing to sell the next MWh of energy at a rate of p_2/MWh. However, they are offered p_2^*/MWh instead which increases their profit by $p_2^* - p_2$. Hence, it is clear form Figure 5.5 that the net loss is more than the benefit obtained from treating a partially-elastic load as an inelastic load. Hence, the net effect on social welfare is a loss of $p_2 - p_1$.

To understand social welfare effects of treating an elastic load as an inelastic load in the load-reduction case, Figure 5.5 and Figure 5.6 are created. There are two ways to interpret Figure 5.6; the intuitive way and the actual way. The intuitive way is to compare social welfare between elastic and inelastic demand scenarios, as seen in Figure 5.4. Figure 5.4 clearly shows that social welfare of an inelastic load is higher than social welfare of an elastic load. However, analyzing the areas in Figure 5.5 and Figure 5.6 shows that social welfare for the inelastic demand is represented by areas A, B, C, D, E, and F. However, social welfare for the partially-inelastic demand is represented by areas B, C, D, and E. Hence, a reduction in social welfare is concluded.

The actual way to look at Figure 5.6 is to measure the change in social welfare from treating an elastic load as an inelastic load. In this case, market price is higher and generator's profit increases by area F. However, consumer surplus decreases by area F and G. Hence, the net effect in social welfare is a reduction by area G as shown in Table 5.1. Also, load payment increases due to the increase in electricity market price which is contributed to by an increase in demand in addition to the deployment of expensive peaker generators. This can be used as an economical motivation to treat the RTPDR load as an elastic load which frequently results in a lower electricity bills for consumers. It can also help strengthening a policy point of view, to create regulations that would transfer benefits from generators to consumers in the form of reduced electricity bills.

Table 5.1. Social Welfare Change from Treating an Elastic Load as an Inelastic Load (case-1)

Δ **Generation profit**	Increase by area F
Δ **Consumer surplus**	decrease by area F and G
Δ **Social welfare**	decrease by area G

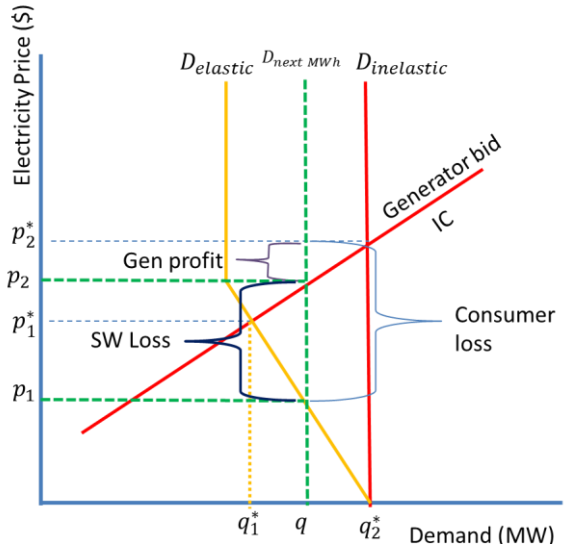

Figure 5.5. Effects of treating a partially-elastic load as an inelastic load (case-1)

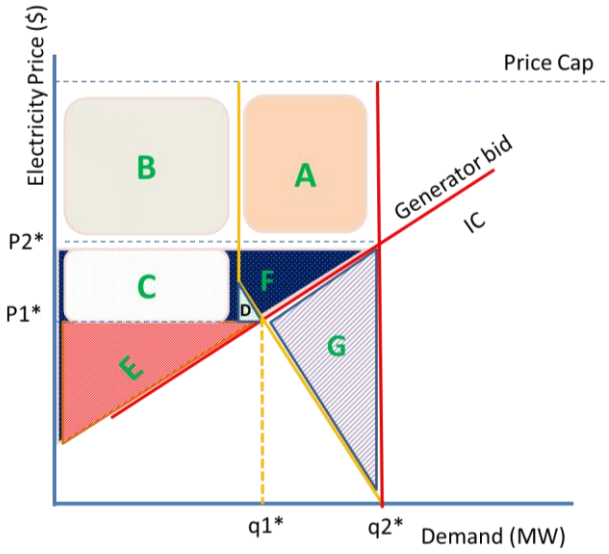

Figure 5.6. Social welfare change from treating an elastic load as an inelastic load (case-1)

In the second case, if the load is treated as partially elastic and partially inelastic load instead of being treated as an inelastic load, then generation profit increases and consumer surplus also increases as per Figure 5.7. In Figure 5.7, the partially-elastic consumer, at q, is willing to pay p_1 for the next MWh of energy. However, if the load is treated as a partially elastic load, then it will pay p_1^* instead causing the consumer to gain $p_1 - p_1^*$. On the other hand, generators at q are willing to sell the next MWh of energy at a rate of p_2/MWh. However, they are offered p_1^*/MWh instead which increases their profit by $p_1^* - p_2$. Hence, it is clear form Figure 5.7 that the net

effect is an improvement of social welfare from treating the load as a partially-elastic load instead of an inelastic load. Hence, the net effect on social welfare is an increase by $p_1 - p_2$ as seen in Figure 5.7.

To understand the effects of treating an elastic load as an inelastic load in the social welfare for the second case, Figure 5.8 has been created. There are two ways to interpret Figure 5.8; the intuitive way and the correct way. The intuitive way is to compare social welfare between the elastic and inelastic demand scenarios. Similar to the load-reduction case, a decrease in social welfare is concluded.

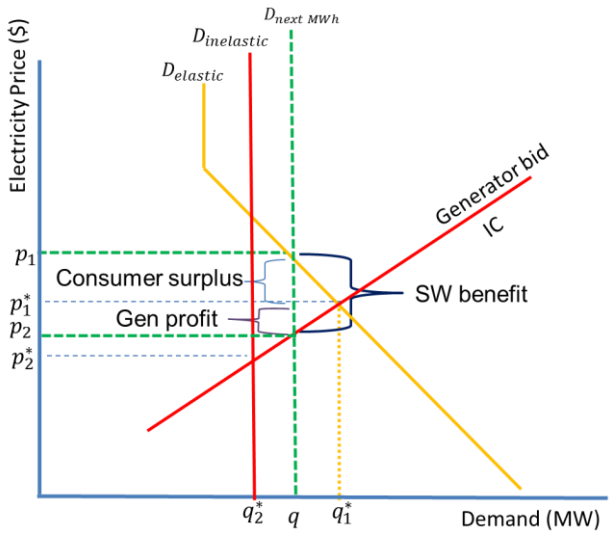

Figure 5.7. Effects of treating a partially-elastic load as an inelastic load (case-2)

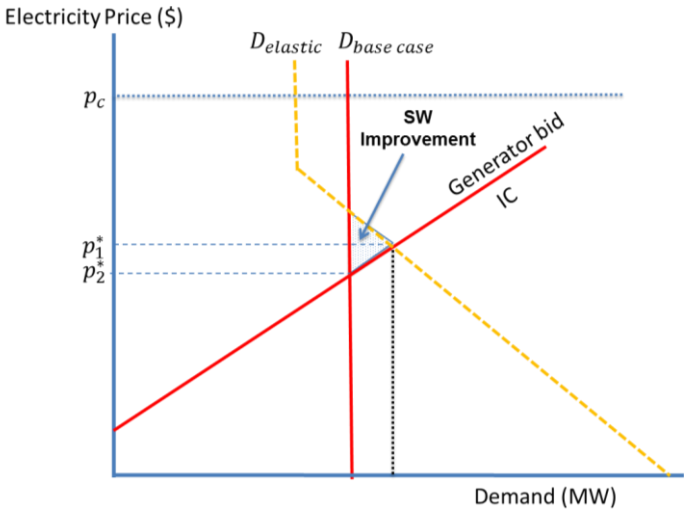

Figure 5.8. Social welfare change from treating an elastic load as an inelastic load (case-2)

The correct way to look at Figure 5.8 is to measure the change in social welfare from treating a price-responsive load as an inelastic load. In this case, market price is lower which decreases generation profit. Consumer surplus faces two effects. The first effect is an increase in consumer surplus by the amount of load payment increase which is $p_1^* - p_2^*$ for every MW of load consumption up to q_2^*. The second effect is an reduction in consumer surplus by $p_1 - p_1^*$ for every MW of load consumption between q_2^* and q_1^*. The net effect is expected to be an improvement of consumer surplus by the difference of the two effects for the inelastic scenario, as seen in Figure 5.8. Note that the improvement effect of consumer surplus is cancelled by the reduction effect on generation profit, up to q_2^*. Hence, social welfare value is not expected to change, up to q_2^*. The area of the shaded triangle in Figure 5.8 is the lost social welfare from treating elastic load as an inelastic load, which represents the area of the difference between worth and cost for the elastic load. Load payment is expected to be higher due to the increased electricity market price, which is contributed to by an increase in load consumption in addition to the deployment of expensive peaker generators.

5.3.2 *Modelling the Saudi Grid*

The Saudi Grid data are not publically available. To create an approximate model the single-bus model for the Saudi Grid, generation data for the Saudi Grid were collected from various resources. This includes the number of generation units per power plant, generation capacity for each unit, type of turbine, and fuel type used [70, 71, 72, 73, 74, 75, 76, 77]. The collected data are then used to identify similar generators for the purpose of constructing the heat curves for all generators in the Saudi Grid. Fuel cost data was collected from [70] as listed in Table 5.2. Data from [70, 78] were filtered and fitted to establish the cost curve for every generator in the Saudi Grid.

Table 5.2. Cost for Different Types of Fuel at the Subsidized Fuel Price [55]

Fuel Type	**Cost ($/MMBTU)**
Gas	0.75
Oil	0.74
Diesel	0.63

5.3.2.1 Social Welfare Contribution of a RTPDR Injection

The total system worth consists of the sum of individual loads' worth for the whole system. Similarly, the total system cost consists of the sum of individual generators' cost for the whole system. The analysis in this section is used to determine the net social welfare contribution of a RTPDR injection that consists of both generation and load by proving that the net injection of a RTPDR injection contributes to the social welfare as a net cost when it is considered as a generator or as a net worth when it is considered as a load, as long as the proper sign is used when representing the net social welfare contribution from a RTPDR injection. Figure 5.9 shows the injection of a RTPDR facility as equivalent to a separate load and generator.

The generator and load of the RTPDR facility in Figure 5.9 should be reflected to their equivalent power injection components. The elastic cost in Figure 5.3 does not change its shape because it follows the sign of the power injection while the elastic worth in Figure 5.2 should be transformed into an equivalent power injection, as seen in the top left side of Figure 5.10. The equivalent curve for the RTPDR injection is shown in the lower side of Figure 5.10.

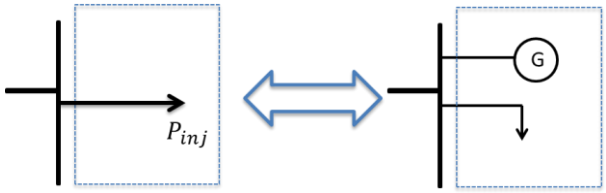

Figure 5.9. The equivalent power injection of a RTPDR facility

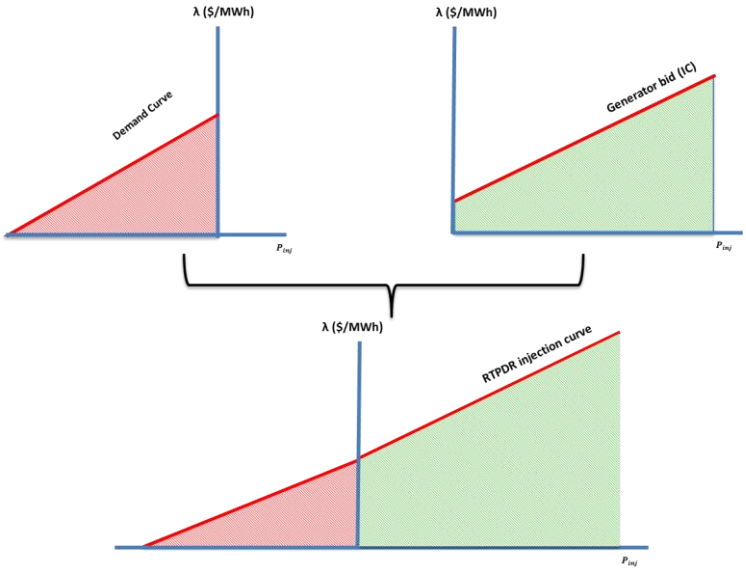

Figure 5.10. The equivalent social welfare contribution of a RTPDR facility

Proof: For the demand curve: $\lambda = f_d(P_d)$ and for the supply curve: $\lambda = f_s(P_g)$

Assume that $f_d(P_d)$ and $f_s(P_g)$ are monotonic. Then, $f_d^{-1}$and f_s^{-1} exist.

Hence, the inverse functions can be written as:

$$P_d = f_d^{-1}(\lambda) = g_d(\lambda)$$

$$P_g = f_s^{-1}(\lambda) = g_s(\lambda)$$

Now, let's calculate the social welfare contribution of individual components:

$$\mathrm{C}(P_G) = \int_0^{P_g} f_s(P_g)\, dP_g$$

$$\lambda = f_s(P_g)$$

$$d\lambda = f_s'(P_g)\, dP_g = f_s'(g_s(\lambda))\, dP_g$$

$$dP_g = \frac{d\lambda}{f_s'(g_s(\lambda))}$$

Using integration by substitution, we get the following:

$$C(P_G) = \int_{f_s(0)}^{f_s(P_g)} \lambda \cdot \frac{d\,\lambda}{f_s'(g_s(\lambda))} = \int_{f_s(0)}^{f_s(P_g)} \frac{\lambda}{f_s'(g_s(\lambda))}\, d\,\lambda \qquad (5.3)$$

Similarly,

$$W(P_d) = \int_0^{P_d} f_d(P_d)\, dP_d$$

$$\lambda = f_d(P_d)$$

$$d\lambda = f_d'(P_d)\, dP_d = f_d'(\mathrm{g_d}(\lambda))\, dP_d$$

$$dP_d = \frac{d\,\lambda}{f_d'(\mathrm{g_d}(\lambda))}$$

By performing integration by substitution, we get the following:

$$W(P_d) = \int_{f_d(0)}^{f_d(P_d)} \lambda \cdot \frac{d\,\lambda}{f_d'(g_d(\lambda))} = \int_{f_d(0)}^{f_d(P_d)} \frac{\lambda}{f_d'(g_d(\lambda))}\, d\,\lambda \tag{5.4}$$

Social welfare contribution of the individual components of the RTPDR injection is:

$$\mathrm{SW} = W(P_d) - C(P_G)$$

$$= \int_{f_d(0)}^{f_d(P_d)} \frac{\lambda}{f_d'(\mathrm{g_d}(\lambda))}\, d\,\lambda - \int_{f_s(0)}^{f_s(P_g)} \frac{\lambda}{f_s'(\mathrm{g_s}(\lambda))}\, d\,\lambda \tag{5.5}$$

The net RTPDR injection can be written as follows:

$$P_{i,DR} = P_{G,DR} - P_{D,DR}$$

Hence, social welfare contribution of the RTPDR injection, as seen in Figure 5.10, is:

$$\mathrm{SW} = -C\left(P_{i,DR}\right) = -\int P_{i,DR}\, dP_i \tag{5.6}$$

$$C(P_{i,DR}) = \int_{-P_d}^{P_g} f\left(P_{i,DR}\right) dP_i \tag{5.7}$$

By properties of integration, (5.7) can be written as:

$$\int_{-P_d}^{0} f_d(P_d)\, dP_i + \int_{0}^{P_g} f_s\left(P_g\right) dP_i$$

Using integration by substitution, we get the following:

$$\int_{f_d(-P_d)}^{f_d(0)} \frac{\lambda}{f_d'(\mathrm{g_d}(\lambda))}\, d\,\lambda \;+\; \int_{f_s(0)}^{f_s(P_g)} \frac{\lambda}{f_s'(\mathrm{g_s}(\lambda))}\, d\,\lambda \tag{5.8}$$

From (5.6), (5.7) and (5.8), social welfare of the RTPDR injection can be written as:

$$\mathrm{SW}(\,P_{i,DR}) = -\left\{ \int_{f_d(-P_d)}^{f_d(0)} \frac{\lambda}{f_d'(\mathrm{g_d}(\lambda))} d\lambda \;+\; \int_{f_s(0)}^{f_s(P_g)} \frac{\lambda}{f_s'(\mathrm{g_s}(\lambda))} d\lambda \right\} \tag{5.9}$$

Using integral properties, (5.9) can be written as:

$$\mathrm{SW}(\,P_{i,DR}) = \int_{f_d(0)}^{f_d(P_d)} \frac{\lambda}{f_d'(\mathrm{g_d}(\lambda))}\, d\,\lambda - \int_{f_s(0)}^{f_s(P_g)} \frac{\lambda}{f_s'(\mathrm{g_s}(\lambda))}\, d\,\lambda \tag{5.10}$$

Combining (5.3), (5.4) and (5.10), we get the following:

$$\mathrm{SW}(\,P_{i,DR}) = \mathrm{W}(P_d) \;-\; \mathrm{C}(P_G) \tag{5.11}$$

Reflecting The RTPDR injection components into the demand curve yields the following:

$$P_{D,net,DR} = P_{d,DR} - \; P_{g,DR}$$

Using similar proof approach, social welfare contribution of the RTPDR injection can be written as:

$$\mathrm{SW}(P_{D,net,DR}) = \mathrm{W}(P_d) \;-\; \mathrm{C}(P_G) \tag{5.12}$$

The above proof confirms our understanding of the social welfare contribution of a RTPDR injection. The social welfare of a RTPDR injection is equal to the social welfare contribution of the RTPDR injection worth plus the social welfare contribution of the RTPDR generation cost.

The contribution of a RTPDR injection to social welfare is the generation cost. Generation cost is usually the integration of the incremental cost and load worth is usually the integration of the demand curve. However, the generation cost of the RTPDR injection in this case is the integration of the incremental cost of the RTPDR generation less the integration of the demand curve of the RTPDR injection. The outcome of this proof is used as the basis for incorporating the RTPDR injection into the DCOPF model.

5.3.2.2 Modelling a RTPDR injection into the Saudi Grid DCOPF

There are two cases that are considered for modelling a RTPDR injection. The first case represents a negative RTPDR injection, which means that the RTPDR injection decides to import power from the utility to maximize its profit. In this case, the chosen method to represent the RTPDR injection in a DC optimal power flow environment is to treat the price-responsive net load of the RTPDR injection as a negative generator with an associated negative cost similar to [79], as seen in Figure 5.11 and Figure 5.12. In this case, the area shaded in orange in Figure 5.12 represents a negative cost or a positive worth for the net load of the RTPDR injection, as discussed in section 5.3.1.1. The second case represents a positive RTPDR injection, when the RTPDR injection decides to export power to the electricity market, based on its profit maximization algorithm that is discussed in Chapter 3, as seen in Figure 5.13 and Figure 5.14. The net bid value of the RTPDR injection is dependent on the bid curve of the price-responsive injection and the LMP value at the RTPDR bus.

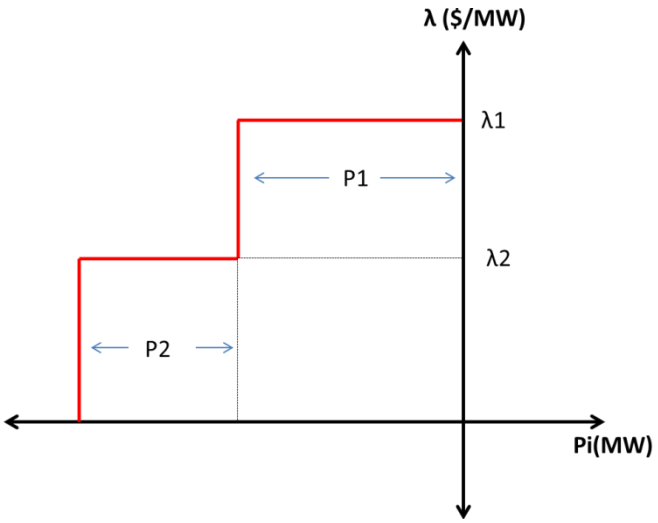

Figure 5.11. Bid Curve for the negative RTPDR injection

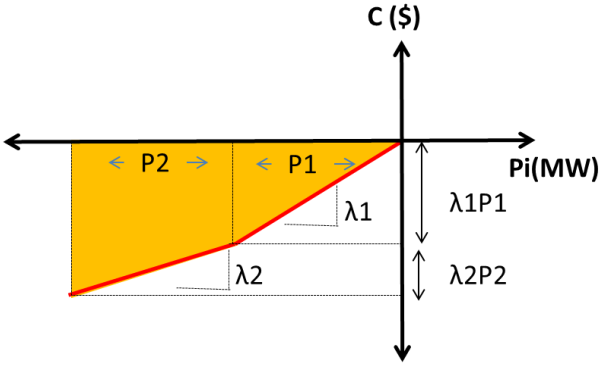

Figure 5.12. Cost function for the negative RTPDR injection

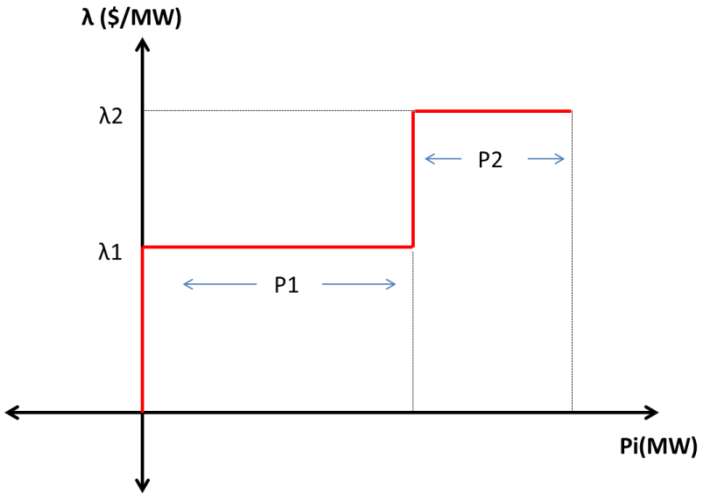

Figure 5.13. Bid Curve for the positive RTPDR injection

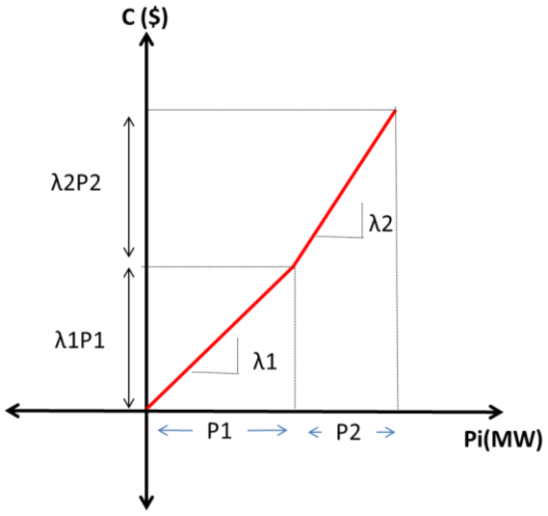

Figure 5.14. Cost function for the positive RTPDR injection

Discussion of the RTPDR Injection Model: The bid curve and the cost function for the positive and negative injections for the RTPDR injection are discussed in the previous section. The cost function of the RTPDR injection converts the bid curve of the RTPDR injection into a benefit function that maximizes the profit for the RTPDR facility.

The RTPDR injection is expected to receive an extra benefit from participating in the electricity market in addition to the benefit obtained from its bid curve. The extra benefit is classified as either a DR profit when the net value of the RTPDR injection is positive or DR surplus when the net value of the RTPDR injection is negative. Demonstrations of the RTPDR surplus are shown in Figure 5.15, Figure 5.16, Figure 5.17, and Figure 5.18. Demonstrations of the RTPDR profit are shown in Figure 5.19, and Figure 5.20.

The worth of the RTPDR injection in Figure 5.15 is represented by the area outlined in orange, which reflects the accepted amount of dispatchable load P_d^*, which depends on the value of the RTP of electricity. Load payment is the area under the market price λ^*. The shaded blue area is the net surplus of the RTPDR injection, which represents the difference between the RTPDR injection worth and the total load payment to the market.

When the market price, λ^*, is negative, as shown in Figure 5.16, then the load payment is negative which is counter-intuitive. Market price can become negative for several reasons such as paying subsidy to renewables, having must-run generators for steam production to a process system, and having transmission system congestion in effect. Hence, load is paid to consume power and load payment becomes negative. In example-2, RTPDR injection worth is the area outlined in orange. Hence, the net RTPDR surplus is the RTPDR worth in addition to the market payment to the load, as shown in the shaded area of Figure 5.16.

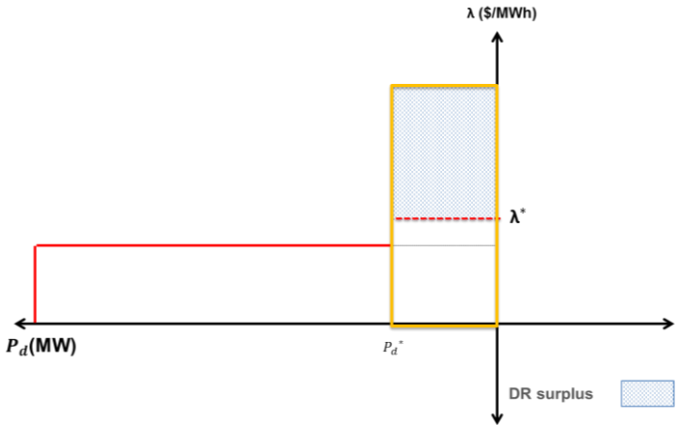

Figure 5.15. RTPDR surplus of a negative injection (example-1)

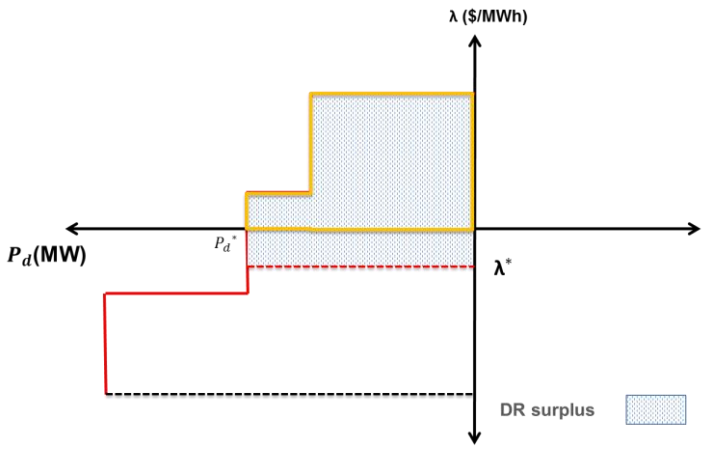

Figure 5.16. RTPDR surplus of a negative injection (example-2)

In Figure 5.17, the RTPDR worth is represented by the area outlined in orange, which consists of a positive and a negative worth. Since λ^* is negative, load payment is negative, which becomes a load profit. Hence, the total RTPDR surplus is the shaded area in Figure 5.17, which consists of the positive worth and load profit, less the negative worth. The RTPDR injection worth in Figure 5.18 is the area outlined in orange, which is negative. Load payment is negative, which is the area under λ^* up to P_d^*. Hence, the net RTPDR surplus is the blue shaded area in Figure 5.18, which consists of the load payment less the negative worth.

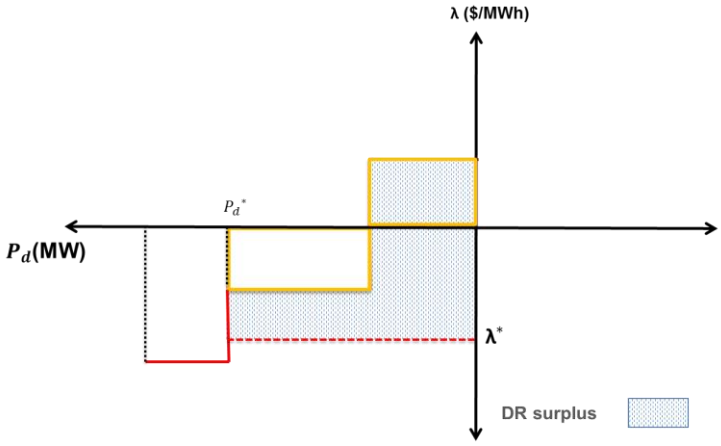

Figure 5.17. RTPDR surplus of a negative injection (example-3)

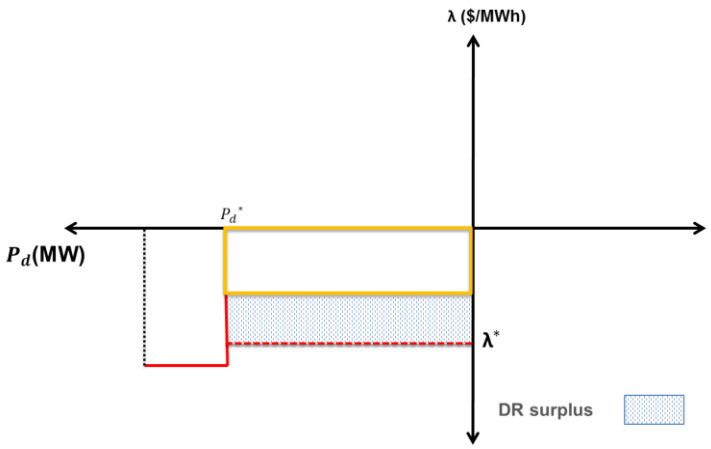

Figure 5.18. RTPDR surplus of a negative injection (example-4)

In Figure 5.19, since λ^* value is less than the second block bid, then the first block of the RTPDR bid is the accepted bid. The RTPDR injection cost is the area outlined in orange. The RTPDR revenue is the area under λ^*. Hence, the RTPDR injection profit is the shaded area in Figure 5.19, which consists of RTPDR revenue less by the RTPDR cost. Using similar analysis steps for the RTPDR injection surplus, Figure 5.20 becomes easy to understand. The RTPDR cost is the area outlined in orange, which consists of a positive and a negative cost. The RTPDR revenue is the area under λ^*. Hence, the RTPDR profit is the shaded area in Figure 5.20, which consists of the RTPDR revenue and the negative cost, less the positive cost.

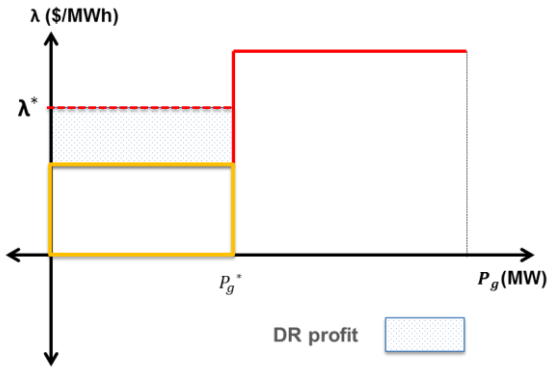

Figure 5.19. RTPDR profit of a positive injection (example-1)

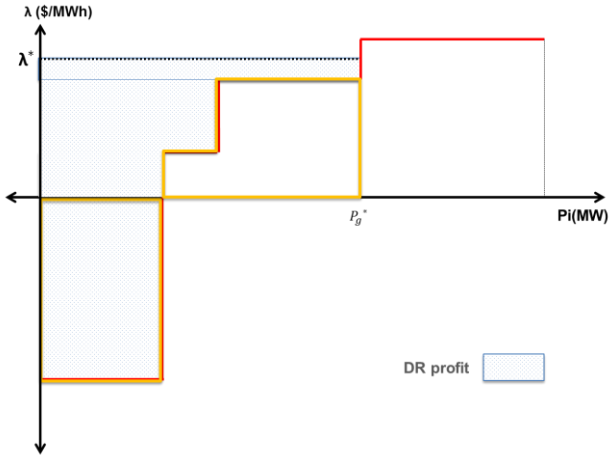

Figure 5.20. RTPDR profit of a positive injection (example-2)

5.3.3 *The Saudi Grid single-bus Analysis*

Two scenarios were used to simulate the single-bus system; a complete inelastic load, and a partially-inelastic load, as shown in Figure 5.1. In the first scenario, the elastic load is treated as a combination of a price-responsive load and generation. The bid of the elastic load is extracted from the profit maximization algorithm discussed in Chapter 2. The bid curve may have a negative power injection, which means that the elastic load is importing power from the utility, which usually occurs at a low RTP. Also, the elastic load may have a positive power injection, which means that the elastic load is exporting power to the utility, which usually occurs at a high RTP. In the second scenario, the elastic load is treated as a completely inelastic load, which means that it is not allowed to change its consumption pattern when the RTP of electricity changes. In this case, DR load is assumed to behave similar to the base case scenario that is discussed in Chapter 2 in which load and generation of the DR load are fixed and cannot be changed. Hence, the net injection of the DR load, then, is the difference between the maximum generation and maximum consumption of the DR load, which can be positive or negative. As a result, the net inelastic load in the second scenario is a combination of the system inelastic load in addition to the net injection of the DR load.

From Table 5.3, there are two sets of observed results; the intuitive results and the counter-intuitive results. The intuitive results confirm our understanding of the effects of RTPDR injection in the electricity market, after deciding the DR load behavior based on Figure 5.6 or Figure 5.8. While the behavior of the DR load is not predictable over the course of the year, it has been

Table 5.3. RTPDR Effects on the Single-bus Model Using the Subsidized Fuel Price

Scenario	Total Cost (M$)	Total Rev/LP (M$)	Total Worth (M$)	SW (M$)	GP (M$)	CS (M$)	Avg Price ($)	Total Load (GW)
elastic	$986.9	$994.1	$71,693	$70,706	$7.24	$70,699	$6.23	156,002
inelastic	$959.8	$938.0	$71,647	$70,687	($21.85)	$70,709	$6.01	151,545

observed that the behavior of DR load will follow the behavior of Figure 5.8 mainly, more than 99%, for the model of DR load under study. Hence, the load-increase case, which follows Figure 5.8, is expected to prevail.

The intuitive results are that the total consumed load is higher in the elastic scenario, which is an expected result as per Figure 5.8. The total consumed load in the elastic scenario is expected to increase because the RTPDR injection is expected to consume more power to take advantage of the low RTP, as seen in Table 5.3. The total worth is expected to be higher for the elastic scenario due to the increased power consumption. Hence, as per (5.13), the total worth for the elastic scenario is expected to be higher, as seen in Table 5.3. The total cost is expected to be higher for the elastic scenario due to the increased power consumption. Hence, as per (5.14), the total cost for the elastic scenario is expected to be higher, as seen in Table 5.3. In theory, the average price is not predictable because we do not know which situation for DR behavior will prevail. The average price for this model is higher in the elastic scenario. As a result, generation revenue and load payment are expected to be higher. Since the increase in total generation revenue is higher than the increase in total cost, generation profit is expected to be higher for the elastic case scenario, as seen in Table 5.3. More importantly, social welfare is higher in the elastic scenario. Since the total worth has increased more than the total cost in the elastic scenario, the net effect as per (5.1) is an improvement of the social welfare of the society by the area of the shaded triangle in Figure 5.8.

On the other hand, the counter-intuitive results are that consumer surplus is lower in the elastic scenario and generation profit is negative for the inelastic scenario, as seen in Table 5.3. Consumer surplus faces two effects. The first effect is a reduction in consumer surplus by the amount of load payment increase which is $p_1^* - p_2^*$ for every MW of load consumption up to q_2^*. The second effect is a consumer surplus increase between q_2^* and q_1^* by the area of the upper half of the shaded triangle in Figure 5.8 which represents the area of the difference between worth and market price, p_1^*, for the elastic load. The net effect is expected to be a reduction in consumer

surplus, as seen in Table 5.3, by the difference of the two effects. The reason for the negative generation profit is that the current practice of the utility is to run generation based on a priority list that considers different factors such as season, efficiency, criticality, and availability of fuel. Also, fuel subsidy is dependent on the type of fuel. Hence, some expensive generators might dispatch, which reduces the profit of the generation companies or can even make it negative as seen in this situation.

The RTPDR injection was observed to bid a net positive injection for all instances over the whole year. Looking into Figure 5.21, it is obvious that the RTPDR injection will always bid a positive value for any price even if it drops as low as zero, which is the lowest possible price for the single-bus model. It should be noted that the behavior of the RTPDR injection might change when it faces negative RTPs, which can occur in presence of any subsidy or even when transmission system congestion is in effect.

$$W(P_d) = \int_0^{P_d^*} D \, dP_d \tag{5.13}$$

$$C(P_G) = \int_0^{P_G^*} IC \, dP_G \tag{5.14}$$

5.3.4 *Fuel Price Sensitivity Analysis*

The current cost of fuel in the Saudi Grid reflects various subsidies depending on the fuel type. It is believed that the RTPDR injection, the process facility, as well as the grid operational philosophy might change when an unsubsidized fuel cost is used. It is believed that the Gulf Grid Interconnection will operate based on financial incentive, the RTP signal, rather than the existing contingency-based operational philosophy. Also, since subsidies vary based on the fuel type, it is believed that some generators, which receive the highest fuel subsidy, might change their dispatch or even experience a complete shutdown. The analysis in this section discusses the effect of removing fuel subsidy from all participants in the Saudi electricity market, which includes the RTPDR injection. The unsubsidized fuel price data, international fuel prices, were obtained from [53, 54, 55] using the closing price of 3/2/2015 and conversion rates from [55]. A comparison

between the bid curves of the combined RTPDR injection in the Saudi Grid using the subsidized and unsubsidized fuel prices is shown in Figure 5.21.

Discussion

From Table 5.5, there are two sets of observed results; the intuitive results and the counter-intuitive results. Once the decision is made about the DR load behavior to follow either Figure 5.6 or Figure 5.8, the intuitive results can confirm our understanding of the effects of the RTPDR injection in the electricity market in presence of unsubsidized fuel price. While the behavior of the RTPDR injection is not predictable over the course of the year, it has been observed that the behavior of the RTPDR injection will follow the behavior of Figure 5.6 mainly, more than 95%, for the model of the RTPDR injection under study. Hence, the load-reduction case, which follows Figure 5.6, is expected to prevail.

The intuitive results are that the total consumed load is lower in the elastic scenario, which is an expected result as per Figure 5.6. The total consumed load in the elastic scenario is expected to be less because the RTPDR injection is expected to consume less power in presence of high RTP, as seen in Table 5.5. The total worth is expected to be lower for the elastic scenario due to the reduced power consumption. Hence, as per (5.3), the total worth for the elastic scenario is lower, as seen in Table 5.5. The total cost is expected to be lower for the elastic scenario due to the reduced power consumption. Hence, as per (5.4), the total cost for the elastic scenario is lower, as seen in Table 5.5. Consumer surplus is expected to be higher in the elastic scenario, as seen in Table 5.5. While the average price is higher in the elastic scenario, the first case is still prevailing, which resulted in a net effect of increased consumer surplus. This can be explained by the reduction of the total load payment that is higher in magnitude than the reduction in worth for the elastic scenario. Hence, a higher consumer surplus is expected for the elastic scenario, as seen in Table 5.5. Even though the numerical analysis determined the direction of consumer surplus for this model, it should be noted that consumer surplus direction is not predictable because the prevailing case for the DR load is not known beforehand. More importantly, social welfare is higher in the elastic scenario. Since the total cost has decreased more than the total worth reduction in the elastic scenario, the net effect as per (5.1) is an improvement of the social welfare of the society by the area of the shaded triangle, area-G of Figure 5.6.

Table 5.4. Fuel Cost at the Subsidized and Unsubsidized Fuel Price [53, 54, 55]

Fuel Type	Subsidized Price ($/MMBTU)	Unsubsidized Cost ($/MMBTU)
Gas	0.75	2.79
Oil	0.74	10.63
Diesel	0.63	13.95

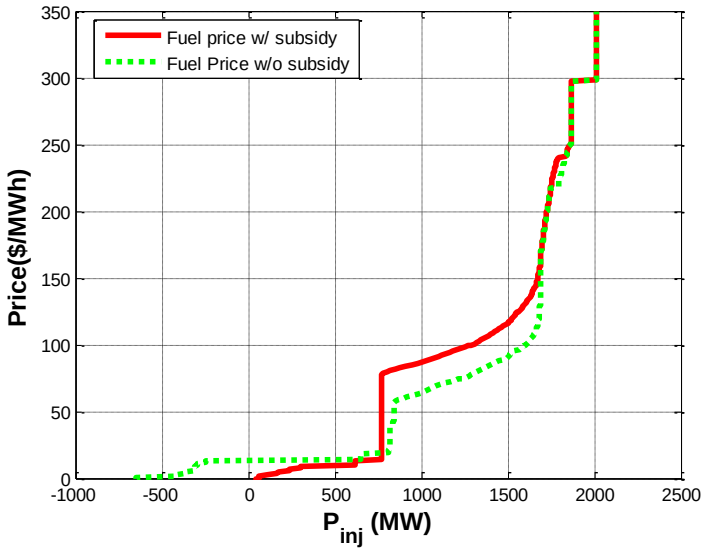

Figure 5.21. Demand curve for the lumped RTPDR injection in the Saudi Grid single-bus model using the subsidized and unsubsidized fuel prices

On the other hand, the counter-intuitive results are that the average price and the generation profit are higher in the elastic scenario as seen in Table 5.5. While the market price is slightly lower in the elastic scenario most of the time (more than 95%), the remaining 5% shows a greater magnitude difference that influenced the average price over the course of year. Hence, it should be noted that the average price cannot be predicted beforehand since it is not known which case will have more effect on the average price. In this case, even though the elastic scenario market price was higher than the inelastic scenario for only 5% of the time over the whole year, the average price for the elastic scenario over the whole year was higher than the inelastic scenario, as seen in Table 5.5. The total generation cost reduced more than the total generation revenue for the

elastic scenario. Hence, the net effect is an increase in the total generation profit, as seen in Table 5.5.

The RTPDR was observed to bid a net positive injection for all instances over the whole year. This can be explained by the bid curve characteristics of the RTPDR injection and the range of price that the RTPDR injection faces over the course of year. Figure 5.21 shows that the RTPDR injection bids a positive value for any RTP that is $14 or higher. Analysis of the market price of electricity shows that the minimum observed price for the elastic scenario was $14. It should be noted that the behavior of the RTPDR injection might change when it faces negative RTPs, which can occur when transmission system congestion is in effect, which will be discussed in the next section.

Table 5.5. RTPDR Effects on the Single-bus Model Using the Unsubsidized Fuel Price

Scenario	Total Cost (M$)	Total Rev/LP (M$)	Total Worth (M$)	SW (M$)	GP (M$)	CS (M$)	Avg Price ($)	Total Load (GW)
elastic	$5,560	$3,655	$71,410	$65,850	($1,905)	$67,755	$23.42	150,766.5
inelastic	$5,581	$3,674	$71,426	$65,845	($1,906)	$67,752	$23.26	151,545.2

5.3.5 *Effects of Higher Penetration Levels of RTPDR Injections on Economic Incentives and the Electricity Market*

Two cases are observed for the theoretical analysis of social welfare effects of a single RTPDR injection versus several RTPDR injections that participate in the electricity market. The first case represents a reduction in load for the multiple-load scenario compared to the single-load scenario, as seen in Figure 5.22. The other case represents an increase in load consumption for the multiple-load scenario, as seen in Figure 5.23.

In the load-reduction case, the RTP of electricity reduces, generation profit decreases, and consumer surplus increases, as seen in Figure 5.22. Following the theoretical analysis of the single-bus model of the Saudi Grid, social welfare of the society is improved by the shaded area shown in Figure 5.22. In the load-increase case, the RTP of electricity increases, generation profit increases, and consumer surplus increases, as seen in Figure 5.23. Social welfare of the society improves by the shaded area shown in Figure 5.23. Results of the theoretical analysis demonstrate that the higher the penetration level of RTPDR injections in the electricity market, the higher the

social welfare value will become, regardless of the injection value of the price-responsive customer in the base case scenario.

Table 5.6 shows that the higher the penetration level of RTPDR injections, the higher the RTP of electricity will become. This result is influenced by the assumption of the net injection in the inelastic scenario and the availability of fuel subsidy in the Saudi Grid. This in turn influenced the RTP of electricity to become cheap and promoted more load consumption, as seen in Table 5.7. It is observed that social welfare of the society increases when more RTPDR injections participate in the electricity market, as seen in Table 5.7.

A RTPDR injection receives its benefit from participation in a RTPDR program from two sources; scheduling benefits and market benefits. Scheduling benefits comes as a direct result from changing a RTPDR facility schedule to maximize profit. The market benefit comes in a form of generation profit when the RTPDR injection is positive or consumer surplus when the RTPDR injection is negative. The market and scheduling benefits for the RTPDR injection are part of the scheduling algorithm discussed in Chapter 3. The net benefit obtained from a RTPDR injection is higher in magnitude compared to the net benefit obtained from the same injection in presence of other responding loads, as seen in Table 5.8, which is an expected result.

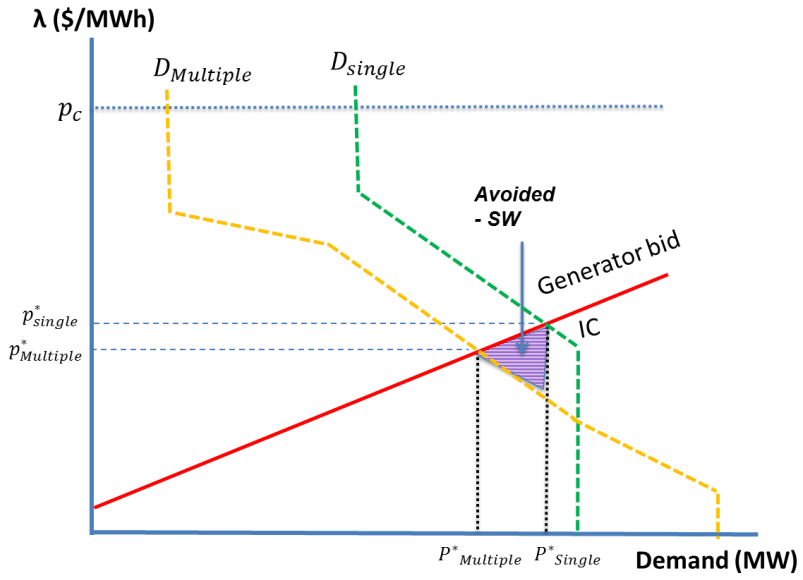

Figure 5.22. Social welfare effects for different penetration levels of RTPDR injections (load-reduction case)

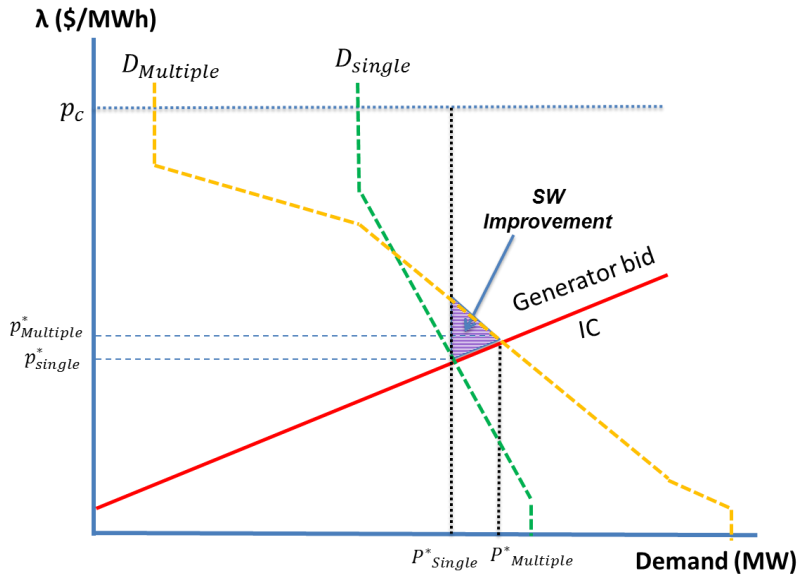

Figure 5.23. Social welfare effects for different penetration levels of RTPDR injections (load-increase case)

Table 5.6. Effects of Higher Penetration Level of RTPDR Injections on RTP Volatility

Case	inelastic	Elastic (single)	Elastic (Multiple)
Average Price ($/MWh)	6.01	6.09	6.23
Highest Price ($/MWh)	34.88	34.88	34.88
Lowest Price ($/MWh)	0	0	4.43
σ	1.20	1.05	0.86

Table 5.7. Comparison of RTPDR Effects between a Single and Multiple RTPDR Injections

Scenario	Total Cost (M$)	Total Rev/LP (M$)	Total Worth (M$)	SW (M$)	GP (M$)	CS (M$)	Total Load (GW)
Inelastic	$960	$938	$71,647	$70,687	($21.85)	$70,709	151,545.2
Elastic (single)	$968	$958	$71,665	$70,697	($10.84)	$70,707	152,972.7
Elastic (Multiple)	$987	$994	$71,693	$70,706	$7.24	$70,699	156,001.8

Table 5.8. Effects of Multiple RTPDR Injections on the Process Facility's Profit

Scenario	Single RTPDR Injection	Several RTPDR Injections
Base case	$72,277,315	$72,536,862
RTPDR	$77,047,136	$77,119,848
Difference	$4,769,821	$4,582,985
% Difference	0	-3.92%

5.4 THE THREE-BUS TEST CASE

The purpose of the three-bus test system is to apply the theory in the single-bus model into a model that has a transmission system. The new model provides an opportunity to study the system-wide effects of a RTPDR injection, such as power flow and transmission congestion effects, which are dependent on the electrical system topology.

A demand curve for a small-size gas processing facility with RTPDR capability is extracted from the output of the algorithm for the model discussed in Chapter 2. Then, the demand curve is used to model a dispatchable load in the three-bus DC Optimal Power Flow (DCOPF). The facility's load is scaled to be suitable for the size of the three-bus test case and it constitutes around 5% of the total system load.

The purpose of the test case is to study the system-wide effects of RTPDR injection on the electricity market with congestion in the transmission system. Hence, the test case will be used to establish the qualitative analysis for the RTPDR injection effects on an electrical system. The test case will specifically evaluate the impact of RTP of electricity on the process facility's profit, evaluate the impact of large load with RTPDR capability on the electricity market price, and assess system improvement resulting from a considerable penetration level of RTPDR resources on the electric grid, specifically transmission congestion and shortage of generation.

An available DC OPF tool, called MATPOWER, can be modified to be suitable for studying RTPDR effects on a small-scale test system, the three-bus case [79]. The test case simulates a counter-intuitive scenario that is discussed in [69], which produces a negative LMP. A transmission congestion scenario in presence of a RTPDR injection is also analyzed. A generation shortage scenario is also presented, which demonstrates that the availability of RTPDR resources

in the gird can prevent a possible market failure. The analysis in this section is part of an effort to understand and quantify the effects of RTPDR resources at different system conditions.

It is expected that, even at low penetration of RTPDR resources, the system price can reduce slightly at normal condition or by a considerable amount during system contingency as stated in [18]. It is expected that a RTPDR injection reduces its consumption as a result of an increase in the RTP of electricity, which is likely to happen during transmission system congestion or loss of generation. If transmission congestion is in effect between two buses, the RTP of electricity is expected to change in all buses of the system and each bus has its own unique LMP. It is also expected that the RTP of electricity reduces slightly at the uncongested side of the transmission line and increases at the remaining buses compared to a no-congestion scenario. The reason for the price increase is the limit on the transmission line, which prevents cheap generation from selling excess power to the load at the congested side of the transmission line. Instead, cheap generation is expected to operate at lower power output to serve the load at the uncongested side which causes the RTP of electricity at the uncongested bus to reduce further. Expensive generators, however, might be dispatched to serve the load at the congested side of the transmission line. This in turn results in an increase of the total cost of generating electricity, which increases the RTP of electricity in the whole system.

When a RTPDR injection changes in one bus as a result of change in the RTP of electricity, the RTP of electricity is expected to reduce slightly in all buses. The reason for the expected price drop is that the expensive peaker generators are expected to reduce their power output or even shutdown, which reduces the total cost of generating electricity. Generation profit, consumer surplus, and social welfare are calculated and discussed as part of the analysis of the three-bus test case.

The analysis was conducted on several scenarios based on the system described in Figure 5.24. Transmission system data are listed for each scenario. Generation cost curves are assumed to be linear for the scenario-I and quadratic for the remaining scenarios.

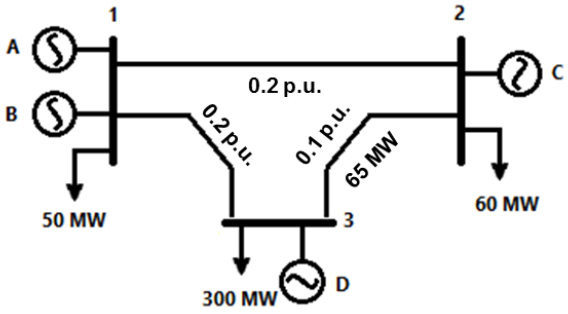

Figure 5.24. The single-line diagram of the 3-bus test system for scenario-I [69]

5.4.1 *Scenario-I*

The transmission system data for scenario-I are listed in Table 5.9. Generation capacity and incremental cost data for each generator in scenario-I are listed in Table 5.10. A price cap of $500/MWh is imposed for social welfare calculation purposes. The selection of the price cap is based on the analysis of the detailed Saudi Grid system, which showed a maximum LMP value of $300/MWh. Hence, it is assumed that a system price higher than $500/MWh, which includes a safety margin, is a sign of a market failure.

Scenario-I simulates a case that produces a negative LMP at bus-2. In this example, bus-2 generator is not dispatched due to transmission congestion of the line between bus-2 and bus-3. If the generator at bus-2 is dispatched, the electrical system will not be able to correct the generation dispatch without violating the transmission line constraint. Hence, the LMP value at bus-2 is determined by a combination of LMP values from other buses in the system. From the definition of LMP, which is the cost of adding an additional MW at a specified bus, LMP_2 can be calculated by dispatching 1 MW to the load at bus-2 while maintaining the value of the line flow at line 2-3. If 1 MW is dispatched from bus-1, it will change the flow in line 2-3 by -0.4 MW. Similarly, If 1 MW is dispatched from bus-3, it will change the flow in line 2-3 by -0.8 MW. These constraints can be written as:

$$\Delta P_1 + \Delta P_3 = \Delta P_2 = 1 \tag{5.15}$$

$$-0.4(\Delta P_1) + (-0.8)(\Delta P_3) = 0 \tag{5.16}$$

Table 5.9. Transmission System Data (scenario-I) [69]

Line	X (p.u.)	TL limit (MW)
1-2	0.2	N/A
1-3	0.2	N/A
2-3	0.1	65

Table 5.10. Generation Cost Data for Scenario-I [69]

Generator	P_{max}(MW)	IC ($/MWh)
A	140	7.5
B	285	6
C	90	3
D	85	20

Solving (5.15) and (5.16) yields the following:

$$\mathrm{LMP}_2 = 2 \cdot \mathrm{LMP}_1 - \mathrm{LMP}_3 \tag{5.17}$$

Since generator-A sets the price at bus-1, then $LMP_1 = \$7.5/MWh$. Similarly, since generator-D sets the price at bus-3, then $LMP_3 = \$20/MWh$. LMP_2 is calculated from (5.17) as follows:

$$LMP_2 = 2\,(7.5) - (20) = -\$5/MWh$$

From Table 5.12, the DCOPF simulation does not converge when the RTPDR injection is placed at bus-2, the sending end of the congestion transmission line, because it creates a system with no feasible solution. This means that there is no feasible way to correct the generation dispatch while satisfying the transmission line constraint. Social welfare maximizes when the RTPDR injection is placed at the receiving end of the congested transmission line. Hence, a comparison between the elastic and inelastic scenarios will only consider placement of the RTPDR injection at bus-3.

RTPDR effects on the electricity market for scenario-I can be analyzed from the results in Table 5.11, Table 5.12, Table 5.13, Table 5.14, Table 5.15 and Table 5.16. In the elastic case, load payment and generation revenue have reduced slightly, as seen in Table 5.11. Merchandising

surplus value did not change in both the elastic and the inelastic cases. Elastic case worth has reduced slightly and generation cost has reduced slightly, as seen in Table 5.11. Consumer surplus has improved slightly while generation profit did not change for the elastic case, as shown in Table 5.11. As a result, the net effect is an improvement of the social welfare of the whole system.

Load payment has reduced slightly due to marginal increase in power export from the RTPDR injection to the grid, as seen in Table 5.11. Hence, the expensive generator-D dispatch has reduced slightly, which resulted in reduced load payment, as seen in Table 5.12 and Table

Table 5.11. Market Effects of the RTPDR injection (scenario-I)

RTPDR Location	**Scenario**	**LP (K$)**	**GR (K$)**	**MS (K$)**	**Worth (K$)**	**GC (K$)**	**CS (K$)**	**GP (K$)**	**SW (K$)**
bus-1	inelastic	$5.78	$3.82	$1.96	$183.55	$3.39	$177.78	$0.43	$180.16
bus-1	elastic	$5.90	$3.87	$2.03	$183.63	$3.44	$177.72	$0.43	$180.18
bus-3	inelastic	$5.48	$3.44	$2.03	$183.55	$3.02	$178.08	$0.43	$180.54
bus-3	elastic	$5.46	$3.43	$2.03	$183.54	$3.00	$178.08	$0.43	$180.54

Table 5.12. Generation Dispatch (scenario-I)

	Bus-1		**Bus-3**	
Generator	Inelastic	Elastic	Inelastic	Elastic
A	17.5	24.2	47.5	47.5
B	285.0	285.0	285.0	285.0
C	0.0	0.0	0.0	0.0
D	77.5	77.5	47.5	46.8
RTPDR injection	10	3.3	10	10.7

Table 5.13. LMP Data (scenario-I); the RTPDR Injection Located at Bus-3

Location	**Inelastic Case**	**Elastic Case**
Bus-1	$7.5	$7.5
Bus-2	-$5.0	-$5.0
Bus-3	$20	$20

5.14. The total worth for the elastic case has reduced due to the increased power export from the RTPDR injection, which resulted in a net effect of slight reduction of load consumption. Since the reduction in load payment is higher in magnitude compared to the reduction of the total worth for the elastic scenario, the net effect is a consumer surplus improvement, as seen in Table 5.11. Generation revenue has been reduced slightly while the generation cost reduced by the same magnitude, as seen in Table 5.11. Hence, generation profit did not change in this particular model. The net effect is a social welfare increase, as seen in Table 5.16.

It should be noted that even though the RTPDR injection did not change the price or LMP value at any bus of the system, it still helped improving the total social welfare of the whole system, when it participated in the electricity market. The change in the net value of the RTPDR injection at bus-3 between the elastic and the inelastic cases is marginal, as seen in Table 5.12. Hence, a marginal change in generation dispatch was noticed, which did not results in a price change at any bus in the system, as seen in Table 5.13. However, it reduced the revenue of the expensive generator, located at bus-3, which has a market power potential, as seen in Table 5.15. Social welfare maximized when the RTPDR injection is placed at the congested side of the transmission line. These results are expected and they are confirmed by this analysis. An interesting result, which is outside the scope of this research, is that a maximum change in social

Table 5.14. Load Payment for the Three-Bus Test Case (scenario-I)

Location	Inelastic Case	Elastic Case
Bus-1	375	$375
Bus-2	-300	-$300
Bus-3 (inelastic load)	5600	$5,600
Bus-3 (elastic load)	-$200.0	-$213.4
Total Load Payment	$5,475	$5,461.6

Table 5.15. Generation Revenue for the Three-Bus Test Case (scenario-I)

Location	Inelastic Case	Elastic Case
Bus-1	$2,493.8	$2,493.8
Bus-2	$0.00	$0.00
Bus-3	950.0	$936.6
Total Generation Revenue	$3,443.8	$3,430.4

Table 5.16. Social Welfare for the Three-bus Test Case (scenario-I)

	Inelastic Case	**Elastic Case**
Generation Revenue ($)	$3,443.8	$3,430.4
Generation Cost ($)	$3,616.2	$3,002.9
Generation Profit ($)	$427.5	$427.5
Load Payment ($)	$5,475	$5,461.6
Consumer Surplus ($)	$178,078	$178,082
Merchandising Surplus ($)	$2,031.2	$2,031.2
Social Welfare ($)	$180,537	$180,541.0

Table 5.17. The RTPDR Injection Market Benefit for the Three-bus Test Case (scenario-I)

RTPDR Location	**RTPDR cost**	**RTPDR revenue**	**RTPDR profit**
Bus-1	$7.53	$24.65	$17.12
Bus-3	$88.30	$213.39	$125.09

welfare between the elastic and inelastic cases has occurred at bus-1 and not at bus-3, the congested side of the transmission line. The result suggest that even though placing a RTPDR injection at the receiving end of a congested transmission line maximized social welfare, it is not necessary that converting an inelastic load into a RTPDR injection at bus-3 will yield a maximum improvement in social welfare. In this example, converting an inelastic load into a RTPDR injection at bus-1 yielded the maximum improvement in social welfare, which is a future research direction that needs to be investigated further. Another interesting result is that placing the RTPDR injection at bus-1 resulted in a bid amount that has a lower power export to the Grid compared to the inelastic case. Hence, more power is dispatched from generator-A at bus-1, which resulted in a higher merchandising surplus in the elastic case.

Looking into the RTPDR injection benefit from market participation beside the scheduling benefit, discussed in section 5.3.2.2, the market benefit is maximized when the RTPDR injection is placed at the receiving end of the congested transmission line, as seen in Table 5.17. The reason for the huge market benefit is that the RTPDR injection power export has increased when it is

placed at bus-3 to take advantage of the high LMP value. Hence, the market benefit is much higher compared to the benefit obtained from placing the RTPDR injection at bus-1, as seen in Table 5.17.

5.4.2 *Scenario-II*

In scenario-II, system topology is similar to scenario-I. However, one generator was removed from bus-1 and the distribution of load across the system has also changed, as seen in Figure 5.25. Transmission system data is tabulated in Table 5.18. Generators' cost data were taken from [63] with small adjustment to generator-C cost coefficients, to make it suitable for scenario-II. Generation cost data is tabulated in Table 5.19.

Scenario-II simulates a case of transmission congestion that creates a market power situation for generator-C due to transmission system congestion at line 1-3. The LMP value at bus-2 is determined by a combination of LMP values from other buses in the system. LMP_2 is calculated by dispatching 1 MW to the load at bus-2 while maintaining the value of the line flow at line 1-3. Using similar analysis steps from scenario-I, the constraints can be written as:

$$\Delta P_1 + \Delta P_3 = \Delta P_2 = 1 \tag{5.18}$$

$$+0.4(\Delta P_1) + (-0.2)(\Delta P_3) = 0 \tag{5.19}$$

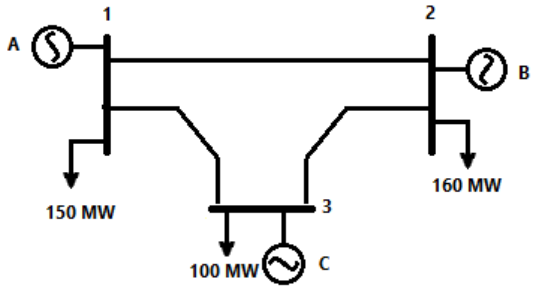

Figure 5.25. The single-line diagram of the 3-bus test system for scenario-II

Table 5.18. Transmission System Data (scenario-II)

Line	X (p.u.)	TL limit (MW)
1-2	0.2	98
1-3	0.2	70
2-3	0.1	60

Table 5.19. Generation Cost Data (scenario-II) [63]

Generator	P_{max} (MW)	a ($/MW^{2}h)	b ($/MWh)	c ($/h)
A	350	0.00158	11.1874	182.3692
B	76	0.0096	13.8095	84.0747
C	100	0.00616	30	225.3385

Solving (5.18) and (5.19) will yield the following:

$$LMP_2 = \frac{1}{3} \cdot LMP_1 + \frac{2}{3} \cdot LMP_3 \tag{5.20}$$

Since generator-A sets the price at bus-1, then $LMP_1 = \$12.12/\text{MWh}$. Similarly, since generator-C sets the price at bus-3, then $LMP_3 = \$30.12/\text{MWh}$. LMP_2 is calculated from (5.20) as follows:

$$LMP_2 = \frac{1}{3} \cdot (12.12) + \frac{2}{3} \cdot (30.12) = \ \$24.12/MWh$$

Social welfare maximizes when the RTPDR injection is placed at the receiving end of the congested transmission line. Hence, a comparison between the elastic and inelastic scenarios will only consider placement of the RTPDR injection at bus-3, which follows the behavior of Figure 5.6. The analysis of placing the RTPDR injection at bus-1 is conducted because it shows different set of results that are needed to have a better analysis of more possible events. This case is expected to behave similar to Figure 5.8 in which the total consumed load in the elastic case is more than the total consumed load in the inelastic case.

Scenario-II simulates a situation of market power that can be exercised by generator-C. Looking into Table 5.22, placement of the RTPDR injection at bus-1 resulted in a slight increase of the LMP value at bus-1 while the placement of the RTPDR injection at bus-3 resulted in a slight reduction of the LMP value at bus-2 and bus-3. The reason for the slight increase in the LMP value at bus-1 can be explained by the reduction of the RTPDR injection power export, as seen in Table 5.21. The reason for the slight decrease in the LMP value at bus-3 is that the RTPDR injection exported slightly more power to the grid which replaced part of the dispatched power from the expensive generator-C, as seen in Table 5.21. Since the LMP value at bus-2 is a function of the LMP value at bus-3, the LMP value at bus-2 has also reduced slightly, as seen in Table 5.22.

Table 5.20. Market Effects of the RTPDR Injection (scenario-II)

RTPDR Location	Scenario	LP (K$)	GR (K$)	MS (K$)	Worth (K$)	GC (K$)	CS (K$)	GP (K$)	SW (K$)
Inelastic	bus-1	$8.38	$6.23	$2.15	$183.55	$5.86	$175.17	$0.37	$177.70
Elastic	bus-1	$8.40	$6.25	$2.15	$183.57	$5.88	$175.17	$0.37	$177.70
inelastic	bus-3	$7.78	$5.69	$2.10	$183.55	$5.31	$175.77	$0.37	$178.24
Elastic	bus-3	$7.76	$5.66	$2.10	$183.54	$5.29	$175.78	$0.37	$178.25

Table 5.21. Generation Dispatch (scenario-II)

	Case			
	Elastic		Inelastic	
Generator	RTPDR injection at bus-1	RTPDR injection at bus-3	RTPDR injection at bus-1	RTPDR injection at bus-3
A	266.2	294.7	264.7	294.7
B	76.0	76.0	76.0	76.0
C	39.3	8.7	39.3	9.3
RTPDR injection	8.5	10.7	10.0	10.0

Table 5.22. LMP Data for the Three-bus Test Case (scenario-II)

	Case			
	Elastic		Inelastic	
Generator	RTPDR injection at bus-1	RTPDR injection at bus-3	RTPDR injection at bus-1	RTPDR injection at bus-3
LMP_1	12.03	12.12	12.02	12.12
LMP_2	24.33	24.11	24.33	24.12
LMP_3	30.49	30.11	30.49	30.12

The RTPDR injection in this scenario was not able to neither influence the market price significantly nor reduce the effect of market power in the system due to the characteristics of the bid curve of the RTPDR injection. Analysis of the bid curve shows that a significant change in the bid amount of the RTPDR injection is seen at a price that is higher than $100/MWh. Hence, the analysis will be carried on a new scenario that simulates a different generator at bus-3, generator-C, which represents a less efficient generator in the electricity market. Generator-C has very high cost coefficients, as seen in Table 5.23. A larger change in the bid value of the RTPDR injection

is expected. The RTP of electricity is expected to be influenced significantly as stated in [18]. The new generation data is tabulated in Table 5.23.

The modified Scenario-II simulates a situation of market power that can be exercised. RTPDR effects on the electricity market for the modified scenario-II can be analyzed from the results in Table 5.24, Table 5.25, Table 5.26, Table 5.27, Table 5.28 and Table 5.29. The expensive generator-C in the inelastic case is dispatched even though the cheap generator-A did not reach its capacity, due to the transmission line congestion at line 1-3, as seen in Table 5.25.

Looking into Table 5.26, placement of the RTPDR injection at bus-1 resulted in a slight increase of the LMP value at bus-1 while the placement of the RTPDR injection at bus-3 resulted in a huge reduction of the LMP value at bus-2 and bus-3. The reason for the slight increase in the LMP value at bus-1 can be explained by the reduction of the RTPDR injection power export, as seen in Table 5.25. Hence, generator-A dispatched more power causing a slight increase in the RTP at bus-1. The reason for the huge reduction of the LMP value at bus-3 is that the RTPDR injection power export to the grid has increased significantly, which caused the expensive generator-C to shutdown, as seen in Table 5.25. Since the LMP value at bus-2 is a function of the LMP value at bus-3, the LMP value at bus-2 has also reduced significantly, as seen in Table 5.26.

When the RTPDR injection is placed at bus-1, load payment and generation revenue for the elastic case have increased slightly, as seen in Table 5.24. Merchandising surplus value did not change in both the elastic and the inelastic cases. Elastic case worth has increased slightly and generation cost has increased slightly, as seen in Table 5.24. Consumer surplus has improved slightly while generation profit increased slightly for the elastic case, as shown in Table 5.24. As a result, the net effect is a slight improvement of the social welfare of the whole system.

Table 5.23. Generation Cost Data (modified scenario-II) [63]

Generator	$\boldsymbol{P_{max}}$ **(MW)**	**a ($/MW^{2}h)**	**b ($/MWh)**	**c ($/h)**
A	350	0.00158	11.1874	182.3692
B	76	0.0096	13.8095	84.0747
C	100	0.00616	450	225.3385

Table 5.24. Market Effects of the RTPDR Injection (modified scenario-II)

RTPDR Location	Scenario	LP (K$)	GR (K$)	MS (K$)	Worth (K$)	GC (K$)	CS (K$)	GP (K$)	SW (K$)
Inelastic	bus-1	$95.2	$44.0	$51.2	$183.6	$22.4	$88.4	$21.7	$161.2
Elastic	bus-1	$95.2	$44.1	$51.2	$183.6	$22.4	$88.4	$21.7	$161.2
inelastic	bus-3	$77.5	$30.9	$51.1	$183.6	$9.2	$101.6	$21.7	$174.3
Elastic	bus-3	$20.5	$9.4	$11.2	$182.7	$5.0	$162.2	$4.3	**$177.7**

Table 5.25. Generation Dispatch (modified scenario-II)

	Case			
	Elastic		Inelastic	
Generator	RTPDR injection at bus-1	RTPDR injection	RTPDR injection	RTPDR injection
A	266.2	294.7	264.7	294.7
B	76.0	76.0	76.0	76.0
C	39.3	0.0	39.3	9.3
RTPDR injection	8.5	19.3	10.0	10.0

Table 5.26. LMP Data for the Three-bus Test Case (modified scenario-II)

	Case			
	Elastic		Inelastic	
Generator	RTPDR injection at bus-1	RTPDR injection	RTPDR injection	RTPDR injection
LMP_1	12.03	12.12	12.02	12.12
LMP_2	304.33	76.04	304.33	304.12
LMP3	450.48	108.00	450.48	450.11

When the RTPDR injection is placed at bus-1, load payment for the elastic case has increased slightly due to marginal reduction in power export from the RTPDR injection to the grid, as seen in Table 5.25. Hence, more power is dispatched from generator-A causing the LMP value at bus-1 to increase slightly, as seen in Table 5.26. The total worth for the elastic case has increased due to the reduced power export from the RTPDR injection, which resulted in a net effect of slight increase of load consumption. Since the increase in load payment is lower in magnitude compared

to the increase of the total worth for the elastic scenario, the net effect is a consumer surplus improvement, as seen in Table 5.24. Generation revenue has increased slightly while the generation cost increased with less magnitude, as seen in Table 5.24. Hence, the generation profit increased slightly. The net effect is a social welfare improvement, as seen in Table 5.24. These results are expected and they are confirmed by the analysis of the RTPDR injection behavior of Figure 5.8.

When the RTPDR injection is placed at bus-3, load payment and generation revenue for the elastic case have reduced significantly, as seen in Table 5.24. Merchandising surplus value reduced significantly in the elastic case. Elastic case worth has reduced slightly and generation cost has reduced significantly, as seen in Table 5.24. Consumer surplus has improved significantly while generation profit reduced significantly for the elastic case, as shown in Table 5.24. The net effect is an improvement of the social welfare of the whole system, as seen in Table 5.24. Load payment has reduced significantly due to the considerable increase in power export from the RTPDR injection to the grid, as seen in Table 5.24. Hence, the expensive generator-D was forced to shut down, which resulted in a huge reduction in load payment, as seen in Table 5.24 and Table 5.27. The total worth for the elastic case has reduced due to the increased power export from the RTPDR injection, which resulted in a net effect of slight reduction of load consumption. Since the reduction in load payment is higher in magnitude compared to the reduction of the total worth for the elastic scenario, the net effect is a considerable improvement of consumer surplus, as seen in Table 5.24. Generation revenue has reduced considerably while the generation cost reduced by a less magnitude. Hence, generation profit has reduced

Table 5.27. Load payment for the Three-bus Test Case (modified scenario-II)

Location	**Inelastic Case**	**Elastic Case**
Bus-1	$1,818	$1,818
Bus-2	$48,659	$12,166
Bus-3 (inelastic load)	$31,508	$8,640
Bus-3 (elastic load)	-$4,501	-$2,088
Total Load Payment	$77,484	$20,536

Table 5.28. Generation Revenue for the Three-bus Test Case (modified scenario-II)

Location	Inelastic Case	Elastic Case
Bus-1	$3,571.1	$3,571.1
Bus-2	$23,113.1	$5,779.0
Bus-3	$4,201.0	$0.0
Total Generation Revenue	$30,885.2	$9,350.1

Table 5.29. Social Welfare for the Three-bus Test Case (modified scenario-II)

	Inelastic Case	Elastic Case
Generation Revenue ($)	$30,885.2	$9,350.1
Generation Cost ($)	$9,231	$5,031
Generation Profit ($)	$21,654	$4,319
Load Payment ($)	$77,484	$20,536
Consumer Surplus ($)	$101,569	$162,212
Merchandising Surplus ($)	$51,100	$11,186
Social Welfare ($)	$174,322	$177,717

significantly, as seen in Table 5.24. Since the reduction in total cost is higher in magnitude compared to the reduction in total worth, the net effect is a social welfare increase, as seen in Table 5.24. These results are expected and they are confirmed by the analysis of the RTPDR injection behavior of Figure 5.6.

The RTPDR injection benefit from market participation, beside the profit maximization bid curve, is the highest when the RTPDR injection is placed at the receiving end of the congested transmission line, as seen in Table 5.30. The reason for the huge extra benefit is that the RTPDR injection power export has increased when it is placed at bus-3 to take advantage of the higher LMP value, as seen in Table 5.25. Hence, the extra benefit is much higher compared to the benefit obtained from placing the RTPDR injection at bus-1, as seen in Table 5.30. Results so far indicate that the RTPDR injection benefit from market participation is not predictable because it is a function of several factors such as system topology, LMP value of the RTPDR injection bus, and the bid characteristic of the RTPDR injection. However, results suggest that the maximum extra

benefit is obtained when the RTPDR injection is placed at the receiving end of a congested transmission line.

Table 5.30. Market Benefit of the RTPDR Injection for the Three-bus Test Case (modified scenario-II)

RTPDR Location	RTPDR cost	RTPDR revenue	RTPDR profit
Bus-1	$58.07	$102.37	$44.29
Bus-3	$884.48	$2,088.00	**$1,203.52**

5.4.3 *Scenario-III*

Scenario-III simulates a situation of generation shortage that could lead into an electricity market failure. Scenario-III does not impose any transmission system constraint. The system topology is similar to the system in Figure 5.25. However, load at bus-3 will vary to simulate different situations of generation shortage. Generator data are tabulated in Table 5.31. Load data for three different loading conditions are tabulated in Table 5.32. RTPDR effects on the electricity market for scenario-III can be analyzed from the results in Table 5.33, and Table 5.34. The location of the RTPDR injection is indifferent for scenario-III since transmission system congestion is not considered.

The electrical system in scenario-III does not converge for the inelastic case when bus-3 load reaches 277 MW, assuming that the RTPDR injection bids a fixed positive injection of 10 MW to the electricity market. At this loading level, the system load exceeds the available generation by 1 MW which leads to a market failure. In practice, the ISO will be forced to implement load shedding, an involuntary load curtailment, which is not acceptable to customers in developed countries, especially industrial facilities whose profit is severely impacted by involuntary shut down. However, in the elastic case, when the RTP of electricity rises due to a power system event, the RTPDR injection reacts to the RTP change by increasing its bid amount to make more profit. Hence, the electricity market stabilizes and prevents market failure. The new market price is influenced by the bid characteristics of the RTPDR injection. Also, note that since transmission system congestion is not considered in this scenario, the system price is uniform in all buses of the test case. In the elastic case, case-1, the RTPDR injection bid was higher than the base case of 10

MW, which helped reducing the dispatch of the expensive generator-C, as seen in Table 5.33. Hence, the system price reduced slightly, as seen in Table 5.34. In case-2, the bid curve of the RTPDR injection shows that it is willing to increase its power export to 11 MW provided that the RTP of electricity reaches $80/MWh, which is needed to supply power to the extra system load. Hence, generator-C is dispatched fully before increasing the power export of the RTPDR injection. Hence, the system price increases to $80/MWh, avoiding a complete market failure. In case-3, the system load has been increased further, which deployed more power export from the RTPDR injection, as seen in Table 5.33. The system price is determined by the bid curve characteristics of the RTPDR injection. In this particular example, the RTP has increased to $298/MWh because the RTPDR injection is willing to increase its power export to 27 MW, which is the amount of power that is needed to compensate the shortage in generation, when the RTP reaches $298/MWh. increasing the system load level higher than 27 MW might result in a condition that could lead to a market failure or load shedding event. Hence, the RTPDR injection in scenario-III can prevent a market failure situation that could lead to an involuntary load shedding event when the power system load increases up to the maximum allowed positive value of the RTPDR injection less the net fixed injection of the inelastic case. In this example, the RTPDR injection bids a fixed positive value of 10 MW in the inelastic case. However, the RTPDR injection can bid up to a maximum positive power value of 27.8 MW, which is the

Table 5.31. Generation Cost Data (scenario-III) [63]

Generator	$\boldsymbol{P_{max}}$ **(MW)**	**a ($/MW^{2}h)**	**b ($/MWh)**	**c ($/h)**
A	350	0.00158	11.1874	182.3692
B	76	0.0096	13.8095	84.0747
C	100	0.00616	18.7460	225.3385

Table 5.32. Load Data at Bus-3 (scenario-III)

Case	**Bus-3 load (MW)**
1	276
2	277
3	293
4	294

Table 5.33. Generation Dispatch for Different Cases (scenario-III)

	Case			
Generator	1	2	3	4
A	350	350	350	Does not converge
B	76	76	76	Does not converge
C	99.33	100	100	Does not converge
RTPDR injection	10.67	11	27	Does not converge

Table 5.34. LMP Data for Different Cases (scenario-III)

	Case				
	Inelastic	1	2	3	4
LMP	20.20	19.97	80.00	298.00	N/A

highest generation capacity of the RTPDR injection, less the auxiliary load of the RTPDR facility. Hence, the electrical grid was able to handle an additional 17.8 MW of load without a need to initiate a load shedding event.

Results of the three-bus test case demonstrated the ability of a RTPDR injection to reduce the RTP of electricity, which confirms the theoretical understanding discussed in section 5.3.1. The RTPDR injection was also able to limit the effect of market power that could be exercised by an expensive generator, when transmission congestion is in effect. Market failure or involuntary load curtailment might be prevented or reduced when a RTPDR injection reduces its own load or even supply power to the utility. The three-bus test case showed, surprisingly, that negative RTPs can occur when transmission system congestion is experienced, which might appear in the future Saudi electricity market.

It should be noted that the results of the three-bus test system are used as a guide for the qualitative analysis of what to expect from a real electricity system, the Saudi Grid. If transmission congestion or loss of generation occurs, a RTPDR injection can reduce the RTP volatility and reduce the price of electricity by varying magnitudes, based on the system topology, location of transmission constraints, and the bid curve characteristics of the RTPDR injection.

Results of the test system are not conclusive without testing the RTPDR injection in a real test case such as the future Saudi electricity market, which is proposed in the next section.

5.5 THE SAUDI ELECTRICITY MARKET

5.5.1 *Objective*

The work in this research attempts to quantify actual benefits from implementing a RTPDR program in a real test system, the Saudi Grid. This can be achieved by creating and modelling the Saudi Grid test system. Several RTPDR injections are modelled at various locations of the Saudi system for the purpose of studying system-wide effects of a RTPDR injection. Scenarios of transmission congestion are analyzed to study the impact of a RTPDR injection during a power system contingency. Results can be analyzed to quantify the benefits of a RTPDR program for consumers, who are motivated to participate based on economics. The analysis simulates the impact of several participating RTPDR injections in one electricity market and their impact on the electricity market as well as on each RTPDR injection profit. It is expected that the whole electricity market will benefit more from having several RTPDR injections in one market due to their impact on the market price as well as their ability to relief congestion. However, if high penetration levels of RTPDR injections participate in the electricity market, DR competition might reduce the expected benefits captured by the RTPDR injection, which is another motivation for studying the effects of RTPDR resources on a realistic test case, the Saudi Grid.

Analysis can also identify the impact of a RTPDR program on the electricity market especially generation profit, load payment, and social welfare. Other system effects from RTPDR program implementation can be observed during the analysis to confirm qualitative results that are obtained from the single-bus and three-bus test cases.

5.5.2 *Overview of the Saudi Electricity Market*

The existing Saudi market consists of a vertically-integrated utility with few private generation entities having a regulated fixed price of $32/MWh as seen in Figure 5.26. However, the existing utility is undergoing deregulation. The deregulation is being carried out in two stages. At the end of the first stage, which is already completed, several independent generation companies participate in the electricity market. Also, the generation and distribution departments within the

utility company are divided into several companies under the utility ownership as seen in Figure 5.27. Once the deregulation is complete, there will be several independent cogeneration participants in addition to the generation companies that are owned by the existing utility company. All the generated power will go to an aggregator, a principal buyer, who deals directly with the new independent transmission company for the dispatch of generation. Also, there will be several service providers in addition to the distribution companies that are owned by the existing utility company, as seen in Figure 5.28. The electricity tariff structure is not clear yet but it is anticipated that the market will implement dynamic pricing scheme such as TOU or RTP scheme, especially after the introduction of smart meters in Saudi Arabia. A contract to install smart meters in the Saudi Grid is already awarded [80]. SEC, the Saudi Electricity Company, is planning to install 12 million smart meters by 2025 across the Saudi Grid [81]. Currently, the first stage of deregulation effort has been completed. The second stage has already been initiated and it is expected to complete at the near future.

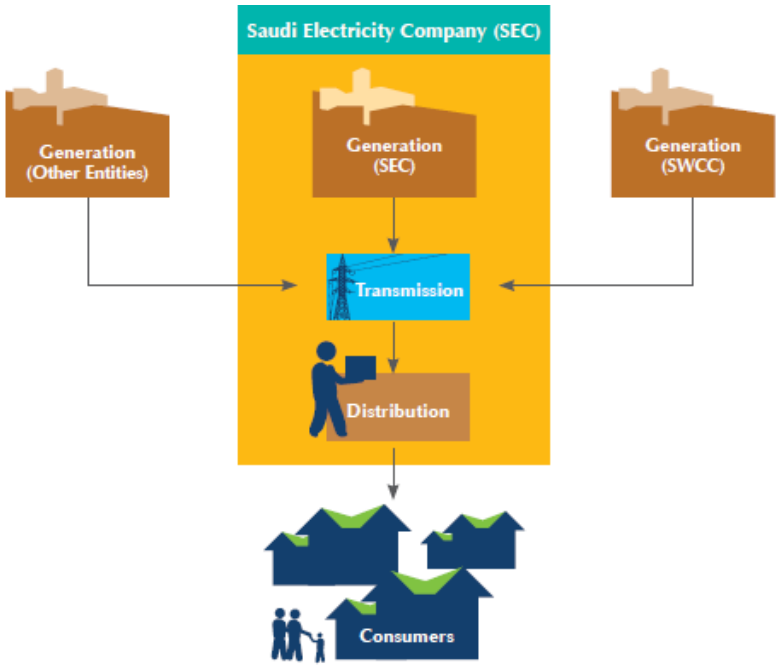

Figure 5.26. The electricity market structure in Saudi Arabia prior to deregulation [38]

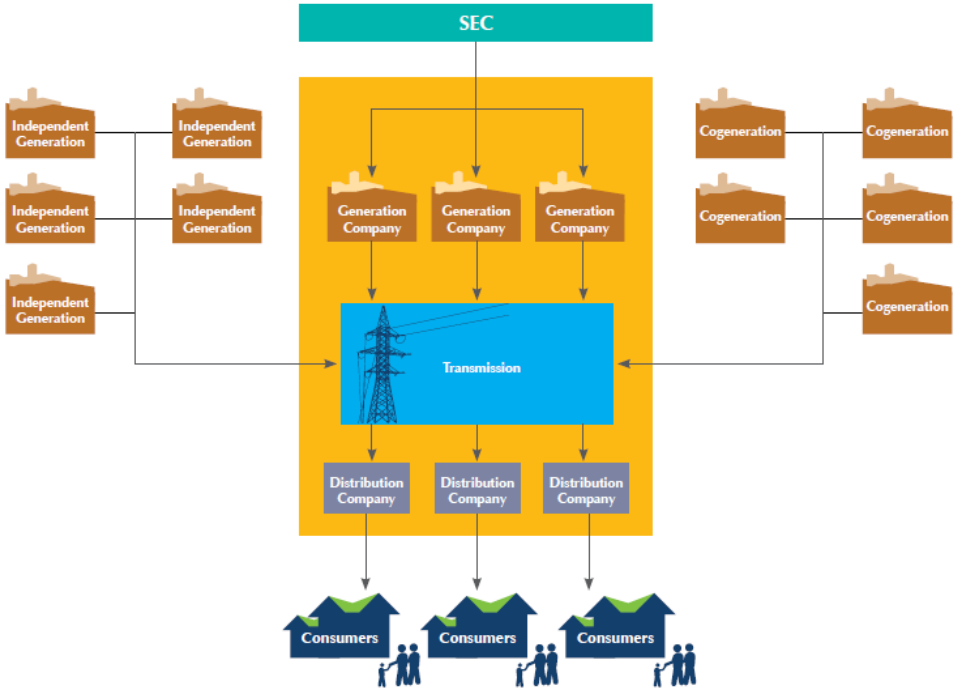

Figure 5.27. The Electricity market structure in Saudi Arabia after phase-I completion [38]

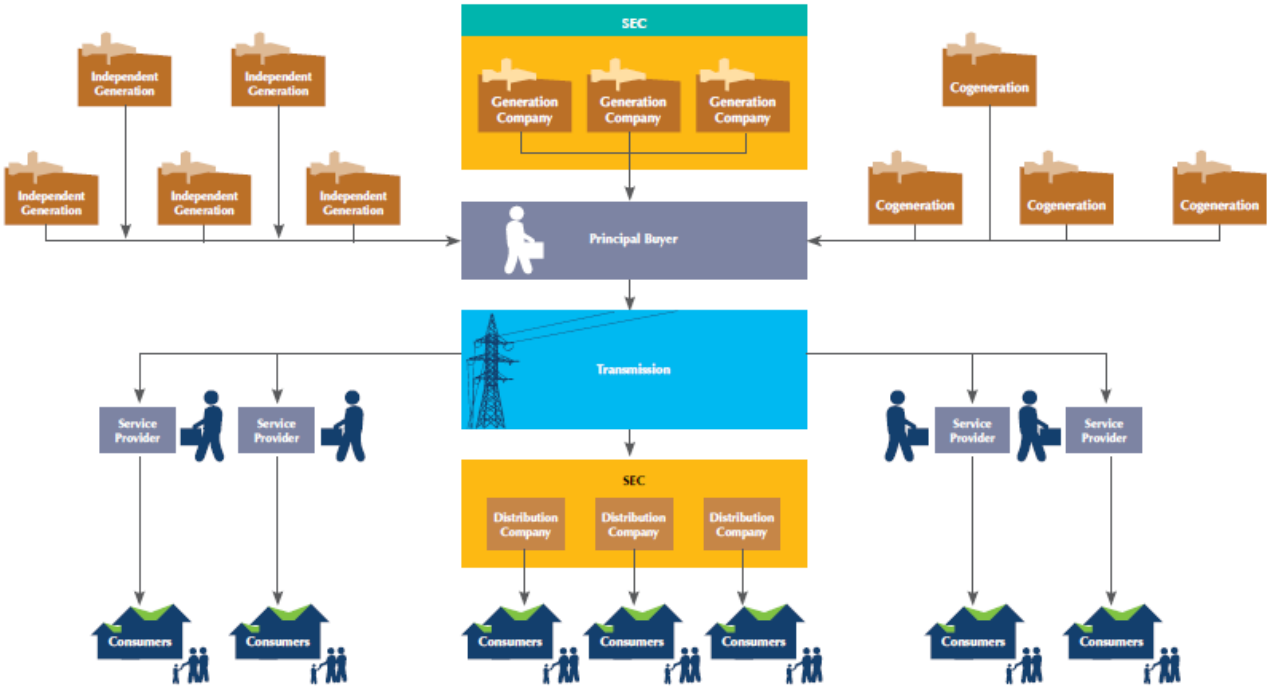

Figure 5.28. The Electricity market structure in Saudi Arabia after complete deregulation [38]

5.5.3 *Development of the Saudi Grid Test System*

Several gas processing facilities that participate in the RTPDR program are connected to the Saudi Grid System. They constitute around 5% of the total system load. The purpose of the study is to evaluate the impact of these facilities on the Saudi Grid, specifically on the RTP volatility due to transmission system congestion or shortage of generation at high demand periods.

The existing electrical system structure in Saudi Arabia is a vertically-integrated utility in which there is only one company that generates and operates the transmission system and distributes load to consumers. Other independent power producers (IPP) exist, especially large industrial customers, such as Aramco, Hadeed, SWCC, etc [55]. Currently, the utility does not release detailed system data. So, IPPs can only benefit from the publically available data, which are collected as part of this research's work. Hence, this work models the Eastern and Central regions of the Saudi Grid, which is called the Eastern-Central interconnection. The Eastern-Central interconnection constitutes more than 60% of the Saudi Grid system, excluding isolated networks [82]. The Eastern-Central interconnection has been connected to the Gulf Grid interconnection that is described in Chapter 1 since 2011 [83].

The current pricing scheme of the Saudi grid is a fixed-price scheme that is set at $32/MWh regardless of the condition of the electric system, even if transmission line congestion exists. However, it was announced by ECRA that the existing system will transform into an electricity market which consists of generation, transmission, and distribution companies. The transformation is performed in three phases. The first phase was completed as planned by the end of 2013 [38]. However, the main purpose of the transformation is to help the utility to cope up with the rapid growth in load by creating a market that provides an incentive for IPPs to participate. The Eastern and Central systems are the main components of the proposed electricity market and they are the main focus of this research. Figure 5.29 presents the existing generation and transmission systems of the Saudi Grid. The Eastern-Central interconnection is the main focus of this work and it is considered a major part of the future electricity market in Saudi Arabia.

The electric grid is divided into three systems; the generation system, the transmission system, and the distribution system. Each system is discussed in detail in the subsequent sections.

5.5.3.1 Generation Modelling

Data for the Generation system in Saudi Arabia were discussed in the single-bus model test case. Generation capability for each area, excluding isolated systems and retired generators, is tabulated in Table 5.35 using data from [55, 38, 2, 72, 84, 35, 77, 70, 71]. The Saudi Grid generation mix for each area is listed in Table 5.36.

Table 5.35. Generation Capacity by Region [55, 38, 2, 72, 84, 35, 77, 70, 71]

Area	Generation Capability (MW)
Central	14,111
East	19,069
Gulf-Interconnection (Eastern)	1,200

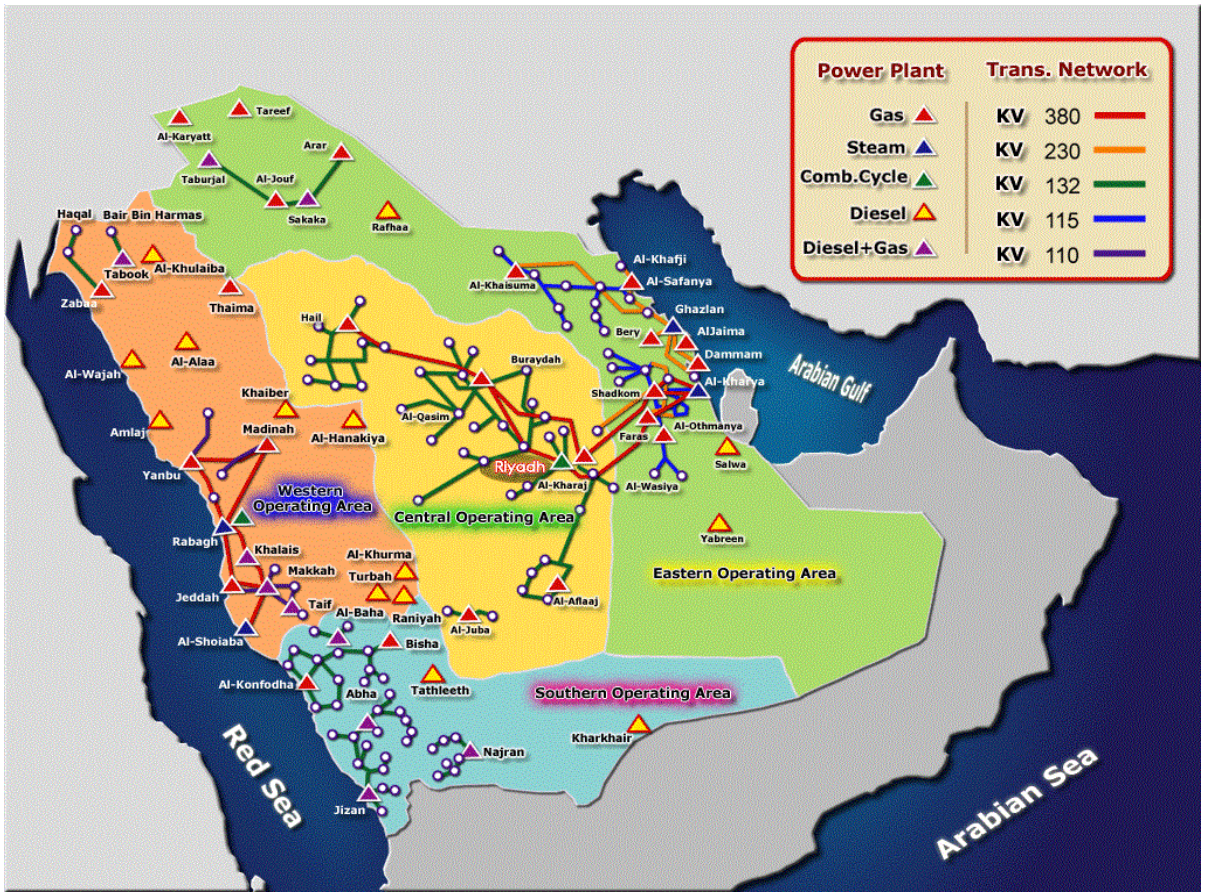

Figure 5.29. Generation and transmission systems for the Central and Eastern regions [84]

Table 5.36. Generation Mix of the Central and Eastern Systems [70]

Area	Fuel Type	Percentage (%)
Central	Combined Cycles, natural gas	21%
	Gas-turbines, natural gas	46%
	Gas-turbines, crude and diesel	33%
Eastern	Steam Cycles, natural gas	75%
	Gas-turbines, natural gas	24%
	Gas-turbines, diesel oil (back-up)	1%

Unit De-commitment: If all the existing generation at the utility is kept operational throughout the year, the utility will face the issue of power balance during light loading conditions such as in the Winter or at off-peak periods such as late night. In this case, even if all generation are dispatched at their minimum allowed power level, the electrical system will still have an excess generation causing the DCOPF not to converge. The typical approach to this issue is to formulate a unit commitment problem that has an objective function that minimizes the total cost of running generation while observing system constraints which includes the power balance constraint. However, this work is intended to deal with the current utility practice, which uses a seasonal priority list rather than performing a typical UTC.

To deal with the excess generation issue, a priority list for generation is used for each season based on generation information and data collection from [85]. The seasons are the winter, autumn/fall, and summer seasons. The winter season is December, January, and February. The summer season is June, July, August, and the first week of September. The Autumn/Fall season is the remaining months. The priority list considers generation efficiency, fuel type, and criticality of the generating unit. A difference in the objective function might arise between the priority list unit commitment and the typical unit commitment generation configuration. The use of the priority list unit commitment is justified by the current utility practice, which is part of the approximation of the Saudi power system, and the less demanding computational time.

5.5.3.2 Transmission Modelling

The transmission system is divided into three parts; the Eastern Province transmission system, the Central Province transmission system, and the transmission system connection between the two areas. The main lines that connect between the two regions are tabulated in Table 5.37. Table 5.37 lists the connection points for each line, the voltage level, the number of lines per connection, and the ampacity of each line. Hence, the transmission system between the Eastern and Central regions is very strong and no stability limits are expected since the longest line length is less than 300 miles [85, 86].

Data for the transmission system were collected as part of this work such as voltage level, transmission line ampacity, transmission line length. This includes all transmission line parameters that are needed for the simulation of the DCOPF model such as system topology and transmission line reactance. Data were obtained from the Saudi Electricity Company representative [85] and actual trace of transmission lines from the provided data using [86].

The modelled Saudi Grid consists of 186 buses with 531 transmission lines. The system topology is shown in Figure 5.30. The interconnection between the Eastern and Central regions is highlighted in red.

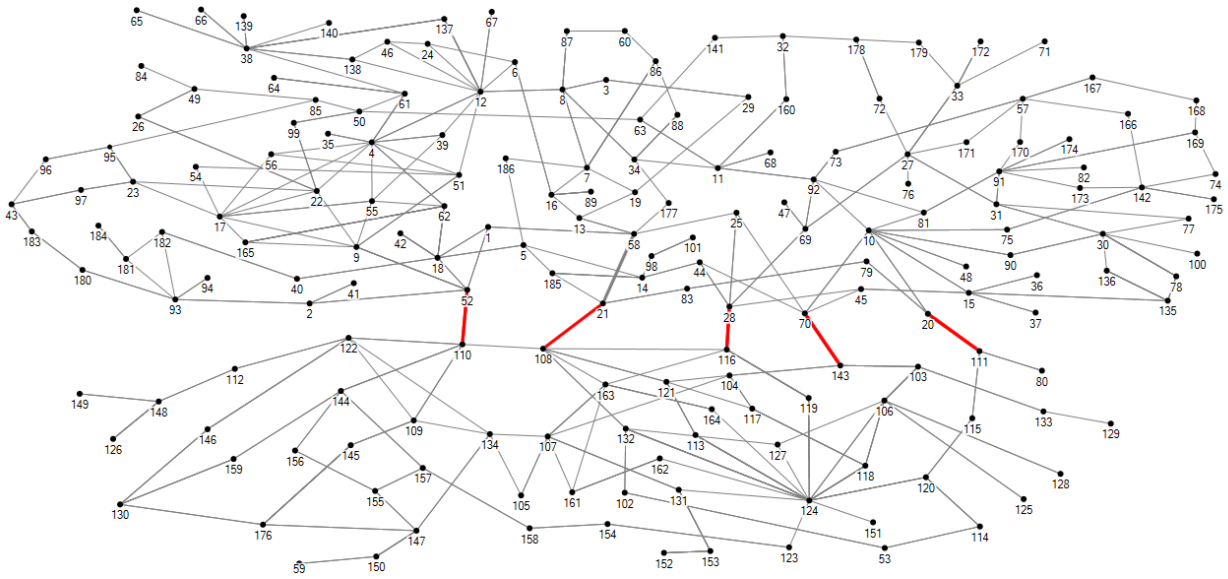

Figure 5.30. System topology of the Saudi Grid

Table 5.37. Major Transmission Lines between the Eastern and Central Regions

From	To	Voltage Level	# of lines	Line Ampacity
Faras	Kharj	380 kV	2	1650 MVA
Shegum	Qurtubah	380 kV	2	1650 MVA
Fadhili	Sudair	380 kV	2	1650 MVA
Khurais	Riyadh-9019	380 kV	2	1650 MVA
Wasia	Majmaah	230 kV	2	741 MVA

Soft Constraints: Running a real test system in an optimal power flow environment may face a convergence issue. A useful approach to deal with the DCOPF infeasibility is to introduce a penalty to the hard constraint, which relaxes the transmission line capacity constraint.

A new variable is introduced to represent the violation of a transmission constraint for each branch l, FV_l. The value of FV_l is positive and the sum of the violation and the transmission line limit must be greater than the flow and the negative flow in the constraint transmission line l [79]. The new soft constraints, then, are:

$$FV_l \geq 0 \tag{5.21}$$

$$FV_l + limit_l \geq P_l \tag{5.22}$$

$$FV_l + limit_l \geq -P_l \tag{5.23}$$

The transmission line capacity soft constraint is chosen such that it is a linear penalty function as seen in Figure 5.31 and equation (5.24). So, a linear cost coefficient $c_{v,l}$ is used for each transmission line violation FV_l. Hence, the new penalty cost function to be added to the objective function is [79]:

$$f_p(P_l) = \sum_{l=1}^{L} c_{v,l} \cdot FV_l \tag{5.24}$$

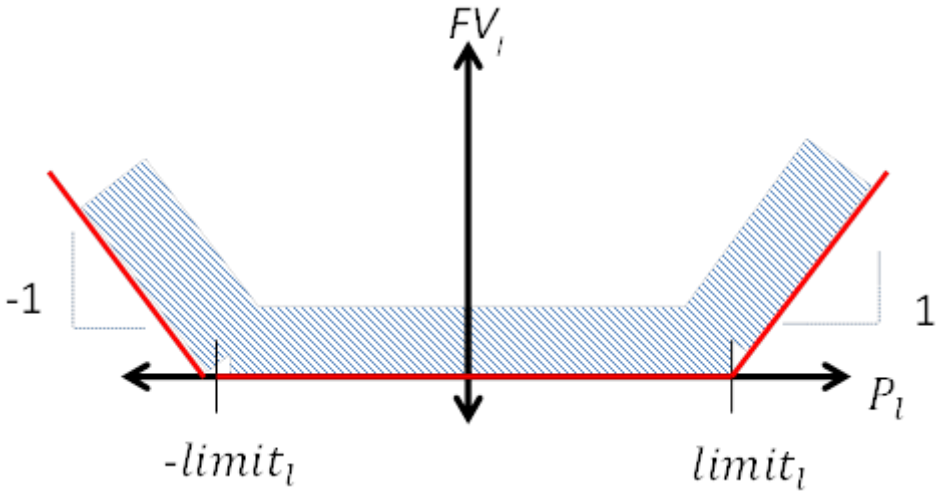

Figure 5.31. Feasibility region for the transmission line violation constraint [79]

5.5.3.3 Distribution System

In the distribution system, load is categorized into either a RTPDR injection or an inelastic load. Large industrial loads, which are price-responsive, are modeled individually, mostly large industrial loads that own a cogeneration system. The modelled Saudi Grid consists of 186 buses. Each bus load is a residential load, industrial load, or a combination of both. The available data only provides the total load for each province [77]. Hence, a residential load is calculated using demographic information from [87] as follows:

$$L_{Bus_i}^{residential} = \frac{Bus_i\ population}{total\ province\ population} \times L_{total}^{residential} \tag{5.25}$$

Industrial load is divided into two parts; price-responsive load and inelastic load. Inelastic industrial load data is collected from [85, 88, 89, 90, 91]. If an industrial load is new, the load is calculated based on the ratio of the completed operational part of the industrial load to its nameplate capacity. Detailed information of the price-responsive industrial loads, which are suitable for RTPDR implementation, is collected and modeled into the Saudi Grid as part of this effort. Detailed data of the price-responsive facilities is binding by a confidentiality agreement. Note that data for the load profile of the Saudi Grid is not publically available. Therefore, it is assumed that the Saudi Grid load profile will follow the load profile of the ERCOT system for the reasons mentioned in section 3.1 of Chapter 3.

5.5.4 *Testing the Saudi Grid System*

The purpose of simulating a RTPDR injection into the Saudi Grid is to determine the effects of the RTPDR injection on consumers, suppliers, social welfare, and the electricity market. More accurate results can also be concluded from testing the RTPDR injection in a real test system, the Saudi Grid. Simulation is intended to quantify RTPDR benefits for participating consumers including price-responsive loads, determine the impact of RTPDR resources on suppliers' profit, and identify any change in social welfare. Transmission congestion (TC) and loss of generation (LG) can be imposed to identify the response of the RTPDR injection and analyze its effects, which are expected to relieve or reduce the effect of TC or mitigate a situation of LG. The testing and analysis of the Saudi Grid is intended to quantify consumer benefits and any possible increase in the social welfare due to the implementation of a RTPDR program. Calculation of consumer surplus, generation profit, change is social welfare will be similar to the calculations provided in the three-bus system.

Simulation of LG in a DCOPF environment resulted in a convergence issue due to the inability of generation resources to meet electricity demand. Hence, a market failure or involuntary load shedding is expected. However, if a RTPDR resource participates in the electricity market, no transmission congestion is in effect, and the RTPDR resource is large enough to compensate for the lost generation, then the RTPDR resource is expected to help the electricity market avoiding a market failure situation.

Demand curves for several process facilities are extracted from the output of the algorithm for the model discussed in Chapter 2. Different generation system size and cost data is implemented for each RTPDR facility based on the actual installed generation capacity at each modelled RTPDR facility. It is expected, in practice, to see a small variation of steam demand and boilers operating cost from one facility to another. However, due to the lack of information, it is assumed that the steam consumption per unit of production and boiler cost data is similar for all RTPDR facilities. Variations in steam consumption and operational cost of boilers are assumed to be negligible in this work.

Demand curves for the RTPDR facilities are used to model several RTPDR injections in the Saudi Grid. Examples of modelling a RTPDR injection from a demand or bid curve in a DCOPF environment are discussed in section 5.3.1.3.

The procedure for testing the Saudi Grid is by scenario creation and simulation in which conditions are either studied or imposed and results are analyzed. Scenarios of interest are created similar to the scenarios developed in the three-bus test system, data is evaluated, and results are discussed. The RTPDR injection, which responds as a function of the RTP of electricity, is compared between the elastic and inelastic cases from social welfare point of view as well as its effects on the RTP of electricity, similar to the three-bus test case.

The existing Saudi Grid is not expected to experience any transmission congestion in the near future because it is overdesigned. However, considering the rapid increase in the peak load of the Saudi Grid, averaging around 7.4% per year, the Saudi Grid peak load is expected to double in less than a decade [3]. Hence, several low ampacity transmission lines, particularly at the 115 KV level, are expected to experience TC in the near future. Also, shortage of generation might be experienced during peak periods. A RTPDR injection is expected to relieve or reduce the effect of TC by reducing load due to the expected increase in the RTP of electricity at the receiving end of the congested transmission line. Hence, a power flow reduction at the congested transmission line is expected, as seen in scenario-II of the three-bus test case. If a loss of generation occurs, market power might be exercised, which might lead to a market failure or involuntary load shedding. As a result, a dramatic increase in the RTP of electricity is expected. However, when the RTPDR injection reacts to an increase of the RTP of electricity, it reduces the chance for generation companies to exercise market power. This is expected to lead to a lower RTP of electricity compared to treating a price-responsive load as an inelastic load, as seen in scenario-III of the three-bus test case.

The expected conclusion is that the RTPDR injection can improve power system reliability, limit the possibility of exercising market power, and reduce the chance for involuntary load curtailment. It is expected that with higher penetration of RTPDR resources that the RTP volatility reduces and the electricity market becomes more stable. It is also expected that the RTP of electricity reduces, which results in a lower profit for generation companies. Load payment is expected to reduce, which increases consumer surplus. Hence, the expected net effect is an improvement of the social welfare for the whole society.

5.6 CONCLUSION

Literature review highlighted the need for studying the impact of price-responsive load participation on the electricity market. The work in this chapter developed a method to do exactly that, by computing RTPDR injection profits and system-wide social welfare. The method was implemented for the natural gas plant load model developed earlier, and a single-bus model of the Saudi Electricity Market. The system included several RTPDR injections that participate in the Saudi Electricity market. The developed method also provided a means to analyze RTPDR injection benefit to the society by calculating the change in social welfare from having a higher penetration level of RTPDR injections. The study of the single-bus model of the Saudi Grid was expanded to a small-size test system that has a transmission network, the three-bus test case, to study system-wide effects of RTPDR injections in an electricity market. The qualitative analysis of the single-bus model of the Saudi Grid is used as a guide for the analysis of the three-bus test system.

The method can be generalized to any other electricity market that allows RTPDR injection participation and operates with a RTP of electricity. The use of a specific RTPDR injection model developed from an actual industrial facility, and system economic parameters based on the actual Saudi Grid make this work more realistic than the generic models and fictitious demand response characteristics in most published work. The quantitative results of the analysis can be generalized to other electricity markets that allow participation of price-responsive loads.

The outcome of this work can influence the debate about the market structure in Saudi Arabia which has the potential to impact a large investment in the future Saudi market that is valued in billions of dollars. The analysis showed that there is less RTP volatility with more RTPDR participation, which is an expected result. The analysis also confirmed the expected result of less market failures, i.e. less RTP volatility, including fewer and lower price spikes, and less involuntary load shedding.

The analysis in this work studied the effects of RTPDR injections on generation profit, consumer surplus, generation cost, load payment, and social welfare. Results demonstrated that the higher the penetration level of RTPDR injections in the electricity market, the higher the social welfare value will become, which benefits all electricity market participants. This in turn

may motivate regulators to more readily approve the RTP scheme for the electricity market and encourage RTPDR participation in the electricity market.

The results of this chapter also demonstrated that the captured benefit by a RTPDR injection is lower when other price-responsive loads participate in the electricity market, which is an expected result. Hence, improved quantification of RTPDR injection benefits should consider the effect of RTPDR injection participation on the electricity market.

Chapter 6. CONTRIBUTIONS OF THE RESEARCH WORK AND FUTURE RESEARCH DIRECTIONS

This chapter lists the contributions of this work and highlights their importance. The contributions of this dissertation are divided into four parts. The first part identified one important characteristic to determine the suitability of industrial facilities for RTPDR participation and applied this insight to a natural gas processing facility. The second part developed an instantaneous scheduling algorithm to maximize profit for an industrial facility. The algorithm was expanded to a time-domain scheduling to develop a method to quantify the benefits of DR participation using a realistic model of the industrial process, which was applied to a specific gas processing facility to generate quantitative results, as requested in the literature review. The third part is a method to modify an industrial facility design to optimize the net benefit from RTPDR participation. The last part of contributions is a methodology to quantify RTPDR load benefits to the electricity market and society, which can influence decisions about the electricity market structure in Saudi Arabia. Subsequent sections discuss each contribution in detail and provide an assessment for its importance.

Future research directions are proposed which use the work in this dissertation as a starting point and expands the research scope beyond this dissertation.

6.1 IDENTIFICATION OF SUITABLE RTPDR FACILITIES

The analysis in Chapter 2 determined candidate ARAMCO facilities that are theoretically suitable for RTPDR implementation. It also identified one important metric, thermal time constant, to use to assess the suitability of a process system for RTPDR program implementation.

Assessment of candidate RTPDR facilities provides a means to prioritize DR implementation based on its suitability. A natural gas processing facility is found to be a suitable candidate for RTPDR program implementation due to its short thermal time constant. If the thermal time constant of a process system is characterized to be short, then it has the flexibility to maneuver fairly quickly in response to fluctuations of the RTP of electricity.

The theoretical viability of RTPDR implementation in a suitable facility, the gas processing facility, is established. The ability to identify suitable industrial facilities for RTPDR

implementation can influence the decision of an industrial facility owner's about the implementation of a RTPDR program.

6.2 Quantification of RTPDR Benefits for an Industrial Facility

Literature review highlighted the need for a tool to quantify DR benefits and motivate customers' participation. This work provides one such tool, as discussed in Chapter 3.

Chapter 2 developed an instantaneous scheduling algorithm and determined that MIP is a suitable solution method. The algorithm was applied to a specific gas processing facility to maximize its profit and generate its bid curve. The algorithm was expanded to a time-domain scheduling to develop a method to quantify the benefits of DR participation using a realistic model of a gas processing facility to generate quantitative results.

The qualitative analysis of this work can be generalized to any other industrial facility that participates in a RTPDR program. However, quantitative results and the benefit obtained by a RTPDR facility will obviously vary in magnitude from one facility to another.

The developed tool analyzes the effects of implementing a RTPDR program on the operation of a process facility in an electricity market with RTP. Quantification of RTPDR benefits demonstrated that there are positive financial incentives for participation in a RTPDR program. The economic feasibility of the implementation of a RTPDR program at the process facility is established. Quantifying DR financial benefits can influence the facility owner's decision about participation in a RTPDR program. This in turn defeats a claim that states that a low penetration level of price-responsive loads is a direct result of lack of incentives for participating customers [6]. The developed tool can be extended to a wide range of industrial facilities. Facilities that realize a benefit (i.e. increased profit) from engagement in a RTPDR program are expected to participate. This in turn makes the electricity market more efficient and improves social welfare of the society.

6.3 A Method for Design Study to Modify an Industrial Facility to Improve its RTPDR Capability

A methodology to conduct a design study for a RTPDR program implementation in a gas processing facility is developed using a cost-benefit approach, as described in Chapter 4. The

design study evaluated the impact of expanding the size of three key parameters of the gas processing facility that could impact the benefit obtained from a RTPDR program in an industrial facility. These parameters are generation system size, storage tank capacity, and process system capacity.

The analysis method of the design study can be applied to any industrial facility that considers participation in a RTPDR program and has thermal and process constraints. However, quantitative results and the size of each design parameter may vary from one facility to another depending on the cost of expansion, required pay-back period, and the realized benefit from participation in a RTPDR program that is influenced by the RTP profile. Once actual Saudi Grid price data becomes available, the quantitative results of the design study are expected to be more accurate.

The design study examined the expansion of each design parameter in isolation. However, initial results indicated that the design parameter of the process facility are interdependent, which suggests there is room for improvement by formulating a multi-variable design study that can determine the size of expansion for each design parameter simultaneously. The formulation of the multi-variable design study involves a major reformulation, which is discussed with details in the future work section.

6.4 A Method for Quantification of RTPDR Benefits for the Electricity Market and Society

Literature review highlighted the need for studying the impact of price-responsive load participation on the electricity market and its performance [20, 21]. The work in Chapter 5 developed a method to do exactly that, by computing RTPDR load profits and system-wide social welfare. The method was implemented for the natural gas plant load model developed earlier, and the likely future Saudi Electricity Market. The analyzed system included several RTPDR loads that participate in the Saudi Electricity market. The method was also used to examine the effect of varying RTPDR penetration on social welfare and on individual RTPDR load benefits.

The method can be generalized to any other electricity market that allows RTPDR load participation and operates with a RTP of electricity. The use of a specific RTPDR load model developed from an actual industrial facility, and system economic parameters based on the actual

Saudi Grid make this work more realistic than the generic models and fictitious demand response characteristics in most published work. The method was implemented for the natural gas plant load model developed earlier and a single-bus model of the Saudi Electricity Market to study the local effects of RTPDR injection. The study of the single-bus model of the Saudi Grid was expanded to a small-size test system that has transmission network, the three-bus test case, to study system-wide effects of RTPDR injections in an electricity market, such as transmission congestion. The qualitative analysis of the single-bus and three-bus test systems can be used as a guide for the analysis of a real test system, the synthesized Saudi Grid.

The outcome of this work can influence the debate about the market structure in Saudi Arabia which has a potential to impact a large investment in the future Saudi market that is valued in billions of dollars. The analysis showed that there is less RTP volatility with more RTPDR participation, which is an expected result. The analysis also confirmed the expected result of fewer market failures, i.e. less RTP volatility, including fewer and lower price spikes, and less involuntary load shedding. Results demonstrated that the higher the penetration level of RTPDR injections in the electricity market, the higher the social welfare value will become, which benefits all electricity market participants. This in turn may motivate regulators to more readily approve the RTP scheme for the electricity market and encourage RTPDR participation in the electricity market. Results also demonstrated that the captured benefit by a RTPDR load is lower when other price-responsive loads participate in the electricity market, which is an expected result. Hence, quantification of RTPDR load benefits should consider this effect.

6.5 FUTURE WORK

6.5.1 *Identification of Characteristics of Suitable RTPDR Facilities*

The analysis in Chapter 2 identified one important metric, thermal time constant, to use to assess the suitability of a process system for RTPDR program implementation. A more general screening process for RTPDR suitability could be identified, which can lead to a less expensive and faster implementation of a RTPDR program in suitable industrial facilities.

While thermal time constant is an important metric to assess the suitability of a process system for RTPDR program implementation, there should be other metrics that determine feasibility that did not arise in this research. A qualitative consideration of plant operations

identifies if they can change their output fairly quickly for RTPDR implementation, i.e. incoming raw material flow rate variation, start-up time for a process system, and ramp up/ramp down capability of a process system

6.5.2 *Expand DR Participation to Other Components of the Load*

It is of interest to expand the idea of RTPDR to other industrial facilities and process models that have RTPDR capability. For example, other types of gas processing and treatment facilities have short thermal time constants, which makes them good candidates for immediate RTPDR participation. Saline Water Conversion Corporation (SWCC) facilities constitute around 10% of electricity generation in Saudi Arabia. It is of interest to study the possibility of implementing a RTPDR program in SWCC facilities, which has the potential of increasing the penetration level of RTPDR resources by a considerable amount. However, each process system is unique and has its own process model, operational philosophy and constraints. If process constraints that limit the flexibility of RTPDR participation are modeled properly, then these facilities can use the formulation in this work to quantify the benefits from participation in a RTPDR program.

6.5.3 *Expansion of the Detailed Model of the Industrial Facility's Process System*

A more accurate model for an industrial facility should be achievable through a multi-disciplinary effort including chemical and mechanical engineers. This is needed to capture the capabilities and dynamics of the process system flow and variations. For example, the ramp up/down limits were taken from the observation of the highest ramp up/down change of the process system from the historical data of the process system. However, there is a possibility that the ramp up/down capability of the process system is less binding, which would enable the process system to maneuver over a better range. Hence, a higher benefit is expected from participation in a RTPDR program. Some process facilities might not favor a continuous change of the incoming raw material flow rate due to the extra maintenance cost and the reduced lifetime of some of the process equipment. An added constraint could be enforced to accommodate this possible operational philosophy requirement. In this case, a cost-benefit approach is suggested, which compares the extra cost with the extra benefit obtained from allowing a continuous change to the incoming raw material flow rate.

6.5.4 *Expanding the Analysis for the Saudi Grid Test System*

The Saudi Grid data are not publically available and the model is built from scratch. The Saudi Grid model was recently completed. The original goal is to extend the three-bus analysis to the synthesized Saudi Grid.

Preliminary results of the Saudi Grid analysis, which are not part of this work, show that negative electricity prices were observed when transmission congestion is imposed. Also, the electricity price in some buses reached as high as $600/MWh. Due to time limitation, a complete analysis was not conducted for the Saudi Grid and it is moved to the future work.

6.5.5 *A Multi-objective Design Study for the Gas Processing Facility Using the Saudi Grid RTP Data*

The design study in Chapter 4 examined the expansion of each design parameter in isolation. A multi-variable design study that can determine the size of expansion for each design parameter simultaneously is expected to yield better results due to the discovered interdependence of the design parameters of the gas processing facility.

Based on initial analysis, the formulation of the multi-variable design study involves a major reformulation and a possible change of the selected optimization technique and solver. In this case, the use of a non-linear solver might be needed. The new formulation would also use the Saudi Grid model to generate more accurate estimates of the RTP of electricity in the Saudi market. Hence, the quantitative analysis will become more accurate.

If the results of the design study are not promising for expanding the existing facilities for RTPDR program implementation, then the question becomes whether a design study of a new industrial facility for RTPDR implementation would yield positive results or not. Considering participation in a RTPDR program at the design stage of an industrial facility can influence the size of parameters that provide the needed flexibility for a RTPDR program implementation. This is economically motivated by the reduced capital cost of implementing a RTPDR program at the design stage due to the flexibility of equipment selection and economy of scale. Also, the ability to modify the process system at the design stage for RTPDR program implementation can be achieved by an inter-disciplinary effort that involves chemical and mechanical engineers. For

example, a refinery design could be modified to accommodate RTPDR participation or at least allow the cogeneration system to respond to the RTP of electricity.

6.6 CONCLUSION

This dissertation investigated the implementation of a RTPDR program in a natural gas processing facility. The analysis was carried out on a detailed facility model that incorporates transition constraints. It quantified RTPDR benefits to the price-responsive facility and to social welfare. This work opens the door to explore RTPDR benefits for other market participants that have RTPDR capability and are motivated to participate based on financial incentives, such as gas processing facilities and water treatment facilities. The current trend for the Saudi Electricity Company is to replace electro-mechanical tariff meters with AMRs, which provides the needed infrastructure for RTPDR implementation and opens the door for residential load participation. The outcome of this work shows that a RTPDR facility can increase its profit in a socially responsible way! The results of this work may influence the decision to move to an electricity market in Saudi Arabia and influence industrial facility owners to seriously consider participation in a RTPDR program.

BIBLIOGRAPHY

[1] C. Janahi, 2009. [Online]. Available: http://www.gccia.com.sa/articles/Arab%20Electricity%20Conference%20by%20Chairman%20Janahi%20Nov-2009.pdf. [Accessed 15 September 2011].

[2] F. Al Jabri and T. Khan, "KPIs for the Saudi Arabian Electricity Sector," in IEEE Energycon, Manama, 2010.

[3] S. H. Ghanam, B. Shahrani, A. Essa, M. M. Hamrani, F. A. Dubaikel and A. T. Awami, "Saudi ARAMCO's efforts in smart grid," in IEE PES Conference on Innovative Smart Grid Technologies, Jeddah, 2011.

[4] H. Asano, M. Takahashi and N. Ymaguchi, "Market Potential and Development of Automated Demand Response System," IEEE Power and Energy Society General Meeting, pp. 1-4, 2011.

[5] S. Mohagheghi and N. Raji, "Intelligent demand response scheme for energy management of industrial systems," in IEEE Industry Applications Society Annual Meeting (IAS), Las Vegas, 2012.

[6] J. Torriti, M. G. Hassan and M. Leach, "Demand response experience in Europe: Policies, programmes and implementation," Energy, vol. 35, no. 4, pp. 1575-1583, 2010.

[7] H. Saele and O. Grande, "Demand Response From Household Customers: Experiences From a Pilot Study in Norway," IEEE Transactions on Smart Grid, vol. 2, no. 1, pp. 102-109, 2011.

[8] N. Lu, "An Evaluation of the HVAC Load Potential for Providing Load Balancing Service," IEEE Transactions on Smart Grid, vol. 3, no. 3, pp. 1263 - 1270, 2012.

[9] Z. Wang, R. Paranjape, A. Sadanand and Z. Chen, "Residential demand response: An overview of recent simulation and modeling applications," in 26th Annual IEEE Canadian Conference on Electrical and Computer Engineering (CCECE), Regina, 2013.

[10] W. Han, L. Zhang and J. Liu, "Demand response model for characteristics analysis of electricity consumers," in IEEE Innovative Smart Grid Technologies - Asia (ISGT Asia), Tianjin, 2012.

[11] K. Kuroda, T. Ichimura and R. Yokoyama, "An effective evaluation approach of demand response programs for residential side," in 9th IET International Conference on Advances in Power System Control, Operation and Management (APSCOM 2012), Hong Kong, 2012.

[12] M. H. Albadi and E. F. El-Saadany, "A summary of demand response in electricity markets," Electric Power Systems Research, vol. 78, no. 11, pp. 1989-1996, 2008.

[13] A. Conchado and P. Linares , "Economics for energy," February 2010. [Online]. Available: http://www.eforenergy.org/docpublicaciones/documentos-de-trabajo/WP02-2010.pdf. [Accessed 7 November 2012].

[14] US Department of Energy, "Benefits of Demand Response in Electricity Markets and Recommendations for Achieving them," Report to the United States Congress, February, 2006.

[15] Y. Tang, F. Xu and L. Chen, "Research into possibility of smart industrial load participating into demand response to supply the power system," in China International Conference on Electricity Distribution (CICED) , Nanjing, 2010.

[16] D. J. Hammerstrom, R. Ambrosio, J. Brous, T. A. Carlon, D. P. Chassin, J. G. DeSteese, R. T. Guttromson, G. R. Horst, O. M. Järvegren, R. Kajfasz, S. Katipamula, L. Kiesling, N. T. Le, P. Michie, T. V. Oliver, R. G. Pratt, S. Thompson and M. Yao, "Pacific Northwest GridWise Testbed Demonstration Projects, Part I. Olympic Peninsula Project," Pacific Northwest National Laboratory, Richland, 2007.

[17] D. Menniti, F. Costanzo, N. Scordino and N. Sorrentino, "Purchase-Bidding Strategies of an Energy Coalition With Demand-Response Capabilities," IEEE Transactions on Power Systems, vol. 24, no. 3, pp. 1241 - 1255, 2009.

[18] D. S. Kirschen, "Demand-side view of electricity markets," IEEE Transactions on Power Systems, vol. 18, no. 2, pp. 520 - 527, 2003.

[19] S. Singh and J. Ostergaard, "Use of demand response in electricity markets: An overview and key issues," in 2010 7th International Conference on the European Energy Market (EEM), Madrid, 2010.

[20] L. Jidong, Z. Zehui, Z. Li and H. Xueshan, "Evaluating short term benefits of demand response," in 4th International Conference on Electric Utility Deregulation and Restructuring

and Power Technologies (DRPT), Weihai, 2011.

[21] D. Yang and Y. Chen, "Demand response and market performance in power economics," in IEEE Power & Energy Society General Meeting (PES), Calgary, 2009.

[22] N. Venkatesan, J. Solanki and S. Solanki, "Market optimization for microgrid with Demand Response model," in North American Power Symposium (NAPS), 2011, Boston, 2011.

[23] A. Kowli and G. Gross, "Quantifying the variable effects of systems with demand response resources," Bulk Power System Dynamics and Control (iREP) - VIII (iREP), 2010 iREP Symposium, pp. 1-10, 2010.

[24] J. L. Adams and W. C. Boyer, "Large fractionation facilities on NGL pipelines," Proceedings of the annual convention of the Gas Processors Association, pp. 178-183, 1981.

[25] "Chicago Tribune," 06 June 2012. [Online]. Available: http://articles.chicagotribune.com/2012-06-06/news/sns-rt-markets-cancrudel1e8h6j83-20120606_1_keystone-pipeline-oversupply-of-canadian-barrels-bpd-crude-distillation-unit. [Accessed 31 May 2013].

[26] M. Abahussain and R. Christie, "Optimal scheduling of a natural gas processing facility with Price-based Demand Response," in 2013 IEEE Power and Energy Society General Meeting (PES), Vancouver, BC, 2013.

[27] A. J. Wood and B. F. Wollenberg, Power Generation, Operation, and Control, 2nd ed., New York: Wiley, 1996.

[28] N. L. Ricker, Interviewee, [Interview]. 20 April 2011.

[29] G. Angevine and D. Hrytzak-Lieffers, "The Fraser Institute," September 2007. [Online]. Available: http://www.fraserinstitute.org/research-news/display.aspx?id=13267. [Accessed 31 1 2014].

[30] S. Farghal, R. El-Dewieny and A. Riad, "Optimum operation of cogeneration plants with energy purchase facilities," IEE Proceedings-Generation, Transmission and Distribution, vol. 134, no. 5, pp. 313-319, 1987.

[31] I. Pan, "Market Realist," Market Realist, Inc., 10 May 2013. [Online]. Available: http://marketrealist.com/2013/05/frac-spreads-decreased-4-last-week-reducing-nat-gas-processors-margins/. [Accessed 29 May 2013].

[32] T. Li and M. Shahidehpour, "Price-based unit commitment: a case of Lagrangian relaxation versus mixed integer programming," IEEE Transactions on Power Systems, vol. 20, no. 4, pp. 2015-2025, 2005.

[33] M. Carrion and J. M. Arroyo, "A computationally efficient mixed-integer linear formulation for the thermal unit commitment problem," IEEE Trans. on Power System, vol. 21, no. 3, pp. 1371-1378, Aug. 2006.

[34] "Fair Isaac Corporation," [Online]. Available: http://www.fico.com/en/Products/DMTools/xpressoverview/Pages/Xpress-Optimizer.aspx.

[35] Saudi Electricity Company, "Annual Report 2011," 22 May 2012. [Online]. Available: http://www.se.com.sa/SEC/English/Panel/Reports/. [Accessed 25 July 2012].

[36] C. A. S. Monroy and R. D. Christie, "Energy storage effects on day-ahead operation of power systems with high wind penetration," in North American Power Symposium (NAPS), Boston, 2011.

[37] P. Wattles, "Electric Reliability Council of Texas," 23 May 2012. [Online]. Available: http://www.ercot.com/content/news/presentations/2012/ERCOT_EEForum_2012.pdf. [Accessed 1 2 2014].

[38] Electricity & Cogeneration Regulatory Authority, "Activities & Achievements of the Authority in 2011," Jun. 2012. [Online]. Available: http://www.ecra.gov.sa/documents/Annual%20Reports/ECRA%20ACTIVITIES%20REPORT-WEB.pdf.

[39] P. Mandal, T. Senjyu, N. Urasaki, T. Funabashi and A. Srivastava, "A Novel Approach to Forecast Electricity Price for PJM Using Neural Network and Similar Days Method," IEEE Transactions on Power Systems, vol. 22, no. 4, pp. 2058 - 2065, 2007.

[40] Y. Wang, "Price-load elasticity analysis by hybrid algorithm," in Third International Conference on Electric Utility Deregulation and Restructuring and Power Technologies, 2008., Nanjuing, 2008.

[41] K. Lo and V. Wu, "Analysis of relationships between hourly electricity price and load in deregulated real-time power markets," IEE Proceedings- Generation, Transmission and Distribution, vol. 151, no. 4, pp. 441- 452 , 2004.

[42] "The Weather Channel," [Online]. Available: http://www.weather.com/weather/wxclimatology/monthly/graph/USTX0617. [Accessed 11 February 2013].

[43] "The Weather Channel," [Online]. Available: http://www.weather.com/weather/wxclimatology/monthly/graph/BAXX0001. [Accessed 11 February 2013].

[44] J. Ostrowski, M. Anjos and A. Vannelli, "Tight Mixed Integer Linear Programming Formulations for the Unit Commitment Problem," IEEE Transactions on Power Systems, vol. 27, no. 1, pp. 39-46, 2012.

[45] H. Pandzic, T. Qiu and D. Kirschen, "Comparison of state-of-the-art transmission constrained unit commitment formulations," in 2013 IEEE Power and Energy Society General Meeting (PES), Vancouver, BC, 2013.

[46] W. L. Winston, M. A. Venkataramanan and J. B. Goldberg, Introduction to mathematical programming, Pacific Grove, CA : Thomson/Brooks/Cole, 2003.

[47] J. Warrington, C. Hohl, P. Goulart and M. Morari, "Rolling Unit Commitment and Dispatch With Multi-Stage Recourse Policies for Heterogeneous Devices," IEEE Transactions on Power Systems, vol. 99, pp. 1-11, 2015.

[48] P. Andrianesis, G. Liberopoulos, P. Biskas and A. Bakirtzis, "Medium-Term Unit Commitment in a pool market," in 2011 8th International Conference on the European Energy Market (EEM), Zagreb, 2011.

[49] S. K. Smith and T. Sincich, "An Empirical Analysis of the Effect of Length of Forecast Horizon on Population Forecast Errors," Demography, vol. 28, no. 2, pp. 261-274, May 1991.

[50] D. J. BOWERSOX, "Logística empresarial: o processo de integração da cadeia de suprimento," São Paulo: Atlas, 2001.

[51] A. P. S. Junior, J. C. Novi, A. C. P. Junior and M. M. B. d. Oliveira, "E-Scm and Inventory Management: A Study of Multiple Cases in a Segment of the Department Store Chain," JISTEM, vol. 8, no. 2, pp. 367-388, 2011.

[52] General Algebraic Modeling System (GAMS) Release 24.0.3, Washington, DC, USA:

Corporation, GAMS Development, 2013.

[53] "U.S. Energy Information Administration," 21 01 2015. [Online]. Available: http://www.eia.gov/dnav/pet/pet_pri_spt_s1_d.htm. [Accessed 22 01 2015].

[54] "U.S. Energy Information Administration," 21 01 2015. [Online]. Available: http://www.eia.gov/dnav/ng/ng_pri_fut_s1_d.htm. [Accessed 22 01 2015].

[55] Center for Engineering Research, "Updated Generation Planning for the Saudi Electricity Sector," KFUPM, Dhahran, 2006.

[56] "The Electric Reliability Council of Texas," [Online]. Available: http://www.ercot.com/mktinfo/loadprofile/alp/. [Accessed 11 November 2012].

[57] A. Mohapatra, M. Mallick, K. Panigrahi, Z. Cui and S. Hong, "A hybrid approach for short term electricity price and load forecasting," in 2011 International Conference on Energy, Automation, and Signal (ICEAS), Bhubaneswar, 28-30 Dec. 2011.

[58] "SUNY Oneonta," [Online]. Available: http://www.oneonta.edu/faculty/vomsaaw/w/psy220/files/SignifOfCorrelations.htm. [Accessed 01 09 2014].

[59] " Electric Reliability Council of Texas," [Online]. Available: http://www.ercot.com/mktinfo/prices/index.html. [Accessed 01 06 2013].

[60] D. Charles, D. Hill, D. Coyle and S. Smith, "http://www.kbr.com/Newsroom/Publications/technical-papers/LNG-Technology-for-the-Commercially-Minded.pdf," in Gastech, Bilbao, 2005.

[61] W. W. Hogan, "Transmission Benefits and Cost Allocation," Mossavar-Rahmani Center for Bus. and Gov., John F. Kennedy School of Gov., Harvard Univ., Cambridge, MA, May 31, 2011.

[62] U. S. Energy Information Administration, "Electricity Market Module," Washington, DC, Apr. 2010.

[63] F. C. Knopf, Engineering Economics with VBA Procedures in Modeling, Analysis and Optimization of Process and Energy Systems, 1 ed., Wiley, 2011, pp. 22-25.

[64] M. Ortega-Vazquez, Optimizing the Spinning Reserve Requirements, Manchester, UK, 2006.

[65] K. Baxter, "Middle East Economic Digest," [Online]. Available: http://www.meed.com/sectors/oil-and-gas/gas/saudi-aramco-awards-saipem-300m-pipeline-deal/3148378.article.

[66] "High Beam Research," [Online]. Available: http://www.highbeam.com/doc/1G1-133839065.html.

[67] G. P. Towler and R. K. Sinnott, "Capital Cost Estimating," in Chemical engineering design : principles, practice, and economics of plant and process design, 2nd ed., Oxford, MA :, Butterworth-Heinemann, 2013, pp. 312-325.

[68] O. Corradi, H. Ochsenfeld, H. Madsen and P. Pinson, "Controlling Electricity Consumption by Forecasting its Response to Varying Prices," IEEE Transactions on Power Systems, vol. 28, no. 1, pp. 421-429, 2013.

[69] D. S. Kirschen and G. Strbac, Fundamentals of Power System Economics, Chichester: Wiley, 2004.

[70] KEMA International B.V., The Netherlands, "Electricity & Cogeneration Regulatory Authority," 28 Mar. 2009. [Online]. Available: http://ecra.gov.sa/documents/Studies/KPI%20Report-Final220509-lower.pdf. [Accessed 23 May 2011].

[71] "Global Energy Observatory," [Online]. Available: http://globalenergyobservatory.org/geoid/5127. [Accessed 15 01 2013].

[72] "Electrcity & Co-generation Regulatory Authority," [Online]. Available: http://www.ecra.gov.sa/generation_station_tab.aspx?id=0&gtype=4&company=0&Print=no. [Accessed 11 03 2014].

[73] power-technology.com, "Riyadh Crude Oil-Fired Power Plant, Saudi Arabia," [Online]. Available: http://www.power-technology.com/projects/riyadh/. [Accessed 19 02 2013].

[74] "675MW Hail Power Plant Expansion Project," alfanar, [Online]. Available: http://www.alfanar.com/catalogs/projects/power_water/hail_2_power.pdf. [Accessed 10 04 2013].

[75] SIEMENS, "Siemens receives another major order for combined cycle power plant in Saudi Arabia," [Online]. Available:

http://www.siemens.com/press/en/pressrelease/?press=/en/pressrelease/2012/energy/fossil-power-generation/efp201202027.htm&content%5b%5d=EF&content%5b%5d=EP. [Accessed 10 05 2014].

[76] "ARABIAN BEMCO CONTRACTING CO.," [Online]. Available: http://www.bemco-ipp.com/press_room_det_Link.php?id=142. [Accessed 10 04 2014].

[77] Saudi Electricity Company, "Annual Report 2012," [Online]. Available: https://www.se.com.sa/en-us/Lists/AnnualReports/Attachments/10/AnnualReport2012En.pdf. [Accessed 17 02 2014].

[78] United States Environmental Protection Agency, "Air Markets Program Data," [Online]. Available: http://ampd.epa.gov/ampd/. [Accessed 12 02 2013].

[79] R. Zimmerman, C. Murillo-Sánchez and R. Thomas, "MATPOWER: Steady-State Operations, Planning, and Analysis Tools for Power Systems Research and Education," IEEE Transactions on Power Systems, vol. 26, no. 1, pp. 12 - 19, Feb. 2011.

[80] "Metering & Smart Energy International," 12 March 2015. [Online]. Available: http://www.metering.com/middle-east-saudi-utility-selects-ziv-smart-meters-for-grid-ops/. [Accessed 24 May 2015].

[81] "Saudi Electricity Company," [Online]. Available: https://www.se.com.sa/en-us/pages/newsdetails.aspx?NId=265. [Accessed 24 May 2015].

[82] S. M. A. Dekhayl, "U.S.-Saudi Arabian Business Council," December 2012. [Online]. Available: http://www.us-sabc.org/files/public/PowerGen2012Presentation.pdf. [Accessed 28 September 2014].

[83] "Gulf Cooperation Council Interconnection Authority," [Online]. Available: http://www.gccia.com.sa/project.aspx?p=P3. [Accessed 2 June 2014].

[84] "Saudi Electricity Company," 2008. [Online]. Available: http://www.se.com.sa/SEC/English/Menu/PowerTransmissionNetwok/Saudi+Arabian+Grid+Code/Saudi+Power+Transmission+Network/.

[85] F. Kateeb, Interviewee, SEC representative. [Interview]. 01 07 2013.

[86] "Wikimapia," [Online]. Available: www.wikimapia.org. [Accessed 01 07 2013].

[87] "Central Department of Statistics and Information," 2010. [Online]. Available:

http://www.cdsi.gov.sa/2010-07-31-07-00-05/cat_view/31-/138----/342---1431-2010/300---. [Accessed 2013 01 10].

[88] "Saudi Industrial Property Authority," 18 March 2014. [Online]. Available: http://www.modon.gov.sa/en/mediacenter/news/Pages/140318.aspx. [Accessed 13 November 2013].

[89] "Power and Water Utility for Jubail and Yanbu," [Online]. Available: http://www.marafiq.com.sa/en/operations/opr_iwppjub.aspx. [Accessed 21 2 2014].

[90] "Saudi Arabian Mining Company," 17 October 2009. [Online]. Available: http://www.maaden.com.sa/en/news_details/26. [Accessed 22 03 2014].

[91] "Saudi Industrial Property Authority," [Online]. Available: http://www.modon.gov.sa/ar/aboutmodon/achievements_authority/Documents/%D8%A7%D9%84%D8%AA%D9%82%D8%B1%D9%8A%D8%B1%20%D8%A7%D9%84%D8%B3%D9%86%D9%88%D9%8A%202013.pdf. [Accessed 31 March 2014].

VITA

Mohammed Abahussain is a PhD candidate in the Electrical Engineering Department at the University of Washington in Seattle. He obtained the BS and MS in electrical engineering from University of the Pacific and the University of Washington respectively. Mohammed joined Saudi Aramco since 2002. He handled various tasks in the Power Distribution and Consulting Services Departments including HV design, project support, and standards review. His research interests include power system operation, power system economics, and smart grid applications.